

Discrete Curves and Surfaces

vorgelegt von
Diplom-Mathematiker
Tim Hoffmann
aus Berlin

Vom Fachbereich 3 Mathematik
der Technischen Universität Berlin
zur Erlangung des akademischen Grades
Doktor der Naturwissenschaften
genehmigte Dissertation

Promotionsausschuß:

Vorsitzender: Prof. Dr. B. Herz

Berichter: Prof. Dr. U. Pinkall

Berichter: Prof. Dr. A. Bobenko

Tag der wissenschaftlichen Aussprache: 12.1.2000

Berlin 2000
D 83

Summary of results

Flows on curves can be discretized in two steps. First one can investigate flows on discrete curves (i.e. polygons) then one can discretize time too. The discretization of flows on curves in \mathbb{CP}^1 that are linked to the KdV and (in its euclidian reduction) the mKdV equation give rise to the famous Volterra model and its discretization as well as discrete KdV and mKdV equations, which in turn gives them a geometric meaning.

The doubly discrete flows in \mathbb{CP}^1 arise as Bäcklund transformations of their smooth counterparts and introduce maps from \mathbb{Z}^2 to \mathbb{C} with all elementary quadrilaterals having constant cross-ratio—these are known as discrete conformal maps. If one extends this to discrete space curves one gets discrete isothermic surfaces.

The Hashimoto or smokering flow and its discretization is discussed and a doubly discrete Hashimoto flow is derived. The smokering flow is linked to both the isotropic Heisenberg magnet model and the nonlinear Schrödinger equation which are known to be gauge equivalent. This equivalence is here also shown for the discrete and doubly discrete case, the first giving rise to the equivalence of two famous discretizations of the nonlinear Schrödinger equation, which was unknown.

Above discrete time evolution can be adopted to generate discrete surfaces of constant mean curvature (cmc surfaces)—which are in particular discrete isothermic surfaces—out of discrete closed curves.

In an other approach discrete versions of rotational cmc surfaces are derived from the standard billiard in an ellipse or hyperbola.

A discrete version of the Dorfmeister-Pedit-Wu-method for generating cmc surfaces out of holomorphic data is presented and discrete Smyth surfaces are derived.

Finally it is shown how discrete K-surfaces can be derived from an analogue of a curvature line stripe.

Zusammenfassung der Ergebnisse

Flüsse auf Kurven können in zwei Schritten diskretisiert werden: Zunächst kann man Flüsse auf diskreten Kurven (also Polygonen) betrachten, dann kann man auch die Zeit diskretisieren. Die Diskretisierung von Flüssen auf Kurven in \mathbb{CP}^1 , die mit der KdV und (in der euklidischen Reduktion) mKdV Gleichung zusammenhängen, führt sowohl zum berühmten Volterra Modell und seiner Diskretisierung, als auch zu diskreten KdV und mKdV Gleichungen, was diesen geometrische Interpretationen gibt.

Die doppelt diskreten Flüsse in \mathbb{CP}^1 entstehen als Bäcklundtransformationen ihrer glatten Analoga und erzeugen Abbildungen von \mathbb{Z}^2 nach \mathbb{C} bei denen alle elementaren Vierecke konstantes Doppelverhältniss haben—solche Abbildungen wurden als diskrete konforme Abbildungen untersucht. Erweitert man das auf Raumkurven erhält man diskrete Isothermflächen.

Der Hashimoto oder Rauchring Fluß und seine Diskretisierung werden untersucht und ein doppelt diskreter Hashimoto Fluß wird hergeleitet. Der Hashimoto Fluß hängt sowohl mit der nichtlinearen Schrödinger Gleichung als auch mit dem anisotropen Heisenberg-Magneten zusammen. Die Eichäquivalenz der beiden Modelle ist bekannt. Diese Äquivalenz wird hier für den diskreten und doppelt diskreten Fall gezeigt, was insbesondere auch zu der Äquivalenz zweier bekannter Diskretisierungen der nichtlinearen Schrödinger Gleichung führt, die nicht bekannt war.

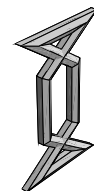
Obige diskrete Zeitevolution für Kurven kann so angepasst werden, daß man aus geschlossenen diskreten Kurven diskrete Flächen mit konstanter mittlerer Krümmung (cmc) erzeugen kann—sie sind insbesondere isotherm. Bei einem anderen Zugang werden diskrete Rotations-cmc-Flächen mit Hilfe des Standardbilliards in der Ellipse oder Hyperbel erzeugt. Eine diskrete Version der Dorfmeister-Pedit-Wu-Methode zur Erzeugung von cmc Flächen aus holomorphen Daten wird vorgestellt und diskrete Smyth Flächen werden konstruiert. Schließlich wird gezeigt, wie man diskrete K-Flächen aus einem Analogon eines Krümmungslinienstreifens erzeugen kann.

Contents

Introduction	11
1 Flows on curves in projective space	14
1.1 Introduction	14
1.2 Discrete calculus	15
1.3 The smooth case	16
1.3.1 Euclidian reduction	17
1.4 Flows on discrete curves in complex projective space	19
1.4.1 Euclidian reduction	22
1.5 Discrete flows	26
2 Discrete Hashimoto surfaces	29
2.1 Introduction	29
2.2 Hashimoto flow, Heisenberg flow, and the NLSE . . .	31
2.2.1 Elastic curves	33
2.2.2 Bäcklund transformations for smooth space curves and Hashimoto surfaces	34
2.3 Discr. Hashimoto flow, Heisenberg flow, and dNLSE .	38
2.3.1 Discrete elastic curves	41
2.3.2 Bäcklund transformations for discrete space curves and Hashimoto surfaces	42
2.4 The doubly discrete Hashimoto flow	49
2.4.1 discrete Elastic Curves	51
2.4.2 Bäcklund transformations for the doubly dis- crete Hashimoto surfaces	53

3	The equiv. of the dNLS and the dIHM models	56
3.1	Introduction	56
3.2	Equivalence of dIHM and dNLSE _{AL}	57
3.2.1	Equivalence of the two discrete nonlinear Schrödinger equations	60
3.3	Doubly discrete IHM and doubly discrete NLSE	62
4	Discrete cmc surfaces from discrete curves	66
4.1	Introduction	66
4.2	Discrete isothermic and cmc surfaces	67
4.3	CMC evolution of discrete curves	68
4.4	Examples	70
4.4.1	Delaunay surfaces	70
4.4.2	Wente tori	70
4.4.3	Trinoidal surfaces	70
5	Discr. Rot. CMC Surf. and Elliptic Billiards	75
5.1	Introduction	75
5.2	Discrete rotational surfaces	76
5.3	Unrolling polygons and discr. surfaces	77
5.4	The Standard Billiard in an Ellipse or Hyperbola	77
5.5	Discrete Rotational CMC Surfaces	78
6	Discrete CMC Surf. and Holom. Maps	83
6.1	Introduction	83
6.2	The DPW method	84
6.3	Discrete cmc surfaces	86
6.4	Splitting in the discrete case	87
6.5	The discrete DPW method	94
6.6	Examples	95
6.6.1	Cylinder and two-legged Mr Bubbles	95
6.6.2	Delaunay tubes	96
6.6.3	n -legged Mr Bubbles and a discrete z^α	100

7	Discrete K-surfaces from discrete curves	103
7.1	Introduction	103
7.2	Discrete K-surfaces from curvature lines	103
7.3	Discrete K-surfaces from asymptotic lines	105
	Acknowledgments	108

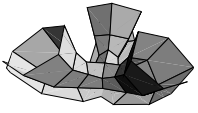


Introduction

The study of discrete geometry has become of great interest in the last years. It turned out that special discrete geometric constructions are directly linked to discrete integrable systems giving them new interpretations as well as establishing new models. At the turn of the century the study of discrete objects often preceded continuous investigations (e.g. differential equations were viewed as limits of difference equations etc.). These discrete objects seemed to be lost for a while but due to the use of computers in our days they are in focus again. Nevertheless already in the early fifties, mathematicians in Vienna like W. Wunderlich and R. Sauer started to study discrete analogs of smooth surfaces. These surfaces were discrete in the sense that they tried to discretize the geometric properties rather than to simply approximate smooth surfaces. In 1994 A. Bobenko and U. Pinkall benefited from this approach when they extended the definitions of Wunderlich [Wun51] for discrete surfaces of negative Gaußian curvature (K-surfaces) and showed that they are equivalent to an integrable difference equation - the now famous discrete Sine Gordon equation [BP96b]. Again A. Bobenko and U. Pinkall found a discretization for isothermic surfaces and surfaces of constant mean curvature (cmc) which lead in turn to integrable discretizations of the corresponding smooth integrable equations [BP96a, BP99].

All these discretizations have in common that the (discrete) surfaces show the typical behavior of their smooth counterparts - even in very rough discretizations. They possess for example discrete versions of Bäcklund transformations, which are well known for the continuous ones. Moreover the construction can be done explicitly





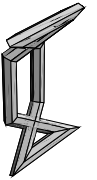
without solving pde's numerically. For example the construction of cmc surfaces is very difficult and general methods need a splitting in some loop group which can usually only be done approximatively for visualization purpose [DPW94]. The discrete version however can be solved exactly (see Chapter 6). We will start here somewhat simpler by investigating discrete curves and flows on them first. A task that has turned out fruitfully already [DS99].

This work is portioned into 7 rather self-contained chapters. They vary in size but all open different views on the interrelationship between discrete curves and surfaces and integrable systems.

In the first chapter we will investigate flows on discrete curves in \mathbb{CP}^1 . It will turn out, that the discretization of the (in the continuous case trivial) tangential flow is linked to the famous Volterra model [FT86]. In fact the cross-ratio of four successive points of a discrete curve plays the rôle of a discrete Schwarzian derivative and will obey the Volterra model.

One can go one step further and discretize time too. The doubly discrete tangential flow (which gives rise to the discrete time Volterra model [Sur99]) is an evolution of the curve in the way that two successive points and their time one images have fixed cross-ratio. This of course gives rise to maps from \mathbb{Z}^2 into \mathbb{CP}^1 . Especially in the case of real negative cross-ratio they can be viewed as discretization of conformal maps and have been studied in [BP96a, HJMP98].

In the second Chapter we will modify this approach to curves in \mathbb{R}^3 getting a discrete and a doubly discrete version of the smoke ring flow. In the continuous case this flow is equivalent to both the nonlinear Schrödinger equation and the isotropic Heisenberg magnet model. We devote the third Chapter to the equivalence of the two in the discrete and doubly discrete case. Chapter 4 is devoted to the above mentioned discrete cmc surfaces. It is shown how one can generate them from a discrete stripe. As examples discrete Wente tori are build from discretizations of the elastic figure eight and discrete trinoidal surfaces are derived.

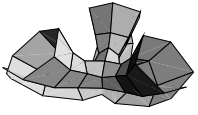


In Chapter 5 we will generate discrete surfaces from curves in a slightly different way: It is known, that every rotational surface allows isothermic parameterization. Since we know what discrete isothermic surfaces are, we can derive the condition for a discrete meridian curve, that its discrete rotation gives an isothermic surface. Moreover one knows that the meridian curve for cmc surfaces are obtained by tracing one focus of an ellipse when rolling it on an straight line. A discrete analog of this is presented, linking these discrete surfaces to another well-known integrable system: The Billiard in an Ellipse.

In Chapter 6 we present a method to generate discrete cmc surfaces from discrete conformal maps (discrete isothermic surfaces in the plane). It is the discrete analog of the DPW recipe introduced by Dorfmeister Pedit and Wu 1994 [DPW94]. To obtain discrete cmc surfaces with umbilics, we have to generalize our definition of discrete isothermic surfaces from the combinatorics of a square grid to some more general graph: Since in each isolated umbilic more than two curvature lines intersect, we need vertices with more than four edges as link.

In the last chapter we shortly mention methods to get discrete K-surfaces from both curvature and asymptotic lines. This is mainly for completeness reasons although it is interesting to compare the Hashimoto and cmc surfaces generated from a discrete elastic eight with the K-surface generated by the same curve.





Chapter 1

Flows on Discrete curves in complex projective space

1.1 Introduction

In this chapter we investigate flows on discrete curves in \mathbb{CP}^1 and \mathbb{C} . We start with a short review of the continuous case, where the KdV equation is derived as evolution equation of the Schwarzian derivative p of a curve c evolving with the flow $\dot{c} = pc'$. This becomes the mKdV equation for the curvature κ of the curve if one changes to the euclidian picture.

In the discrete case however already the tangential flow is not trivial and the cross-ratio q of four neighboring points of the discrete curve (which is a discretization of the Schwarzian derivative) will evolve with the famous Volterra model

$$\dot{q}_k = q_k(q_{k+1} - q_{k-1}).$$

The next higher flow will give a discrete KdV equation and again one gets a discrete mKdV equation for the curvature if one restricts oneself to arclength parameterized discrete curves.

In the last section it will be shown, that one gets the doubly discrete Volterra model if one Bäcklund transforms the discrete curve with the condition that any two neighboring points of the curve and their transforms should have a fixed cross-ratio.

We start by giving some notations and facts about discrete curves.



1.2 Discrete calculus

Let f and g be maps from \mathbb{Z} into an associative algebra. We denote successors and predecessors by subscript "+", "++", "-", "--" etc. So f_-, f, f_+ will stand for f_{n-1}, f_n, f_{n+1} for some $n \in \mathbb{Z}$. Define the following operators

$$\begin{aligned} Df &:= \frac{1}{2}(f_+ - f) \\ Mf &:= \frac{1}{2}(f_+ + f) \\ f \cdot g &:= \frac{1}{2}(f_+g + fg_+). \end{aligned}$$

The meaning of these operators is quite obvious: While D is a discretization of the differentiation, M and \cdot discretize the identity and the product in a sense compatible with D (one should think of Df, Mf etc. to live on the "dual chain" $\mathbb{Z} + \frac{1}{2}$):

$$\begin{aligned} DM &= MD \\ Dfg &= DfMg + MfDg \\ Df \cdot g &= (DMf)g + fDMg \end{aligned}$$

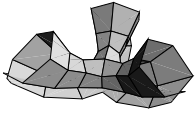
We will use one more discrete operator: the inverse harmonic mean of D

$$D^h f := \left(\frac{1}{2}((Df)^{-1} + (Df_+)^{-1}) \right)^{-1} = \frac{Df Df_+}{DMf}.$$

A discrete curve in \mathbb{R}^n is a map $c : \mathbb{Z} \rightarrow \mathbb{R}^n$. It will be called regular or immersed, if $\|Dc\|$ and $\|DMc\| \neq 0$. It is called *arclength parameterized* if $\|2Dc\| = 1$. Some times we will use the shorthand $S := 2Dc$. For an arclength parameterized curve c the *curvature* κ is defined as follows:

$$\kappa = \tan \frac{\angle(Dc_-, Dc)}{2}. \quad (1.1)$$





1.3 The smooth case

Before we turn to flows on discrete curves we give—without laying claim to completeness—a short review of the continuous case. Let $c : \mathbb{R} \rightarrow \mathbb{CP}^1$ be a smooth immersed curve and $\gamma : \mathbb{R} \rightarrow \mathbb{C}^2$ be a lift in homogenous coordinates normalized by the condition

$$\det(\gamma, \gamma') = 1. \quad (1.2)$$

In this case we have $\det(\gamma, \gamma'') = 0$, so γ and γ'' are linear dependend and we can define p by

$$\gamma'' =: p\gamma. \quad (1.3)$$

Lemma 1 $-2p$ is the Schwarzian derivative of f :

$$-2p = S(c) := \frac{c'''}{c'} - \frac{3}{2} \left(\frac{c''}{c'} \right)^2.$$

Remark If c is an euclidian curve and arclength parameterized one has

$$S(\gamma) = \left(\frac{1}{2}\kappa^2 + i\kappa' \right) \quad (1.4)$$

where $\kappa = \frac{c''}{ic'}$ is the curvature of c .

We will now investigate flows on γ that preserve the normalization (1.2). Any Flow on γ can be written as a linear combination of γ and γ' :

$$\dot{\gamma} = \alpha\gamma + \beta\gamma'. \quad (1.5)$$

Lemma 2 A flow on γ written in above form preserves the normalization (1.2) iff

$$2\alpha + \beta' = 0. \quad (1.6)$$

Proof Compute $0 = \det(\dot{\gamma}, \gamma') + \det(\gamma, \dot{\gamma}')$. □

Thus prescribing β along γ gives a unique flow of the desired form. A trivial choice is of course $\beta = \text{const}$ which results in the tangential flow $\dot{\gamma} = \gamma'$.



Lemma 3 *If γ evolves with a flow preserving the normalization (1.2) p evolves as follows:*

$$\dot{p} = -\frac{\beta'''}{2} + p'p + \beta p' + 2\beta'p. \quad (1.7)$$

Proof Again straight forward calculation. □

If we choose $\beta = -2p$ p itself will evolve with the well known KdV equation:

$$\dot{p} = p''' - 6pp'. \quad (1.8)$$

1.3.1 Euclidian reduction

If c does not hit ∞ , γ obeying the normalization (1.2) is given by

$$\gamma = \frac{1}{\sqrt{-c'}} \begin{pmatrix} c \\ 1 \end{pmatrix}.$$

Lemma 4 *If γ now flows with (1.5) c flows with*

$$\dot{c} = \beta f' \quad (1.9)$$

Proof The evolution equation (1.5) for γ gives

$$\begin{aligned} \dot{c} \frac{\sqrt{-c'}}{-c'} + \frac{\frac{1}{2}c \frac{\dot{c}'}{\sqrt{-c'}}}{-c'} &= \alpha \frac{c}{\sqrt{-c'}} + \beta \frac{c' \sqrt{-c'} + \frac{1}{2}c \frac{c''}{\sqrt{-c'}}}{-c'} \\ \frac{\frac{1}{2} \frac{\dot{c}'}{\sqrt{-c'}}}{-c'} &= \alpha \frac{1}{\sqrt{-c'}} + \beta \frac{\frac{1}{2}c \frac{c''}{\sqrt{-c'}}}{-c'}. \end{aligned}$$

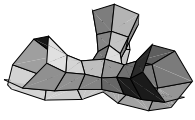
Combining these two equations gives equation (1.9) □

In the special case that c is arclength parameterized (i.e. $|c'| = 1$) we get with the choice $\beta = -2p$:

$$\dot{c} = S(c)c' = \left(\frac{1}{2}\kappa^2 T + \kappa' N\right) \quad (1.10)$$

with T and N being the tangent and the oriented normal of c . Because of the following lemma we will call this flow mKdV flow.





Lemma 5 *If c is arclength parameterized and flows with (1.10) the curvature κ of c solves the mKdV equation*

$$\dot{\kappa} = \kappa''' + \frac{3}{2}\kappa^2\kappa'. \quad (1.11)$$

Proof One has

$$\begin{aligned} c'' &= i\kappa c' \\ \dot{c}' &= i(\kappa'' + \frac{\kappa^3}{2})c' \\ \dot{c}'' &= (i\kappa''' + \frac{3}{2}i\kappa^2\kappa' - \kappa\kappa'' - \frac{1}{2}\kappa^4)c \end{aligned} \quad (1.12)$$

and therefore $i\dot{\kappa} = \frac{\dot{c}''}{c'} - i\kappa\frac{\dot{c}'}{c'} = i(\kappa''' + \frac{3}{2}\kappa^2\kappa')$. \square

Generalized elastic curves

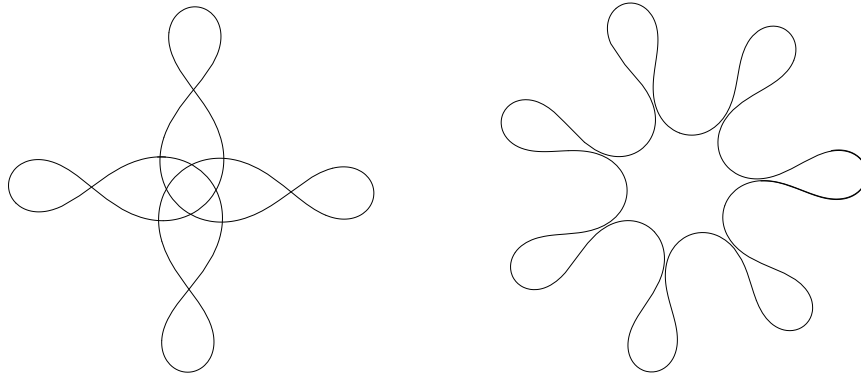


Figure 1.1: Two closed generalized elastic curves.

One can ask for curves, that evolve up to reparametrization (i.e. tangential flow) by euclidian motion only under the mKdV flow. In other words $a\kappa' = \dot{\kappa} = \kappa''' + \frac{3}{2}\kappa^2\kappa'$ for some (real) constant a . One can integrate this equation once getting

$$\kappa'' = b + (a - \frac{1}{2}\kappa^2)\kappa. \quad (1.13)$$

Figure 1.1 shows two closed examples of such curves.

In the case $b = 0$ equation 1.13 reduces to the characterization of elastic curves (2.14) which is discussed in the Chapter 2.¹

¹Taking the norm there comes from the fact that we have no oriented normal in \mathbb{R}^3 .



1.4 Flows on discrete curves in complex projective space

Let $c : \mathbb{Z} \rightarrow \mathbb{CP}^1$ be a discrete curve in the complex projective space. We assume c is immersed, i.e. c_-, c and c_+ are pairwise disjoint. By introducing homogenous coordinates, we can lift c to a map $\gamma : \mathbb{Z} \rightarrow \mathbb{C}^2$ with $c = \gamma_1 \gamma_2^{-1}$. Obviously γ is not uniquely defined: For $\lambda : \mathbb{Z} \rightarrow \mathbb{C}^*$, $\lambda\gamma$ is also valid lift. Therefore we demand γ to satisfy the normalization

$$\det(\gamma, \gamma_+) = 1. \quad (1.14)$$

Note that this is always possible, since c is immersed and after choosing an initial γ_0 , γ is fixed.

Definition 1 *The cross-ratio of four points $a, b, c, d \in \mathbb{CP}^1$ is defined by*

$$\text{cr}(a, b, c, d) = \frac{\det(a, b) \det(c, d)}{\det(b, c) \det(d, a)}.$$

Let us denote the cross-ratio of four neighboring points of γ by q :

$$q := \text{cr}(\gamma_-, \gamma, \gamma_{++}, \gamma_+). \quad (1.15)$$

Up to a Möbius transformation (which is basically the free choice of three initial points of c) γ is determined completely by q and q does not depend on the choice of the initial γ_0 . We can introduce the *associated family* $\gamma(\lambda)$ of γ by the condition $q(\lambda) = \lambda q$.

If γ is normalized by equation (1.14) we can set

$$u := \det(\gamma_-, \gamma_+). \quad (1.16)$$

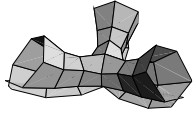
Then

$$\frac{1}{uu_+} = \text{cr}(\gamma_-, \gamma, \gamma_{++}, \gamma_+) = q. \quad (1.17)$$

We shall now study flows on γ that preserve condition (1.14). Since $\det(\gamma, \gamma_+ - \gamma_-) = 2$ any flow on γ can be written in the following way:

$$\dot{\gamma} = \alpha\gamma + \frac{\beta}{2u}(\gamma_+ - \gamma_-). \quad (1.18)$$





Lemma 6 *A flow on the discrete curve γ preserves the conformal arclength iff*

$$2 M \alpha + D \beta = 0. \quad (1.19)$$

Proof To get this condition on α and β we differentiate equation (1.14):

$$\begin{aligned} 0 &= \det(\dot{\gamma}, \gamma_+) + \det(\gamma, \dot{\gamma}_+) \\ &= \det\left(\alpha\gamma + \frac{\beta}{2u}(\gamma_+ - \gamma_-), \gamma_+\right) + \det\left(\gamma, \alpha_+\gamma_+ + \frac{\beta_+}{2u_+}(\gamma_{++} - \gamma)\right) \\ &= \alpha - \frac{\beta}{2} + \alpha_+ + \frac{\beta_+}{2}. \end{aligned} \quad (1.20)$$

So the flow must satisfy equation (1.19). \square

A trivial solution to this is obvious: Choosing $\beta \equiv 0$ induces $\alpha_+ = -\alpha$. This flow corresponds to the freedom of the initial choice of γ_0 and has no effect on c . Note also that (1.19) is a linear equation. So one can always add any two flows solving it.

Lemma 7 *If $\gamma : \mathbb{Z} \rightarrow \mathbb{CP}^1$ evolves with an arclength preserving flow, u and the cross-ratio q evolve as follows:*

$$\dot{u} = -2\left(\alpha u + 2 D M \frac{\beta}{u}\right) \quad (1.21)$$

$$\dot{q} = 2q(q-1) D \beta + q(\beta_{++}q_+ - \beta_-q_-). \quad (1.22)$$

Proof One has

$$\begin{aligned} \dot{u} &= \det(\dot{\gamma}_-, \gamma_+) + \det(\gamma_-, \dot{\gamma}_+) \\ &= \det\left(\alpha_-\gamma_- + \frac{\beta_-}{2u_-}(\gamma - \gamma_{--}), \gamma_+\right) + \det\left(\gamma, \alpha_+\gamma_+ + \frac{\beta_+}{2u_+}(\gamma_{++} - \gamma)\right) \\ &= u(\alpha_+ + \alpha_-) + \frac{\beta_-}{2u_-} - \frac{\beta_+}{2u_+} - \frac{\beta_-}{2u_-}(uu_- - 1) + \frac{\beta_+}{2u_+}(uu_+ - 1) \\ &= -2\left(\alpha u + 2 D M \frac{\beta}{u}\right) \end{aligned}$$

which proves equation (1.21). Now one can use this to compute

$$\begin{aligned} \dot{q} &= -q(\dot{u}u_+ + u\dot{u}_+) \\ &= 2q(q-1) D \beta + q(\beta_{++}q_+ - \beta_-q_-). \end{aligned}$$



□

If we choose $\beta \equiv 1$ and $\alpha \equiv 0$. We get for the curve

$$\dot{\gamma} = \frac{1}{2u}(\gamma_+ - \gamma_-). \quad (1.23)$$

This is what we will call the *conformal tangential flow*. Then $\dot{u} = \frac{1}{u_-} - \frac{1}{u_+}$ and q will solve the famous Volterra model [FT86, Sur99]:

$$\dot{q} = q(q_+ - q_-) = 4q \text{ D M } q. \quad (1.24)$$

If we want this equation for the whole associated family of γ we must scale time by λ :

$$\lambda \dot{q}(\lambda) = q(\lambda)(q_+(\lambda) - q_-(\lambda))$$

One obtains the next higher flow of the Volterra hierarchy [Sur99] when one chooses $\beta = 2 \text{ M } q + 1$. This implies

$$\dot{q} = q(q_+(q_{++} + q_+ + q) - q_-(q + q_- + q_{--})). \quad (1.25)$$

To make contact with the classical results we will now derive the 2×2 -Lax representation of the Volterra model:

Define $e_1 = \begin{pmatrix} 0 \\ 1 \end{pmatrix}$, $e_2 = \begin{pmatrix} -1 \\ 0 \end{pmatrix}$ and $e_3 = \begin{pmatrix} 1 \\ -1 \end{pmatrix}$. Moreover define the matrix $\tilde{\mathcal{F}} = (u\gamma, \gamma_+)$. Then $\tilde{\mathcal{F}}e_1 = u\gamma$, $\tilde{\mathcal{F}}e_2 = \gamma_+$ and $\tilde{\mathcal{F}}e_3 = u\gamma - \gamma_+ = \gamma_-$ and one has $\tilde{\mathcal{F}}_+^{-1}\tilde{\mathcal{F}}e_1 = ue_3$ and $\tilde{\mathcal{F}}_+^{-1}\tilde{\mathcal{F}}e_2 = uqe_1$. Thus

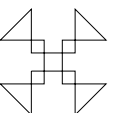
$$\tilde{L} := \tilde{\mathcal{F}}_+^{-1}\tilde{\mathcal{F}} = u \begin{pmatrix} 1 & q \\ -1 & 0 \end{pmatrix}.$$

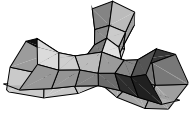
So if we define $\mathcal{F}_n = \prod_{i=0}^{n-1} u_i \tilde{\mathcal{F}}_i$ and $L := \mathcal{F}_+^{-1}\mathcal{F}$ we get

$$L = \begin{pmatrix} 1 & q \\ -1 & 0 \end{pmatrix} \quad (1.26)$$

which is the Lax matrix of the Volterra model [Sur99]. If we differentiate L we get

$$\dot{L} = -\mathcal{F}_+^{-1}\dot{\mathcal{F}}_+\mathcal{F}_+^{-1}\mathcal{F} + \mathcal{F}_+^{-1}\mathcal{F}\mathcal{F}_+^{-1}\dot{\mathcal{F}} = \tilde{M}L - L\tilde{M}_-$$





with the auxiliary matrix $\widetilde{M} = -\mathcal{F}_+^{-1}\dot{\mathcal{F}}_+$.

$$\begin{aligned}
\widetilde{M} &= -\prod_{i=0}^n u_i \widetilde{\mathcal{F}}_+^{-1} \left(\frac{d}{dt} \left(\prod_{i=0}^n u_i \right) \widetilde{\mathcal{F}}_+ + \prod_{i=0}^n u_i \dot{\widetilde{\mathcal{F}}}_+ \right) \\
&= -\frac{d}{dt} \log \left(\prod_{i=0}^n u_i \right) \mathbb{I} - \widetilde{\mathcal{F}}_+^{-1} \dot{\widetilde{\mathcal{F}}}_+ \\
&= (-q_{-1} + q_n) \mathbb{I} \\
&\quad - \widetilde{\mathcal{F}}_+^{-1} \left(\left(\frac{1}{u} - \frac{1}{u_{++}} \right) \gamma_+ + \frac{1}{2} (\gamma_{++} - \gamma), \frac{1}{2u_+} (\gamma_{+++} - \gamma_+) \right) \\
&= (-q_{-1} + q_n) \mathbb{I} - \left((q - q_+) e_1 + \frac{1}{2} e_2 - \frac{1}{2} e_3, \frac{1}{2} e_2 - q_+ e_1 \right) \\
&= \begin{pmatrix} -q_{-1} - \frac{1}{2} & 0 \\ 0 & -q_{-1} - \frac{1}{2} \end{pmatrix} + \begin{pmatrix} 1 + q_+ & q_+ \\ -1 & q \end{pmatrix}.
\end{aligned} \tag{1.27}$$

The first summand is constant and can therefore be omitted. For the whole associated family we get now

$$\begin{aligned}
\lambda \dot{L}(\lambda) &= M(\lambda) L(\lambda) - L(\lambda) M_-(\lambda) \\
L(\lambda) &= \begin{pmatrix} 1 & \lambda q \\ -1 & 0 \end{pmatrix} \\
M(\lambda) &= \begin{pmatrix} 1 + \lambda q_+ & \lambda q_+ \\ -1 & \lambda q \end{pmatrix}.
\end{aligned} \tag{1.28}$$

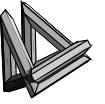
This is up to the change $\lambda \rightarrow \lambda^{-2}$ and a gauge transformation with $E = \begin{pmatrix} \lambda^{1/2} & 0 \\ 0 & \lambda^{-1/2} \end{pmatrix}$ the known form of the Volterra Lax-pair [Sur99].

1.4.1 Euclidian reduction

If c does not hit ∞ we can write $\gamma = \lambda \binom{c}{1}$ with $\lambda_+ = \frac{-1}{\lambda S}$ to satisfy our normalization. We then get for the general evolution of c :

Lemma 8 *If γ flows with (1.18) c evolves with*

$$\dot{c} = \beta \frac{S_- S}{S_- + S} =: \beta D^h c. \tag{1.29}$$



Proof Equation (1.18) gives

$$\begin{aligned}\dot{\lambda}c + \lambda\dot{c} &= \alpha\lambda c + \frac{\beta}{2u}(\lambda_+c_+ - \lambda_-c_-) \\ \dot{\lambda} &= \alpha\lambda + \frac{\beta}{2u}(\lambda_+ + -\lambda_-).\end{aligned}$$

Combining these two equations gives equation (1.29). □

Now let us assume, that c is an arclength parameterized curve in \mathbb{C} . In this case we can write

$$2\frac{S_-S}{S_- + S} = \frac{S_- + S}{1 + \langle S_-, S \rangle}$$

since

$$\left\langle 2\frac{S_-S}{S_- + S}, S_- \right\rangle = \text{Re}\left(2\frac{S_-S}{S_- + S}\bar{S}_-\right) = 1 = \left\langle \frac{S_- + S}{1 + \langle S_-, S \rangle}, S_- \right\rangle$$

and the same for the scalar product with S . So for $\beta = 2$ we get the well known tangential flow for discrete curves [DS99, BS99]:

$$\dot{c} = \frac{S_- + S}{1 + \langle S_-, S \rangle}.$$

Now let us rewrite q to get an interpretation for the choice $\beta = 2Mq + 1$:

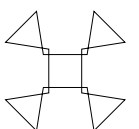
$$\begin{aligned}q &= \frac{S_-S_+}{(S_-+S)(S_++S)} = \frac{1}{(1+\frac{S}{S_-})(\frac{S}{S_+}+1)} = \frac{1}{(1+\frac{i-\kappa}{i+\kappa})(1+\frac{i+\kappa_{\pm}}{i-\kappa_{\pm}})} \\ &= -\frac{1}{4}(i + \kappa)(i - \kappa_+) \\ &= \frac{1}{2}(i D \kappa + \frac{1}{2}\kappa \cdot \kappa + \frac{1}{2}).\end{aligned}$$

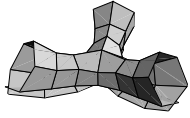
With this on hand the second Volterra flow becomes:

$$\dot{c} = \left(\frac{1}{2}M\kappa \cdot \kappa + iDM\kappa\right)D^h c + \frac{3}{2}D^h c \tag{1.30}$$

which is up to an additional tangential flow part clearly a discretization of (1.10).

Lemma 9 *The discrete tangential flow and the discrete mKdV flow both preserve the discrete arclength parametrization.*





Proof We calculate $\langle S, \dot{S} \rangle$ for a general flow:

$$\begin{aligned} \langle S, \dot{S} \rangle &= \operatorname{Re}(\overline{S}(\beta_+ D^h \gamma_+ - \beta D^h \gamma)) \\ &= \operatorname{Re}\left(\frac{\beta_+}{1+s_+} - \frac{\beta}{1+s_-}\right) = \operatorname{Re}(\beta_+(1+i\kappa_+) - \beta(1-i\kappa)). \end{aligned}$$

So the condition for a flow of the form $\dot{c} = \beta D^h c$ to preserve the discrete arclength is

$$\operatorname{Re} D \beta = \operatorname{Im} M(\kappa\beta). \quad (1.31)$$

for the tangential flow this clearly holds. In the case of the mKdV flow it is an easy exercise to show equation (1.31). \square

Discrete generalized elastic curves

Elastic curves will play some rôle in the next chapter. As in the smooth case we will derive planar elastic curves here as special case of curves that move up to a reparametrization by euclidian motion only when evolved with the mKdV flow. In other words there must exist a (real) constant a such that

$$\dot{c} - a D^h c = \dot{c}_+ - a D^h c_+. \quad (1.32)$$

Lemma 10 *The curvature of a discrete curve, that evolves up to some tangential flow by euclidian motion under the mKdV flow satisfies*

$$\kappa_+ = \frac{2a\kappa}{1+\kappa^2} - \kappa_- + b \quad (1.33)$$

for some constants a and b .

Proof Insert the flow in equation (1.32). \square

Figure 1.2 shows two closed discrete generalized elastic curves and the thumb nail movie on the lower right shows a one parameter family of them.

Remark In the case $b = 0$ this gives the equation for planar elastic curves (2.31) from Chapter 2.

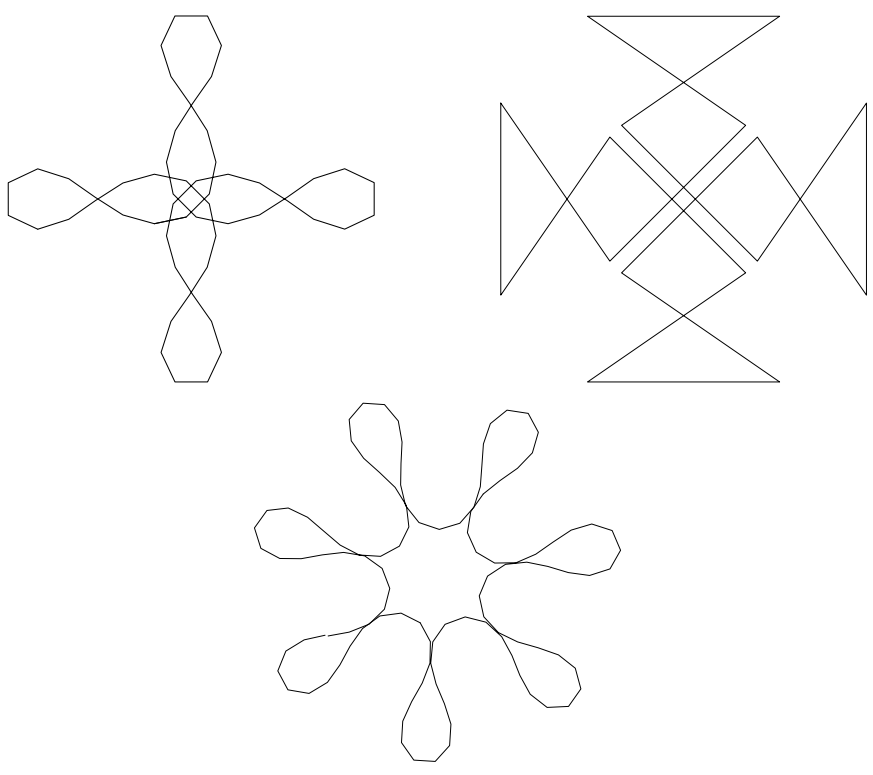
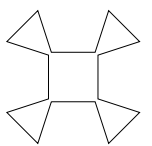
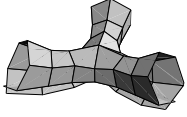


Figure 1.2: Three closed generalized elastic curves.





1.5 Discrete flows

As in the previous section let γ be the lift of a immersed discrete curve in \mathbb{CP}^1 into \mathbb{C}^2 satisfying the normalization (1.19).

Lemma 11 *Given an initial $\tilde{\gamma}_0$ and a complex parameter μ there is an unique map $\tilde{\gamma} : \mathbb{Z} \rightarrow \mathbb{C}^2$ satisfying normalization (1.19) and*

$$\mu = \text{cr}(\gamma, \gamma_+, \tilde{\gamma}_+, \tilde{\gamma}). \quad (1.34)$$

We will call $\tilde{\gamma}$ a Bäcklund transform of γ .

Proof Solving equation (1.34) for $\tilde{\gamma}_+$ gives that $\tilde{\gamma}_+$ is a Möbius transform of $\tilde{\gamma}$. \square

Lemma 12 *If $\tilde{\gamma}$ is a Bäcklund transform of γ with parameter μ then*

$$\begin{aligned} \tilde{q} &= q \frac{s}{s_+}, \\ (1 - \mu)q &= \frac{s_+}{(1 - s)(s_+ - 1)} \end{aligned} \quad (1.35)$$

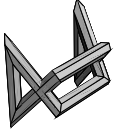
with $s = \text{cr}(\gamma_-, \tilde{\gamma}, \gamma_+, \gamma)$.

Proof Due to the properties of the cross-ratio (a useful table of the identities can be found in [HJHP99]) we have

$$\begin{aligned} 1 - \mu &= \text{cr}(\gamma, \tilde{\gamma}_+, \gamma_+, \tilde{\gamma}) = \frac{\det(\gamma, \tilde{\gamma}_+) \det(\gamma_+, \tilde{\gamma})}{\det(\tilde{\gamma}_+, \gamma_+) \det(\tilde{\gamma}, \gamma)} \\ q &= \frac{\det(\gamma_-, \gamma) \det(\gamma_{++}, \gamma_+)}{\det(\gamma, \gamma_{++}) \det(\gamma_+, \gamma_-)} \\ \frac{1}{1 - s} &= \text{cr}(\gamma_-, \gamma, \tilde{\gamma}, \gamma_+) = \frac{\det(\gamma_-, \gamma) \det(\tilde{\gamma}, \gamma_+)}{\det(\gamma, \tilde{\gamma}) \det(\gamma_+, \gamma_-)} \\ \frac{s_+}{s_+ - 1} &= \text{cr}(\gamma, \tilde{\gamma}_+, \gamma_+, \gamma_{++}) = \frac{\det(\gamma, \tilde{\gamma}_+) \det(\gamma_+, \gamma_{++})}{\det(\tilde{\gamma}_+, \gamma_+) \det(\gamma_{++}, \gamma)}. \end{aligned}$$

Multiplying the first two and the second two equations proves the second statement. If we set $\tilde{s} = \text{cr}(\tilde{\gamma}_-, \gamma, \tilde{\gamma}_+, \tilde{\gamma})$ we see that $\frac{s}{\tilde{s}} = 1$ and therefore

$$(i - \mu)\tilde{q} = \frac{\tilde{s}_+}{(1 - \tilde{s})(\tilde{s}_+ - 1)} = \frac{\frac{1}{s_+}}{(1 - \frac{1}{s})(\frac{1}{s_+} - 1)} = \frac{s}{(1 - s)(s_+ - 1)}$$



which proves the first statement. \square

If c is a periodic curve with period N , we can ask for \tilde{c} to be periodic too. Since the map sending c_0 to c_N is a Möbius transformation it has at least one but in general two fix-points. These special choices of initial points give two Bäcklund transforms that can be viewed as past and future in a discrete time evolution.

We will now show, that this Bäcklund transformation can serve as a discretization of the tangential flow since the evolution on the q 's are a discrete version of the Volterra model.

The discretization of the Volterra model first appeared in Tsujimoto, e. al. 1993. We will refer to the version stated in [Sur99]. There it is given in the form

$$\tilde{\alpha} = \alpha \frac{\beta_+}{\beta} \quad (1.36)$$

$$\beta - h\alpha = \frac{\beta_-}{\beta_- - h\alpha_-} \quad (1.37)$$

with h being the discretization constant.

Theorem 13 *Let \tilde{q} be a Bäcklund transform of q with parameter μ . The map sending q to \tilde{q}_+ is the discrete time Volterra model (1.36) with $\alpha = q$, $\tilde{\alpha} = \tilde{q}_+$, $\frac{\beta}{h} = \frac{q}{s_+}$ and $h = \mu - 1$.*

Proof With the settings from the theorem we have

$$\tilde{\alpha} = \tilde{q}_+ = q_+ \frac{s_+}{s_{++}} = q \frac{q_+ s_+}{s_{++} q} = \alpha \frac{\beta_+}{\beta}$$

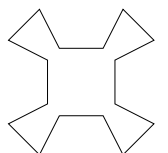
and on the other hand

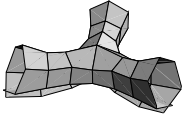
$$\beta - hq = (\mu - 1)q \left(\frac{1}{s_+} - 1 \right) = \frac{1}{1 - s}$$

and

$$\frac{\beta_-}{\beta_- - hq_-} = \frac{\frac{hq_-}{s}}{hq_- \left(\frac{1}{s} - 1 \right)} = \frac{1}{1 - s}.$$

This proves the theorem. \square





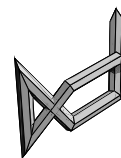
The continued Bäcklund transformations give rise to maps $\gamma : \mathbb{Z}^2 \rightarrow \mathbb{CP}^1$ that can be viewed as discrete conformal maps—especially in the case when μ is real negative (which is quite far from the tangential flow, that is approximated with $\mu \approx 1$) [BP96a, BP99, HJMP98].

On the other hand in case of real μ the transformation is not restricted to the plane: Four points with real cross-ratio always lie on a circle. Thus the map that sends $\tilde{\gamma}$ to $\tilde{\gamma}_+$ is well defined in any dimension. Maps from \mathbb{Z}^2 to \mathbb{R}^3 with cross-ratio -1 for all elementary quadrilaterals² serve as discretization of isothermic surfaces and have been investigated in [BP96a]. A method to construct discrete cmc surfaces (which are in particular isothermic) from discrete conformal maps is presented in Chapter 6.

If one does not restrict oneself to planar evolution the set of closed Bäcklund transforms of a closed curve can be a whole circle: In Chapter 5 the case of a regular n -gon gives rise to discrete rotational isothermic surfaces.

In the next chapter we will modify the discrete time evolution for discrete (euclidian) space curves to get a discrete Hashimoto flow.

²More general one can demand $\text{cr} = \frac{\alpha_n}{\beta_m}$ —see Chapter 4.



Chapter 2

Discrete Hashimoto surfaces and a doubly discrete smoke ring flow

2.1 Introduction

Many of the surfaces that can be described by integrable equations have been discretized. Among them are surfaces of constant negative Gaussian curvature, surfaces of constant mean curvature, minimal surfaces, and affine spheres. This chapter continues the program by adding Hashimoto surfaces to the list. These surfaces are obtained by evolving a regular space curve γ by the Hashimoto or *smoke ring flow*

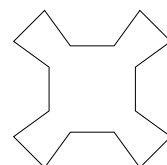
$$\dot{\gamma} = \gamma' \times \gamma''.$$

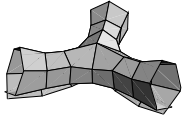
As shown by Hashimoto [Has77] this evolution is directly linked to the famous nonlinear Schrödinger equation (NLSE)

$$i\dot{\Psi} + \Psi'' + \frac{1}{2}|\Psi|^2\Psi = 0.$$

In [AL76] and [AL77] Ablowitz and Ladik gave a differential-difference and a difference-difference discretization of the NLSE. In Chapter 3 we will show¹ that they correspond to a Hashimoto flow on discrete curves (i. e. polygons) [BS99, DS99] and a doubly discrete Hashimoto flow respectively. This discrete evolution is derived in section 2.3.2 from a discretization of the Bäcklund transformations for regular space curves and Hashimoto surfaces.

¹The equivalence for the differential-difference case appeared first in [Ish82].





In Section 2.2 a short review of the smooth Hashimoto flow and its connection to the isotropic Heisenberg magnet model and the nonlinear Schrödinger equation is given. It is shown that the solutions to the auxiliary problems of these integrable equations serve as frames for the Hashimoto surfaces and a Sym formula is derived. In section 2.2.2 the dressing procedure or Bäcklund transformation is discussed and applied on the vacuum. A geometric interpretation of this transformation as a generalization of the Traktrix construction for a curve is given.

In Section 2.3 the same program is carried out for the Hashimoto flow on discrete curves. Then in Section 2.4 special double Bäcklund transformations (for discrete curves) are singled out to get a unique evolution which serves as our doubly discrete Hashimoto flow.

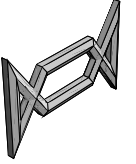
Elastic curves (curves that evolve by rigid motion under the Hashimoto flow) are discussed in all these cases. It turns out that discrete elastic curves for the discrete and the doubly discrete Hashimoto flow coincide.

Through this chapter we use a quaternionic description. Quaternions are the algebra generated by $1, \mathbf{i}, \mathbf{j}$, and \mathbf{k} with the relations $\mathbf{i}^2 = \mathbf{j}^2 = \mathbf{k}^2 = -1$, $\mathbf{ij} = \mathbf{k}, \mathbf{jk} = \mathbf{i}$, and $\mathbf{ki} = \mathbf{j}$. Real and imaginary part of a quaternion are defined in an obvious manner: If $q = \alpha + \beta\mathbf{i} + \gamma\mathbf{j} + \delta\mathbf{k}$ we set $\text{Re}(q) = \alpha$ and $\text{Im}(q) = \beta\mathbf{i} + \gamma\mathbf{j} + \delta\mathbf{k}$. Note that unlike in the complex case the imaginary part is not a real number. We identify the 3-dimensional euclidian space with the imaginary quaternions i. e. the span of \mathbf{i}, \mathbf{j} , and \mathbf{k} . Then for two imaginary quaternions q, r the following formula holds:

$$qr = -\langle q, r \rangle + q \times r$$

with $\langle \cdot, \cdot \rangle$ and $\cdot \times \cdot$ denoting the usual scalar and cross products of vectors in 3-space. A rotation of an imaginary quaternion around the axis $r, |r| = 1$ with angle ϕ can be written as conjugation with the unit length quaternion $(\cos \frac{\phi}{2} + \sin \frac{\phi}{2} r)$.

Especially when dealing with the Lax representations of the various equations it will be convenient to identify the quaternions with



complex 2 by 2 matrices:

$$\mathbf{i} = i\sigma_3 = \begin{pmatrix} i & 0 \\ 0 & -i \end{pmatrix} \quad \mathbf{j} = i\sigma_1 = \begin{pmatrix} 0 & i \\ i & 0 \end{pmatrix}$$

$$\mathbf{k} = -i\sigma_2 = \begin{pmatrix} 0 & -1 \\ 1 & 0 \end{pmatrix}.$$

2.2 The Hashimoto flow, the Heisenberg flow and the nonlinear Schrödinger equation

Let $\gamma : \mathbb{R} \rightarrow \mathbb{R}^3 = \text{Im } \mathbb{H}$ be an arclength parametrized regular curve and $\mathcal{F} : \mathbb{R} \rightarrow \mathbb{H}^*$ be a parallel frame for it, i. e.

$$\mathcal{F}^{-1}\mathbf{i}\mathcal{F} = \gamma' = \gamma_x \quad (2.1)$$

$$(\mathcal{F}^{-1}\mathbf{j}\mathcal{F})' \parallel \gamma'. \quad (2.2)$$

The second equation says that $\mathcal{F}^{-1}\mathbf{j}\mathcal{F}$ is a parallel section in the normal bundle of γ . which justifies the name. Moreover let $A = \mathcal{F}'\mathcal{F}^{-1}$ be the logarithmic derivative of \mathcal{F} . Equation (2.2) gives, that A must lie in the \mathbf{j} - \mathbf{k} -plane and thus can be written as

$$A = -\frac{\Psi}{2}\mathbf{k} \quad (2.3)$$

with $\Psi \in \text{span}(1, \mathbf{i}) \cong \mathbb{C}$.

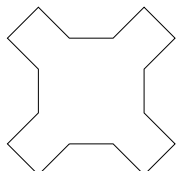
Definition 2 We call Ψ the complex curvature of γ .

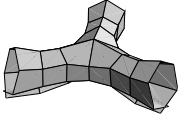
Now let us evolve γ with the following flow:

$$\dot{\gamma} = \gamma' \times \gamma'' = \gamma'\gamma''. \quad (2.4)$$

Here $\dot{\gamma}$ denotes the derivative in time. This is an evolution in binormal direction with velocity equal to the (real) curvature. It is known as the *Hashimoto* or *smoke ring flow*. Hashimoto was the first to show, that under this flow the complex curvature Ψ of γ solves the nonlinear Schrödinger equation (NLSE) [Has77]

$$i\dot{\Psi} + \Psi'' + \frac{1}{2}|\Psi|^2\Psi = 0. \quad (2.5)$$





or written for A :

$$i\dot{A} + A'' = 2A^3. \quad (2.6)$$

Definition 3 *The surfaces $\gamma(x, t)$ wiped out by the flow given in equation (2.4) are called Hashimoto surfaces.*

Equation (2.5) arises as the zero curvature condition $\widehat{L}_t - \widehat{M}_x + [\widehat{L}, \widehat{M}] = 0$ of the system

$$\begin{aligned} \widehat{\mathcal{F}}_x(\mu) &= \widehat{L}(\mu)\widehat{\mathcal{F}}(\mu) \\ \widehat{\mathcal{F}}_t(\mu) &= \widehat{M}(\mu)\widehat{\mathcal{F}}(\mu) \end{aligned} \quad (2.7)$$

with

$$\begin{aligned} \widehat{L}(\mu) &= \mu\mathbf{i} - \frac{\Psi}{2}\mathbf{k} \\ \widehat{M}(\mu) &= \frac{|\Psi|^2}{4}\mathbf{i} + \frac{\Psi_x}{2}\mathbf{j} - 2\mu\widehat{L}(\mu). \end{aligned} \quad (2.8)$$

To make the connection to the description with the parallel frame \mathcal{F} we add torsion to the curve γ by setting

$$A(\mu) = e^{-2\mu x i}\Psi\mathbf{k}.$$

This gives rise to a family of curves $\gamma(\mu)$ the so-called *associated family* of γ . Now one can gauge the corresponding parallel frame $\mathcal{F}(\mu)$ with $e^{\mu x i}$ and get

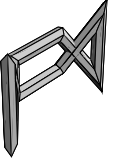
$$(e^{\mu x i}\mathcal{F}(\mu))_x = ((e^{\mu x i})_x e^{-\mu x i} + e^{\mu x i}A(\mu)e^{-\mu x i})e^{\mu x i}\mathcal{F}(\mu) = L(\mu)e^{\mu x i}\mathcal{F}(\mu)$$

with $L(\mu)$ as in (2.7). So above $\widehat{\mathcal{F}}(\mu) = e^{\mu x i}\mathcal{F}(\mu)$ is for each t_0 a frame for the curve $\gamma(x, t_0)$.

Theorem 14 (Sym formula) *Let $\Psi(x, t)$ be a solution of the NLSE (equation (2.5)). Then up to an euclidian motion the corresponding Hashimoto surface $\gamma(x, t)$ can be obtained by*

$$\gamma(x, t) = \widehat{\mathcal{F}}^{-1}\widehat{\mathcal{F}}_\lambda|_{\lambda=0} \quad (2.9)$$

where $\widehat{\mathcal{F}}$ is a solution to (2.7).



Proof Obviously $\widehat{\mathcal{F}}|_{\lambda=0}(x, t_0)$ is a parallel frame for each $\gamma(x, t_0)$. So writing $\widehat{\mathcal{F}}(x, t_0)|_{\lambda=0} =: \mathcal{F}(x)$, one easily computes $(\widehat{\mathcal{F}}^{-1}\widehat{\mathcal{F}}_\lambda|_{\lambda=0})_x = \mathcal{F}^{-1}\mathbf{i}\mathcal{F} = \gamma_x$ and $(\widehat{\mathcal{F}}^{-1}\widehat{\mathcal{F}}_\lambda|_{\lambda=0})_y = \mathcal{F}^{-1}\Psi\mathbf{k}\mathcal{F}$. But $\gamma_t = \gamma_x\gamma_{xx} = \mathcal{F}^{-1}\Psi\mathbf{k}\mathcal{F}$. \square

If one differentiates equation (2.4) with respect to x one gets the so-called isotropic Heisenberg magnet model (IHM):

$$\dot{S} = S \times S'' = S \times S_{xx} \quad (2.10)$$

with $S = \gamma'$. This equation arises as zero curvature condition $U_t - V_x + [U, V] = 0$ with matrices

$$\begin{aligned} U(\lambda) &= \lambda S \\ V(\lambda) &= -2\lambda^2 S - \lambda S' S \end{aligned} \quad (2.11)$$

In fact if G is a solution to

$$\begin{aligned} G_x &= U(\lambda)G \\ G_t &= V(\lambda)G \end{aligned} \quad (2.12)$$

it can be viewed as a frame for the Hashimoto surface too and one has a similar Sym formula:

$$\gamma(x, t) = G^{-1}G_\lambda|_{\lambda=0} \quad (2.13)$$

The system (2.12) is known to be gauge equivalent to (2.7) [FT86].

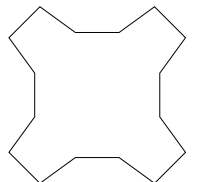
2.2.1 Elastic curves

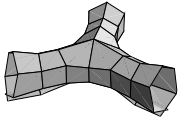
The stationary solutions of the NLSE (i. e. the curves that evolve by rigid motion under the Hashimoto flow) are known to be the *elastic curves* [BS99]. They are the critical points of the functional

$$E(\gamma) = \int \kappa^2$$

with $\kappa = |\Psi|$ the curvature of γ . The fact that they evolve by rigid motion under the Hashimoto flow can be used to give a characterization by their complex curvature Ψ only: When the curve evolves by rigid motion Ψ may get a phase factor only. Thus $\dot{\Psi} = ci\Psi$. Inserted into equation (2.5) this gives

$$\Psi'' = (c - \frac{1}{2}|\Psi|^2)\Psi. \quad (2.14)$$





2.2.2 Bäcklund transformations for smooth space curves and Hashimoto surfaces

Now we want to describe the dressing procedure or Bäcklund transformation for the IHM model and the Hashimoto surfaces. This is a method to generate new solutions of our equations from a given one in a purely algebraic way. Afterwards we give some geometric interpretation for this transformation.

Algebraic description of the Bäcklund transformation

Theorem 15 *Let G be a solution to equations (2.12) with U and V as in (2.11) (i. e. $U(1)$ solves the IHM model). Choose $\lambda_0, s_0 \in \mathbb{C}$. Then $\tilde{G}(\lambda) := B(\lambda)G(\lambda)$ with $B(\lambda) = (\mathbb{I} + \lambda\rho)$, $\rho \in \mathbb{H}$ defined by the conditions that $\lambda_0, \bar{\lambda}_0$ are the zeroes of $\det(B(\lambda))$ and*

$$\tilde{G}(\lambda_0) \begin{pmatrix} s_0 \\ 1 \end{pmatrix} = 0 \quad \text{and} \quad \tilde{G}(\bar{\lambda}_0) \begin{pmatrix} 1 \\ -\bar{s}_0 \end{pmatrix} = 0 \quad (2.15)$$

solves a system of the same type. In particular $\tilde{U}(1) = \tilde{G}_x(1)\tilde{G}^{-1}(1)$ solves again the Heisenberg magnet model (2.10).

Proof We define $\tilde{U}(\lambda) = \tilde{G}_x \tilde{G}^{-1}$ and $\tilde{V}(\lambda) = \tilde{G}_t \tilde{G}^{-1}$. Equation (2.15) ensures that $\tilde{U}(\lambda)$ and $\tilde{V}(\lambda)$ are smooth at λ_0 and $\bar{\lambda}_0$. Using $\tilde{U}(\lambda) = B_x(\lambda)B^{-1}(\lambda) + B(\lambda)\tilde{U}(\lambda)B^{-1}(\lambda)$ this in turn implies that $\tilde{U}(\lambda)$ has the form $\tilde{U}(\lambda) = \lambda\tilde{S}$ for some \tilde{S} .

Since the zeroes of $\det(B(\lambda))$ are fixed we know that $r := \text{Re}(\rho)$ and $l := |\text{Im}(\rho)|$ are constant. We write $\rho = r + v$.

One gets $\tilde{S} = S + v_x$ and

$$v_x = \frac{2rl}{r^2 + l^2} \frac{v \times S}{l} + \frac{2l^2}{r^2 + l^2} \frac{\langle v, S \rangle}{l^2} v - \frac{2l^2}{r^2 + l^2} S. \quad (2.16)$$

This can be used to show $|\tilde{S}| = 1$.

Again equation (2.15) ensures that $\tilde{V}(\lambda) = \lambda^2 X + \lambda Y$ for some X and Y . But then the integrability condition $\tilde{U}_t - \tilde{V}_x + [\tilde{U}, \tilde{V}]$ gives up to a factor c and possible constant real parts x and y that X and Y are fixed to be $X = x + c\tilde{S}_x\tilde{S} + d\tilde{S}$ and $Y = y + 2c\tilde{S}$.

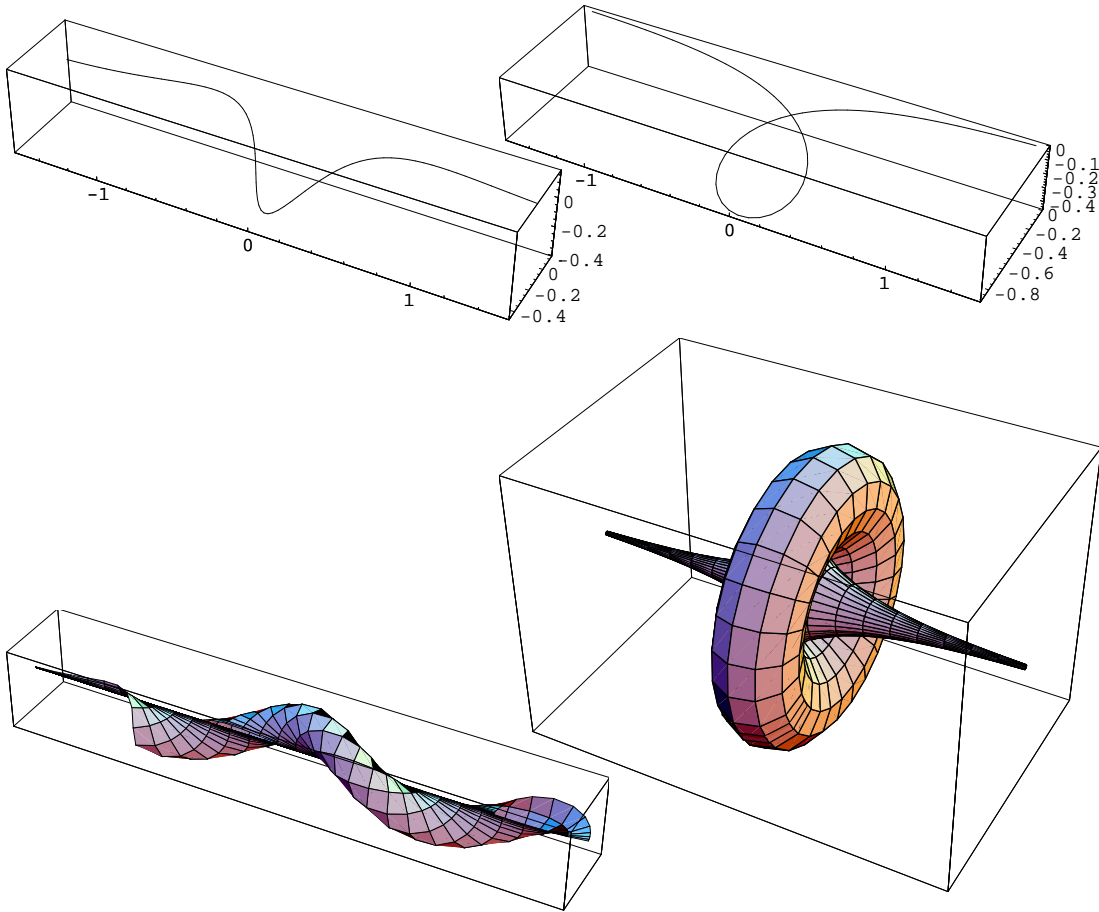
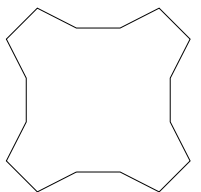
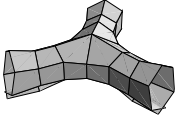


Figure 2.1: Two dressed straight lines and the corresponding Hashimoto surfaces

The additional term $d\tilde{S}$ in X corresponds to the (trivial) tangential flow which always can be added. The form $\tilde{V}(\lambda) = B_t(\lambda)B^{-1}(\lambda) + B(\lambda)V(\lambda)B^{-1}(\lambda)$ gives $c = -1$ and $d = 0$. Thus one ends up with $\tilde{V}(\lambda) = -2\lambda^2\tilde{S} - \lambda\tilde{S}_x\tilde{S}$. \square

So we get a four parameter family (λ_0 and s_0 give two real parameters each) of transformations for our curve γ that are compatible with the Hashimoto flow. They correspond to the four parameter family of Bäcklund transformations of the NLSE.





Example Let us do this procedure in the easiest case: We choose $S \equiv \mathbf{i}$ (or $\gamma(x, t) = x\mathbf{i}$) which gives

$$G(\lambda) = \exp((\lambda x - 2\lambda^2 t)\mathbf{i}) = \begin{pmatrix} e^{i(\lambda x - 2\lambda^2 t)} & 0 \\ 0 & e^{-i(\lambda x - 2\lambda^2 t)} \end{pmatrix}.$$

After choosing λ_0 and s_0 and writing $\rho = \begin{pmatrix} a & b \\ -\bar{b} & \bar{a} \end{pmatrix}$ one gets with equation (2.15)

$$\begin{aligned} -e^{i(\lambda_0 x - 2\lambda_0^2 t)} &= \lambda_0(e^{i(\lambda_0 x - 2\lambda_0^2 t)}a + s_0 e^{-i(\lambda_0 x - 2\lambda_0^2 t)}b) \\ s_0 e^{-i(\lambda_0 x - 2\lambda_0^2 t)} &= \lambda_0(e^{i(\lambda_0 x - 2\lambda_0^2 t)}\bar{b} - s_0 e^{-i(\lambda_0 x - 2\lambda_0^2 t)}\bar{a}). \end{aligned} \quad (2.17)$$

These equations can be solved for a and b :

$$\begin{aligned} a &= -\frac{\frac{1}{\lambda_0} + \frac{s_0 \bar{s}_0}{\lambda_0} e^{-2i(\lambda_0 - \bar{\lambda}_0)x + 4i(\lambda_0^2 - \bar{\lambda}_0^2)t}}{1 + s_0 \bar{s}_0 e^{-2i(\lambda_0 - \bar{\lambda}_0)x + 4i(\lambda_0^2 - \bar{\lambda}_0^2)t}} \\ b &= \bar{s}_0 e^{2i\bar{\lambda}_0 x - 4i\bar{\lambda}_0^2 t} \frac{\frac{1}{\lambda_0} - \frac{1}{\bar{\lambda}_0}}{1 + s_0 \bar{s}_0 e^{-2i(\lambda_0 - \bar{\lambda}_0)x + 4i(\lambda_0^2 - \bar{\lambda}_0^2)t}} \end{aligned} \quad (2.18)$$

Using the Sym formula (2.13) one can immediately write the formula for the resulting Hashimoto surface $\tilde{\gamma}$:

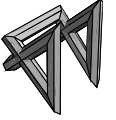
$$\tilde{\gamma} = \text{Im}(\rho) + \gamma = \begin{pmatrix} \text{Im}(a) + ix & b \\ -\bar{b} & -\text{Im}(a) - ix \end{pmatrix}.$$

The need for taking the imaginary part is due to the fact that we did not normalize $B(\lambda)$ to $\det(B(\lambda)) = 1$.

If one wants to have the result in a plane $\arg b$ should be constant. This can be achieved by choosing $\lambda \in i\mathbb{R}$. Figure 2.1 shows the result for $s_0 = 0.5 + i$ and $\lambda_0 = 1 - i$ and $\lambda_0 = -i$ respectively.

Of course one can iterate the dressing procedure to get new curves (or surfaces) and it is a natural question how many one can get. This leads immediately to the Bianchi permutability theorem

Theorem 16 (Bianchi permutability) *Let $\tilde{\gamma}$ and $\hat{\gamma}$ be two Bäcklund transforms of γ . Then there is a unique Hashimoto surface $\hat{\tilde{\gamma}}$ that is Bäcklund transform of $\tilde{\gamma}$ and $\hat{\gamma}$.*



Proof Let G, \widehat{G} , and \widetilde{G} be the solutions to (2.12) corresponding to $\gamma, \widehat{\gamma}$, and $\widetilde{\gamma}$. One has $\widehat{G} = \widehat{B}G$ and $\widetilde{G} = \widetilde{B}G$ with $\widehat{B} = \mathbb{I} + \lambda\widehat{\rho}$ and $\widetilde{B} = \mathbb{I} + \lambda\widetilde{\rho}$. The ansatz $\widetilde{B}\widehat{G} = \widehat{B}\widetilde{G}$ leads to the compatibility condition $\widetilde{B}\widehat{B} = \widehat{B}\widetilde{B}$ or

$$(\mathbb{I} + \lambda\widetilde{\rho})(\mathbb{I} + \lambda\widehat{\rho}) = (\mathbb{I} + \lambda\widehat{\rho})(\mathbb{I} + \lambda\widetilde{\rho}) \quad (2.19)$$

which gives:

$$\begin{aligned} \widetilde{\rho} &= (\widehat{\rho} - \widetilde{\rho}) \widetilde{\rho} (\widehat{\rho} - \widetilde{\rho})^{-1} \\ \widehat{\rho} &= (\widehat{\rho} - \widetilde{\rho}) \widehat{\rho} (\widehat{\rho} - \widetilde{\rho})^{-1}. \end{aligned} \quad (2.20)$$

Thus \widetilde{B} and \widehat{B} are completely determined. To show that they give dressed solutions we note that since $\det \widetilde{B} \det \widehat{B} = \det \widehat{B} \det \widetilde{B}$ the zeroes of $\det \widehat{B}$ are the same as the ones of $\det \widetilde{B}$ (and the ones of $\det \widetilde{B}$ coincide with those of $\det \widehat{B}$). Therefore they do not depend on x and t . Moreover at these points the kernel of $\widetilde{B}\widehat{G}$ coincides with the one of \widetilde{G} . Thus it does not depend on x or t either. Now theorem 15 gives the desired result. \square

Geometry of the Bäcklund transformation

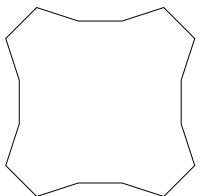
As before let $\gamma : I \rightarrow \mathbb{R}^3 = \text{Im } \mathbb{H}$ be an arclength parametrized regular curve. Moreover let $v : I \rightarrow \mathbb{R}^3 = \text{Im } \mathbb{H}$, $|v| = l$ be a solution to the following system:

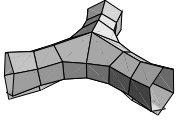
$$\begin{aligned} \widehat{\gamma} &= \gamma + \frac{1}{2}v \\ \widehat{\gamma}' &\parallel v. \end{aligned} \quad (2.21)$$

Then $\widehat{\gamma}$ is called a Traktrix of γ . The forthcoming definition in this section is motivated by the following observation: If we set $\widetilde{\gamma} = \gamma + v$ it is again an arclength parametrized curve and $\widehat{\gamma}$ is a Traktrix of $\widetilde{\gamma}$ too. One can generalize this in the following way:

Lemma 17 *Let $v : I \rightarrow \text{Im } \mathbb{H}$ be a vector field along γ of constant length l satisfying*

$$v' = 2\sqrt{b - b^2} \frac{v \times \gamma'}{l} + 2b \frac{\langle v, \gamma' \rangle}{l^2} v - 2b\gamma' \quad (2.22)$$





with $0 \leq b \leq 1$. Then $\tilde{\gamma} = \gamma + v$ is arclength parametrized.

Proof Obviously the above transformation coincides with the dressing described in the last section with $b = \frac{l^2}{r^2+l^2}$ in formula (2.16). This proves the lemma. \square

So $\text{Im}(\rho)$ from theorem 15 is nothing but the difference vector between the original curve and the Bäcklund transform. Note that in the case $b = 1$ one gets the above Traktrix construction, that is for $\hat{\gamma} = \gamma + v$ holds $\hat{\gamma}' \parallel v$. This motivates the following

Definition 4 The curve $\hat{\gamma} = \gamma + \frac{1}{2}v$ with v as in lemma 17 is called a twisted Traktrix of the curve γ and $\tilde{\gamma} = \gamma + v$ is called a Bäcklund transform of γ .

Moreover equation (2.22) gives that $v' \perp v$ and therefore $|v| \equiv \text{const}$. Since $v = \tilde{\gamma} - \gamma$ we see that the Bäcklund transform is in constant distance to the original curve.

2.3 The Hashimoto flow, the Heisenberg flow, and the nonlinear Schrödinger equation in the discrete case

In this section we give a short review on the discretization (in space) of the Hashimoto flow, the isotropic Heisenberg magnetic model, and the nonlinear Schrödinger equation. For more details on this topic see [FT86, BS99, DS99] and Chapter 3.

We call a map $\gamma : \mathbb{Z} \rightarrow \text{Im } \mathbb{H}$ a discrete regular curve if any two successive points do not coincide. It will be called arclength parametrized curve, if $|\gamma_{n+1} - \gamma_n| = 1$ for all $n \in \mathbb{Z}$. We will use the notation $S_n := \gamma_{n+1} - \gamma_n$. The binormals of the discrete curve can be defined as $\frac{S_n \times S_{n-1}}{|S_n \times S_{n-1}|}$.

There is a natural discrete analog of a parallel frame:

Definition 5 A discrete parallel frame is a map $\mathcal{F} : \mathbb{Z} \rightarrow \mathbb{H}^*$ with $|\mathcal{F}_k| = 1$ satisfying

$$S_n = \mathcal{F}_n^{-1} \mathbf{i} \mathcal{F}_n \quad (2.23)$$



$$\text{Im}((\mathcal{F}_{n+1}^{-1} \mathbf{j} \mathcal{F}_{n+1})(\mathcal{F}_n^{-1} \mathbf{j} \mathcal{F}_n)) \parallel \text{Im}(S_{n+1} S_n). \quad (2.24)$$

Again we set $\mathcal{F}_{n+1} = A_n \mathcal{F}_n$ and in complete analogy to the continuous case eqn (2.24) gives the following form for A :

$$A = \cos \frac{\phi_n}{2} - \sin \frac{\phi_n}{2} \exp \left(\mathbf{i} \sum_{k=0}^n \tau_k \right) \mathbf{k}$$

with $\phi_n = \angle(S_n, S_{n+1})$ the folding angles and τ_n the angles between successive binormals. If we drop the condition that \mathcal{F} should be of unit length we can renormalize A_n to be $1 - \tan \frac{\phi_n}{2} \exp(\mathbf{i} \sum_{k=0}^n \tau_k) \mathbf{k} =: 1 - \Psi_n \mathbf{k}$ with $\Psi_n \in \text{span}(1, \mathbf{i}) \cong \mathbb{C}$ and $|\Psi_n| = \kappa_n$ the discrete (real) curvature.

Definition 6 We call Ψ the complex curvature² of the discrete curve γ .

Discretizations of the Hashimoto flow (2.4) (i. e. a Hashimoto flow for a discrete arclength parametrized curve) and the isotropic Heisenberg model (eqn (2.10)) are well known [FT86] (see also [BS99] for a good discussion of the topic). In particular a discrete version of (2.4) is given by:

$$\dot{\gamma}_k = 2 \frac{S_k \times S_{k-1}}{1 + \langle S_k, S_{k-1} \rangle} \quad (2.25)$$

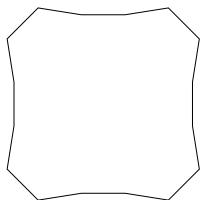
which implies for a discretization of (2.10)

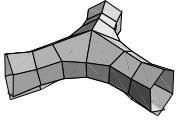
$$\dot{S}_k = 2 \frac{S_{k+1} \times S_k}{1 + \langle S_{k+1}, S_k \rangle} - 2 \frac{S_k \times S_{k-1}}{1 + \langle S_k, S_{k-1} \rangle} \quad (2.26)$$

Let us state the zero curvature representation for this equation too: Equation (2.26) is the compatibility condition of $\dot{U}_k = V_{k+1} U_k - U_k V_k$ with

$$\begin{aligned} U_k &= \mathbb{I} + \lambda S_k \\ V_k &= -\frac{1}{1+\lambda^2} \left(2\lambda^2 \frac{S_k + S_{k-1}}{1 + \langle S_k, S_{k-1} \rangle} + 2\lambda \frac{S_k \times S_{k-1}}{1 + \langle S_k, S_{k-1} \rangle} \right) \end{aligned} \quad (2.27)$$

²It would be more reasonable to define $A = 1 - \frac{\Psi_n}{2} \mathbf{k}$. which implies $\kappa_n = 2 \tan \frac{\phi_n}{2}$ but notational simplicity makes the given definition more convenient.





The solution to the auxiliary problem

$$\begin{aligned} G_{k+1} &= U_k(\lambda)G_k \\ \dot{G}_k &= V_k(\lambda)G_k \end{aligned} \quad (2.28)$$

can be viewed as the frame to a discrete Hashimoto surface $\gamma_k(t)$ and one has the same Sym formula as in the continuous case:

Theorem 18 *Given a solution G to the system (2.28) the corresponding discrete Hashimoto surface can be obtained up to an euclidian motion by*

$$\gamma_k(t) = (G_k^{-1} \frac{\partial}{\partial \lambda} G_k)|_{\lambda=0}. \quad (2.29)$$

Proof One has $G_k^{-1} \frac{\partial}{\partial \lambda} G_k|_{\lambda=0} = \sum_{i=0}^{k-1} S_i = \gamma_k$ for fixed time t_0 and

$$(G_k^{-1} \frac{\partial}{\partial \lambda} G_k|_{\lambda=0})_t = (\frac{\partial}{\partial \lambda} V_k(\lambda)|_{\lambda=0}) = 2 \frac{S_k \times S_{k-1}}{1 + \langle S_k, S_{k-1} \rangle}.$$

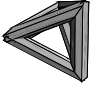
□

To complete the analogy to the smooth case we give a discretization of the NLSE that can be found in [AL76] (see also [FT86, Sur97]):

$$-i\dot{\Psi}_k = \Psi_{k+1} - 2\Psi_k + \Psi_{k-1} + |\Psi_k|^2(\Psi_{k+1} + \Psi_{k-1}). \quad (2.30)$$

Theorem 19 *Let γ be a discrete arclength parametrized curve. If γ evolves with the discrete Hashimoto flow (2.25) then its complex curvature Ψ evolves with the discrete nonlinear Schrödinger equation (2.30)*

A proof of this theorem can be found in [Ish82] and Chapter 3. There is another famous discretization of the NLSE in literature that is related to the dIHM [IK81, FT86]. Again in Chapter 3 it is shown that it is in fact gauge equivalent to the above cited which turns out to be more natural from a geometric point of view.



2.3.1 Discrete elastic curves

As mentioned in Section 2.2.1 the stationary solutions of the NLSE (i. e. the curves that evolve by rigid motion under the Hashimoto flow) are known to be the *elastic curves*. They have a natural discretization using this property:

Definition 7 *A discrete elastic curve is a curve γ for which the evolution of γ_n under the Hashimoto flow (2.25) is a rigid motion which means that its tangents evolve under the discrete isotropic Heisenberg model (2.26) by rigid rotation.*

In [BS99] Bobenko and Suris showed the equivalence of this definition to a variational description.

The fact that (2.26) has to be a rigid rotation means that the left hand side must be $S_n \times p$ with a unit imaginary quaternion p . We will now give a description of elastic curves by their complex curvature function only:

Theorem 20 *The complex curvature Ψ_n of a discrete elastic curve γ_n satisfies the following difference equation:*

$$\mathcal{C} \frac{\Psi_n}{1 + |\Psi_n|^2} = \Psi_{n+1} + \Psi_{n-1} \quad (2.31)$$

for some real constant \mathcal{C} .

Equation (2.31) is a special case of a discrete-time Garnier system (see [Sur94]).

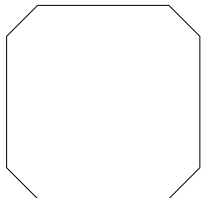
Proof One can proof the theorem by direct calculations or using the equivalence of the dIHM model and the dNLSE stated in theorem 19. If the curve γ evolves by rigid motion its complex curvature may vary by a phase factor only: $\Psi(x, t) = e^{i\lambda(t)}\Psi(x, t_0)$ or $\dot{\Psi} = i\dot{\lambda}\Psi$. Plugging this in eqn (2.30) gives

$$-\dot{\lambda}\Psi_k = \Psi_{k+1} - 2\Psi_k + \Psi_{k-1} + |\Psi_k|^2(\Psi_{k+1} + \Psi_{k-1})$$

which is equivalent to (2.31) with $\mathcal{C} = 2 - \dot{\lambda}$.

□

As an example Fig 2.2 shows two discretizations of the elastic figure eight.



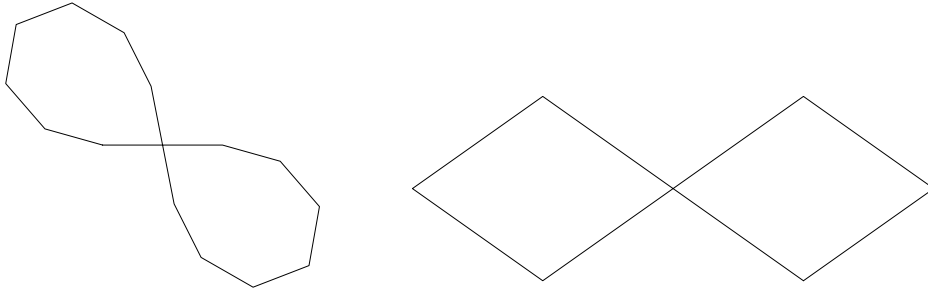
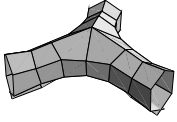


Figure 2.2: Two discretizations of the elastic figure eight.

2.3.2 Bäcklund transformations for discrete space curves and Hashimoto surfaces

Algebraic description

In complete analogy to Section 2.2.2 we state

Theorem 21 *Let G_k be a solution to equations (2.28) with U_k and V_k as in (2.27) (i. e. $U(1) - \mathbb{I}$ solves the dIHM model). Choose $\lambda_0, s_0 \in \mathbb{C}$. Then $\tilde{G}_k(\lambda) := B_k(\lambda)G_k(\lambda)$ with $B_k(\lambda) = (\mathbb{I} + \lambda\rho_k)$, $\rho_k \in \mathbb{H}$ defined by the conditions that $\lambda_0, \bar{\lambda}_0$ are the zeroes of $\det(B_k(\lambda))$ and*

$$\tilde{G}_k(\lambda_0) \begin{pmatrix} s_0 \\ 1 \end{pmatrix} = 0 \quad \text{and} \quad \tilde{G}_k(\bar{\lambda}_0) \begin{pmatrix} 1 \\ -\bar{s}_0 \end{pmatrix} = 0 \quad (2.32)$$

solves a system of the same type. In particular

$$\tilde{U}_k(1) - \mathbb{I} = \tilde{G}_x(1)\tilde{G}^{-1}(1) - \mathbb{I}$$

solves again the discrete Heisenberg magnet model (2.26).

Proof Analogous to the smooth case. □

Example Let us dress the (this time discrete) straight line again: We set $S_n \equiv \mathbf{i}$ and get

$$\begin{aligned} G_n(\lambda) &= (\mathbb{I} + \lambda\mathbf{i})^n \exp\left(-2\frac{\lambda^2}{1+\lambda^2}t\mathbf{i}\right) \\ &= \begin{pmatrix} (1+i\lambda)^n e^{-2i\frac{\lambda^2}{1+\lambda^2}t} & 0 \\ 0 & (1-i\lambda)^n e^{2i\frac{\lambda^2}{1+\lambda^2}t} \end{pmatrix}. \end{aligned}$$



After choosing λ_0 and s_0 and writing again $\rho = \begin{pmatrix} a & b \\ -\bar{b} & \bar{a} \end{pmatrix}$ we get with the shorthands $p = (1 + i\lambda)^n e^{-2i\frac{\lambda^2}{1+\lambda^2}t}$ and $q = (1 - i\lambda)^n e^{2i\frac{\lambda^2}{1+\lambda^2}t}$

$$\begin{aligned} p &= -\lambda_0(pa + s_0qb) \\ q &= \lambda_0(p\bar{b} - s_0q\bar{a}) \end{aligned}$$

which can be solved for a and b :

$$\begin{aligned} a &= -\frac{\frac{1}{\lambda_0} \frac{\bar{p}}{q} + \frac{s_0 \bar{s}_0}{\lambda_0} \frac{q}{p}}{\frac{\bar{p}}{q} + s_0 \bar{s}_0 \frac{q}{p}} \\ b &= \bar{s}_0 \frac{\frac{1}{\lambda_0} - \frac{1}{\lambda_0}}{\frac{\bar{p}}{q} + s_0 \bar{s}_0 \frac{q}{p}}. \end{aligned} \tag{2.33}$$

Again we can write the formula for the curve $\tilde{\gamma}$:

$$\tilde{\gamma}_n = \text{Im}(\rho_n) + \gamma_n = \begin{pmatrix} \text{Im}(a_n) + in & b_n \\ -\bar{b}_n & -\text{Im}(a_n) - in \end{pmatrix}.$$

Figure 2.3 shows two solutions with $s_0 = 0.5 + i$ and $\lambda_0 = 0.4 - 0.4i$ and $\lambda_0 = -0.4i$ respectively. The second one is again planar. Note the strong similarity to the smooth examples in Figure 2.1.

Of course one has again a permutability theorem:

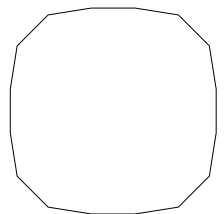
Theorem 22 (Bianchi permutability) *Let $\tilde{\gamma}$ and $\hat{\gamma}$ be two Bäcklund transforms of γ . Then there is a unique discrete Hashimoto surface $\hat{\tilde{\gamma}}$ that is Bäcklund transform of $\tilde{\gamma}$ and $\hat{\gamma}$.*

Proof Literally the same as for theorem 16. □

Geometry of the discrete Bäcklund transformation

In this section we want to derive the discrete Bäcklund transformations by mimicing the twisted Traktrix construction from Lemma 17:

Let $\gamma : \mathbb{Z} \rightarrow \text{Im } \mathbb{H}$ be an discrete arclength parametrized curve. To any initial vector v_n of length l there is a S^1 -family of vectors v_{n+1} of length l satisfying $|\gamma_n + v_n - (\gamma_{n+1} + v_{n+1})| = 1$. This is basically folding the parallelogram spanned by v_n and S_n along the



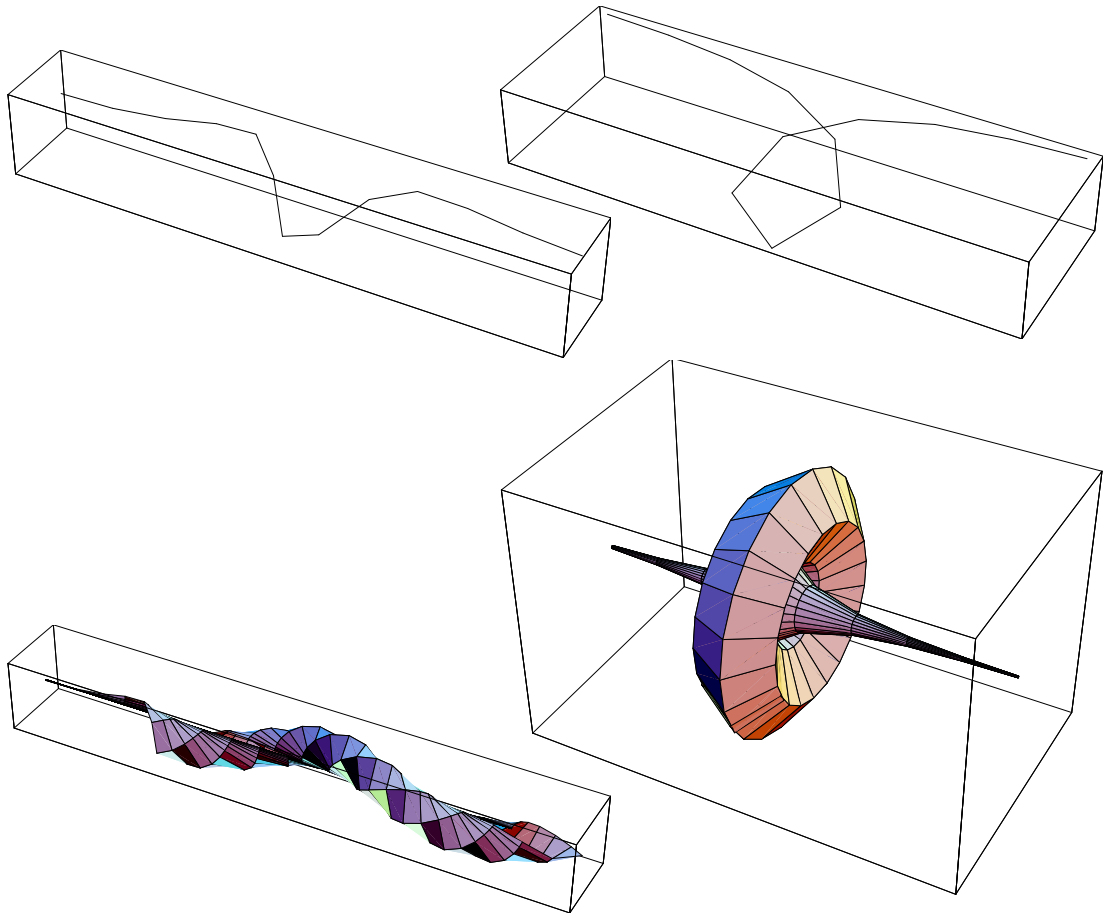
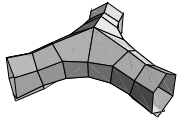


Figure 2.3: Two discrete dressed straight lines and the corresponding Hashimoto surfaces

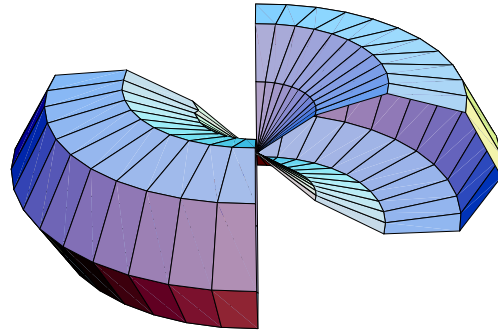


Figure 2.4: The Hashimoto surface from a discrete elastic eight.

diagonal $S_n - v_n$. To single out one of these new vectors let us fix the angle δ_1 between the planes spanned by v_n and S_n and v_{n+1} and S_n (see Fig. 2.5). This furnishes a unique evolution of an initial v_0 along γ . The polygon $\tilde{\gamma}_n = \gamma_n + v_n$ is again a discrete arclength parametrized curve which we will call a *Bäcklund transform* of γ .

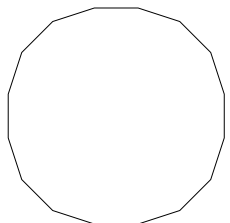
There are two cases in which the elementary quadrilaterals $(\gamma_n, \gamma_{n+1}, \tilde{\gamma}_{n+1}, \tilde{\gamma}_n)$ are planar. One is the parallelogram case. The other can be viewed as a discrete version of the Traktrix construction.

Definition 8 Let γ be a discrete arclength parametrized curve. Given δ_1 and v_0 , $|v_0| = l$ there is a unique discrete arclength parametrized curve $\tilde{\gamma}_n = \gamma_n + v_n$ with $|v_n| = l$ and $\angle(\text{span}(v_n, S_n), \text{span}(v_{n+1}, S_n)) = \delta_1$.

$\tilde{\gamma}$ is called a Bäcklund transform of γ and $\hat{\gamma} = \gamma + \frac{1}{2}v$ is called a discrete twisted Traktrix. for γ (and $\tilde{\gamma}$).

Remark Note that in case of $\delta = \pi$ the $\text{cr}(\gamma, \tilde{\gamma}, \tilde{\gamma}_+, \gamma_+) = l^2$. So this Bäcklund transformation is a special case of the ones from Chapter 1 then.

Of course we will show, that this notion of Bäcklund transformation coincides with the one from the last section. Let us investigate this Bäcklund transformation in greater detail. For now we do not restrict our selves to arclength parametrized curves. We state the following



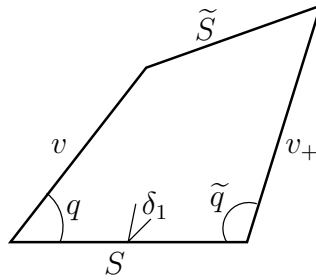
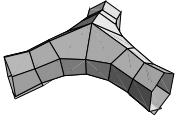


Figure 2.5: An elementary quadrilateral of the discrete Bäcklund transformation

Lemma 23 *The map M sending v_n to v_{n+1} in above Bäcklund transformation is a Möbius transformation.*

Proof Let us look at an elementary quadrilateral: For notational simplicity let us write $S = \gamma_{n+1} - \gamma_n$, $\tilde{S} = \tilde{\gamma}_{n+1} - \tilde{\gamma}_n$, $|S| = s$, $v = v_n$, and $v_+ = v_{n+1}$. If we denote the angles $\angle(S, v)$ and $\angle(v_+, S)$ with q and \tilde{q} , we get

$$e^{i\tilde{q}} = \frac{ke^{iq} - 1}{e^{iq} - k} \quad (2.34)$$

with $k = \tan \frac{\delta_1}{2} \tan \frac{\delta_2}{2}$ and δ_1 and δ_2 as in Fig. 2.5. Note that l , s , k , δ_1 , and δ_2 are coupled by

$$k = \tan \frac{\delta_1}{2} \tan \frac{\delta_2}{2} \quad \frac{l}{s} = \frac{\sin \delta_2}{\sin \delta_1}. \quad (2.35)$$

To get an equation for v_+ from this we need to have all vectors in one plane. So set $\sigma = \cos \frac{\delta_1}{2} + \sin \frac{\delta_1}{2} \frac{S}{s}$. Then conjugation with σ is a rotation around S with angle δ_1 . If we replace e^{iq} by $\frac{\sigma v \sigma^{-1}}{l} \left(\frac{S}{s}\right)^{-1}$ and $e^{i\tilde{q}}$ by $-\frac{S}{s} v_+^{-1} l$ equation (2.34) becomes quaternionic but stays valid (one can think of it as a complex equation with different “ i ”). Equation (2.34) now reads

$$\frac{v_+ S}{l s} = \frac{\frac{s}{l} \sigma v \sigma^{-1} S^{-1} - k}{\frac{k s}{l} \sigma v \sigma^{-1} S^{-1} - 1}.$$

We can write this in homogenous coordinates: \mathbb{H}^2 carries a natural right \mathbb{H} -modul structure, so one can identify a point in $\mathbb{H}\mathbb{P}^1$



with a quaternionic line in \mathbb{H}^2 by $p \cong (r, s) \iff p = rs^{-1}$. In this picture our equation gets

$$\begin{pmatrix} \frac{1}{ls}v_+S \\ 1 \end{pmatrix} \lambda = \begin{pmatrix} \frac{s}{l}\sigma & -kS\sigma \\ \frac{ks}{l}\sigma & -S\sigma \end{pmatrix} \begin{pmatrix} v \\ 1 \end{pmatrix}.$$

Bringing ls and S on the right hand side gives us finally the matrix

$$\mathcal{M} := \begin{pmatrix} \frac{1}{k}\sigma & -\frac{l}{s}S\sigma \\ \frac{1}{ls}S\sigma & \frac{1}{k}\sigma \end{pmatrix}. \tag{2.36}$$

Since we know that this map sends a sphere of radius l onto itself, we can project this sphere stereographically to get a complex matrix. The matrix

$$P = \begin{pmatrix} 2i & -2l \\ \frac{i}{l} & \mathfrak{k} \end{pmatrix}$$

projects lS^2 onto \mathbb{C} . Its inverse is given by

$$P^{-1} = -\frac{1}{4} \begin{pmatrix} i & 2lj \\ \frac{1}{l} & 2\mathfrak{k} \end{pmatrix}.$$

One easily computes

$$\mathcal{M}_{\mathbb{C}} = P\mathcal{M}P^{-1} = -\frac{1}{4} \begin{pmatrix} \nu + i \operatorname{Re}(Si) & 2l \operatorname{Im}(Si)j \\ -\frac{1}{2l} \operatorname{Im}(Si)j & \nu - i \operatorname{Re}(Si) \end{pmatrix} \tag{2.37}$$

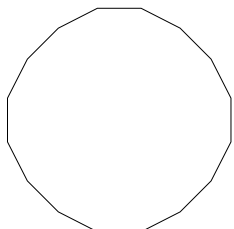
with $\nu = is \frac{\tan \frac{\delta_1}{2} i - \frac{1}{k}}{\frac{\tan \frac{\delta_1}{2}}{k} i - 1}$. This completes our proof. \square

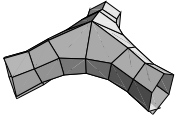
Remark

– Using equation (2.35) one can compute

$$\nu = s \tan \frac{\delta_1}{2} \frac{1 - k^2}{\tan^2 \frac{\delta_1}{2} + k^2} + il = l \tan \frac{\delta_2}{2} \frac{1 - k^2}{\tan^2 \frac{\delta_2}{2} + k^2} + il. \tag{2.38}$$

So the real part of ν is invariant under the change $s \leftrightarrow l$, $\delta_1 \leftrightarrow \delta_2$. Therefore instead of thinking of \tilde{S} as an transform of S with parameter ν one could view v_+ a transform of v with parameter $\nu + i(s - l)$.





- One can gauge $\mathcal{M}_{\mathbb{C}}$ to get rid of the off-diagonal $2l$ factors

$$M = \begin{pmatrix} \frac{1}{\sqrt{2l}} & 0 \\ 0 & \sqrt{2l} \end{pmatrix} \mathcal{M}_{\mathbb{C}} \begin{pmatrix} \sqrt{2l} & 0 \\ 0 & \frac{1}{\sqrt{2l}} \end{pmatrix}.$$

Then we can write in abuse of notation

$$M = \nu \mathbb{I} - S \quad (2.39)$$

Here $\nu \mathbb{I}$ is no quaternion if ν is complex. The eigenvalues of $\mathcal{M}_{\mathbb{C}}$ and M clearly coincide and M obviously coincides with the Lax matrix U_k of the dIHM model in equation (2.27) up to a factor $\frac{1}{\nu}$ with $\lambda = -\frac{1}{\nu}$.

As promised the next lemma shows that the geometric Bäcklund transformation discussed in this section coincides with the one from the algebraic description.

Lemma 24 *Let $S, v \in \text{Im } \mathbb{H}$ be nonzero vectors, $|v| = l$, \tilde{S} and v_+ be the evolved vectors in the sense of our Bäcklund transformation with parameter ν ($\text{Im } \nu = l$). then*

$$(\lambda \mathbb{I} + \tilde{S})(\lambda \mathbb{I} + \text{Re } \nu + v) = (\lambda \mathbb{I} + \text{Re } \nu + v_+)(\lambda \mathbb{I} + S) \quad (2.40)$$

holds for all λ .

Proof Comparing the orders in λ on both sides in equation (2.40) gives two equations

$$\tilde{S} + \text{Re } \nu + v = \text{Re } \nu + v_+ + S \quad (2.41)$$

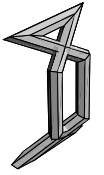
$$\tilde{S}(\text{Re } \nu + v) = (\text{Re } \nu + v_+)S. \quad (2.42)$$

The first holds trivially from construction the second gives

$$\text{Re } \nu = (v_+S - \tilde{S}v)(\tilde{S} - S)^{-1}.$$

This can be checked by elementary calculations using equation (2.38) for the real part of ν . \square

Like in the continuous case we can deduce that $\text{Im}(\rho_n) = v_n = \tilde{\gamma}_n - \gamma_n$ which gives us the constant distance between the original curve γ_n and its Bäcklund transform $\tilde{\gamma}_n$.



2.4 The doubly discrete Hashimoto flow

From now on let $\gamma : \mathbb{Z} \rightarrow \text{Im } \mathbb{H}$ be periodic or have at least periodic tangents $S_n = \gamma_{n+1} - \gamma_n$ with period N (we will see later that rapidly decreasing boundary conditions are valid also). As before let $\tilde{\gamma}$ be a Bäcklund transform of γ with initial point $\tilde{\gamma}_0 = \gamma_0 + v_0$, $|v_0| = l$. As we have seen the map sending v_n to v_{n+1} is a Möbius transformation and therefore the map sending v_0 to v_N is one too. As such it has in general two but at least one fix point. Thus starting with one of them as initial point the Bäcklund transform $\tilde{\gamma}$ is periodic too (or has periodic tangents S). Clearly this can be iterated to get a discrete evolution of our discrete curve γ .

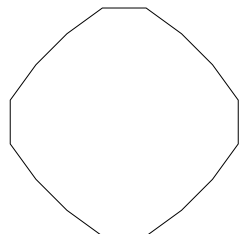
Lemma 25 *Let γ be a discrete curve with periodic tangents S of period N . Then the tangents \tilde{S} of a dressed curve $\tilde{\gamma}$ with the parameters λ_0 and s_0 are again periodic if and only if the vector $(1, s_0)$ is an eigenvector of the monodromy matrix $G_N(\lambda)$ at $\lambda = \lambda_0$.*

Proof We use the notation from Theorem 21. Since $\tilde{\gamma}_n - \gamma_n = v_n = \text{Im}(\rho_n)$ and since $B(\lambda) = \mathbb{I} + \lambda\rho$ is completely determined by λ_0 and v we have, that $B_0(\lambda) = B_N(\lambda)$. On the other hand one can determine $B(\lambda)$ by λ_0 and s_0 . Since $G_0(\lambda) = \mathbb{I}$ condition 2.32 says that $\begin{pmatrix} 1 \\ s_0 \end{pmatrix}$ and $G_n(\lambda_0)\begin{pmatrix} 1 \\ s_0 \end{pmatrix}$ must lie in $\ker B_0(\lambda_0)$. \square

A Lax representation for this evolution is given by equation (2.42) which is basically the Bianchi permutability of the Bäcklund transformation.

In the following we will show that for the special choice $l = 1$ and $\delta_1 \approx \frac{\pi}{2}$ the resulting evolution can be viewed as a discrete smoke ring flow. More precisely one has to apply the transformation twice: once with δ_1 and once with $-\delta_1$. In Chapter 3 we will show, that under this evolution the complex curvature of the discrete curve solves the doubly discrete NLSE introduced by Ablowitz and Ladik [AL77], which of course is an other good argument.

Proposition 26 *A Möbius transformation that sends a disc into its inner has a fix point in it.*



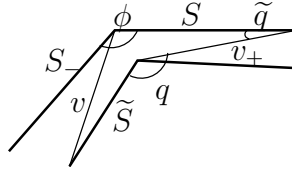
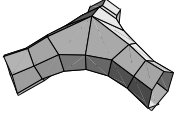


Figure 2.6: An elementary quadrilateral if $l = 1$ and $\delta_1 \approx \frac{\pi}{2}$

Now we show the following

Lemma 27 *If $\angle(-S_-, v) \leq \epsilon$, ϵ sufficiently small, there exists a δ_1 such that $\angle(-S, v_+) < \epsilon$.*

Proof With notations as in Fig 2.6 we know $e^{i\tilde{q}} = \frac{ke^{iq} - 1}{k - e^{iq}}$ and $q \in [\phi - \epsilon, \phi + \epsilon]$ giving us

$$2i \sin \tilde{q} = 2i \operatorname{Im} e^{i\tilde{q}} = 2i \frac{(k^2 - 1) \sin(\phi \pm \epsilon)}{(k^2 + 1) - 2k \cos(\phi \pm \epsilon)}$$

which proves the claim since k goes to 1 if δ_1 tends to $\frac{\pi}{2}$. \square

Knowing this one can see that an initial v_0 with $\angle(-S_{N-1}, v_0) \leq \epsilon$ is mapped to a v_N with $\angle(-S_{N-1}, v_N) < \epsilon$. Above Proposition gives that there must be a fix point p_0 with $\angle(-S_{N-1}, p_0) < \epsilon$.

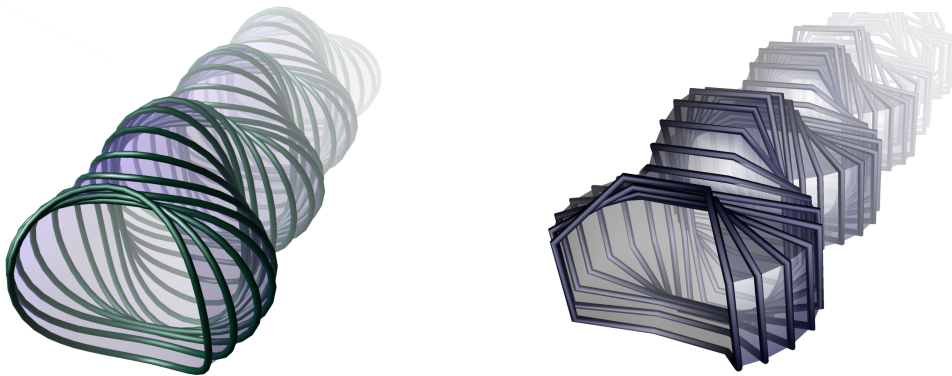
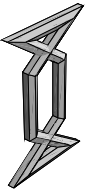


Figure 2.7: An oval curve under the Hashimoto flow and the discrete evolution of its discrete pendant.



But if $p_n \approx -S_{n-1}$ we get $\tilde{\gamma}_n \approx \gamma_{n-1}$ and $\tilde{\gamma}_n - \gamma_{n-1}$ is close to be orthogonal to $\text{span}(S_{n-2}, S_{n-1})$. So it is a discrete version of an evolution in binormal direction—plus a shift. To get rid of this shift, one has to do the transformation twice but with opposite sign for δ_1 . Figure 2.7 shows some stages of the smooth Hashimoto flow for an oval curve and the discrete evolution of its discrete counterpart. In general the double Bäcklund transformation can be viewed as a discrete version of a linear combination of Hashimoto and tangential flow—this is emphasized by the fact that the curves that evolve under such a linear combination by rigid motion only coincide in the smooth and discrete case:

2.4.1 discrete Elastic Curves

As a spin off of the last section one can easily show, that the elastic curves defined in Section 2.3 as curves that evolve under the Hashimoto flow by rigid motion only do the same for the doubly discrete Hashimoto flow. Again we will use the evolution of the complex curvature of the discrete curve. We mentioned before that in the doubly discrete case the complex curvature evolves with the doubly discrete NLSE given by Ablowitz and Ladik [AL77, Hof99b].

We start by quoting a special case of their result which can be summarized in the following form (see also [Sur97])

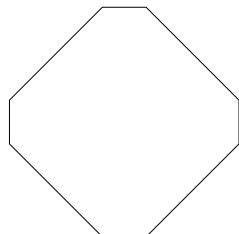
Theorem 28 (Ablowitz and Ladik) *given*

$$L_n(\mu) = \begin{pmatrix} \mu & q_n \\ -\bar{q}_n & \mu^{-1} \end{pmatrix}$$

and $V_n(\mu)$ with the following μ -dependency:

$$V_n(\mu) = \mu^{-2}V_{-2n} + \mu^{-1}V_{-1n} + V_{0n} + \mu^1V_{1n} + \mu^2V_{2n}.$$

Then the zero curvature condition $V_{n+1}(\mu)L_n(\mu) = \tilde{L}_n(\mu)V_n(\mu)$ gives





the following equations:

$$\begin{aligned}
(\tilde{q}_n - q_n)/i &= \alpha_+ q_{n+1} - \alpha_0 q_n + \bar{\alpha}_0 \tilde{q}_n - \bar{\alpha}_+ \tilde{q}_{n-1} \\
&\quad + (\alpha_+ q_n \mathcal{A}_{n+1} - \bar{\alpha}_+ \tilde{q}_n \bar{\mathcal{A}}_n) \\
&\quad + (-\bar{\alpha}_- \tilde{q}_{n+1} + \alpha_- q_{n-1})(1 + |\tilde{q}_n|^2) \Lambda_n \quad (2.43) \\
\mathcal{A}_{n+1} - \mathcal{A}_n &= \tilde{q}_n \bar{\tilde{q}}_{n-1} - q_{n+1} \bar{q}_n \\
\Lambda_{n+1}(1 + |q_n|^2) &= \Lambda_n(1 + |\tilde{q}_n|^2)
\end{aligned}$$

with constants α_+ , α_0 and α_- .

In the case of periodic or rapidly decreasing boundary conditions the natural conditions $\mathcal{A}_n \rightarrow 0$, and $\Lambda_n \rightarrow 1$ for $n \rightarrow \pm\infty$ give formulas for \mathcal{A}_n and Λ_n :

$$\begin{aligned}
\mathcal{A}_n &= q_n \bar{q}_{n-1} + \sum_{j=j_0}^{n-1} (q_j \bar{q}_{j-1} - \tilde{q}_j \bar{\tilde{q}}_{j-1}) \\
\Lambda_n &= \prod_{j=j_0}^{n-1} \frac{1 + |\tilde{q}_j|^2}{1 + |q_j|^2}
\end{aligned}$$

with $j_0 = 0$ in the periodic case and $j_0 = -\infty$ in case of rapidly decreasing boundary conditions.

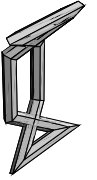
Theorem 29 *The discrete elastic curves evolve by rigid motion under the doubly discrete Hashimoto flow.*

Proof Evolving by rigid motion means for the complex curvature of a discrete curve, that it must stay constant up to a possible global phase, i. e. $\tilde{\psi}_n = e^{2i\theta} \Psi_n$. Due to Theorem 28 the evolution equation for ψ_n reads

$$\begin{aligned}
\frac{(\tilde{\Psi}_n - \Psi_n)}{i} &= \alpha_+ \Psi_{n+1} - \alpha_0 \Psi_n + \bar{\alpha}_0 \tilde{\Psi}_n - \bar{\alpha}_+ \tilde{\Psi}_{n-1} + (\alpha_+ \Psi_n \mathcal{A}_{n+1} \\
&\quad - \bar{\alpha}_+ \tilde{\Psi}_n \bar{\mathcal{A}}_n) + (-\bar{\alpha}_- \tilde{\Psi}_{n+1} + \alpha_- \Psi_{n-1})(1 + |\tilde{\Psi}_n|^2) \Lambda_n
\end{aligned}$$

Using $e^{-i\theta} \tilde{\psi}_n = e^{i\theta} \Psi_n$ gives $\Delta_n = 1$, $\mathcal{A}_n = e^{2i\theta} \Psi_n \bar{\Psi}_{n-1}$, and finally

$$2 (\sin \theta + \operatorname{Re}(e^{i\theta} \alpha_0)) \frac{\Psi_n}{1 + |\Psi_n|^2} =$$



$$= \left(e^{i\theta} \alpha_+ + \overline{e^{i\theta} \alpha_-} \right) \Psi_{n+1} + \left(\overline{e^{i\theta} \alpha_+} + e^{i\theta} \alpha_- \right) \Psi_{n-1}.$$

So the complex curvature of curves that move by rigid motion solve

$$\mathcal{C} \frac{\Psi_n}{1 + |\Psi_n|^2} = e^{i\mu} \Psi_{n+1} + e^{-i\mu} \Psi_{n-1} \quad (2.44)$$

with some real parameters \mathcal{C} and μ which clearly holds for discrete elastic curves. \square

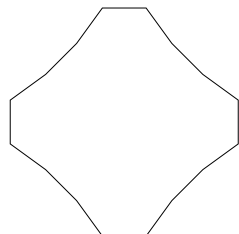
Remark The additional parameter μ in eqn (2.44) is due to the fact that the Ablowitz Ladik system is the general double Bäcklund transformation and not only the one with parameters ν and $-\bar{\nu}$. This is compensated by the extra torsion μ and the resulting curve is in the associated family of an elastic curve. These curves are called *elastic rods* [BS99].

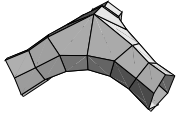
2.4.2 Bäcklund transformations for the doubly discrete Hashimoto surfaces

Since the doubly discrete Hashimoto surfaces are build from Bäcklund transformations themselves the Bianchi permutability theorem (Theorem 22) ensures that the Bäcklund transformations for discrete curves give rise to Bäcklund transformations for the doubly discrete Hashimoto surfaces too. Thus every thing said in section 2.3.2 holds in the doubly discrete case too.

Conclusion

We presented an integrable doubly discrete Hashimoto or Heisenberg flow, that arises from the Bäcklund transformation of the (singly) discrete flow and showed how the equivalence of the discrete and doubly discrete Heisenberg magnet model with the discrete and doubly discrete nonlinear Schrödinger equation can be understood from the geometric point of view. The fact that the stationary solutions of the dNLSE and the ddNLSE coincide stresses the strong similarity of the both and the power of the concept of integrable discrete geometry.





Let us end by giving some more figures of examples of the doubly discrete Hashimoto flow.

The thumb nail movie in the upper right side and Figure 2.8 show a periodic smoke ring flow . The curve is a double eight that is in the family of generalized elastic curves from Chapter 1. This one parameter allows to kill the translational part of the evolution.

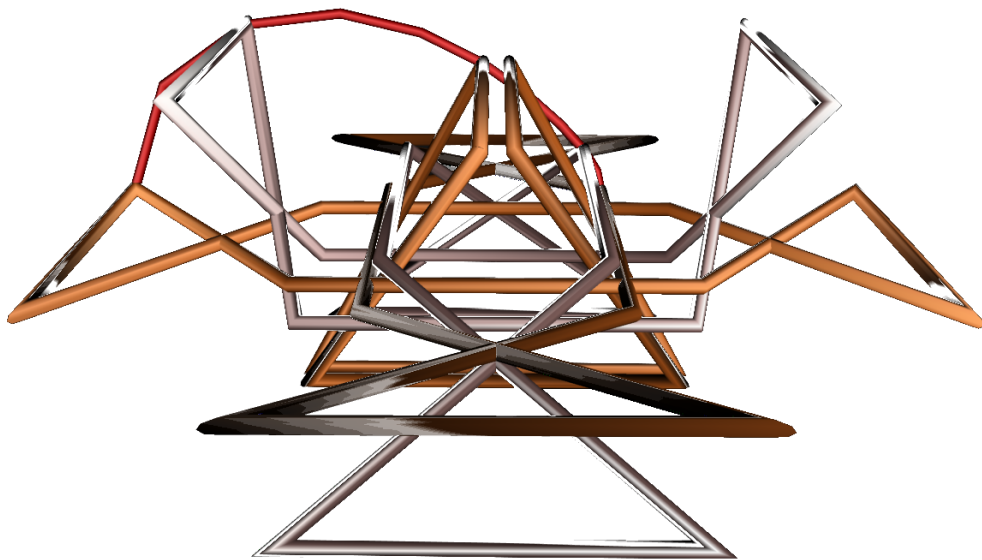


Figure 2.8: A discrete double eight that gives a Hashimoto torus. The green line is the trace of one vertex.

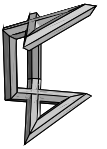
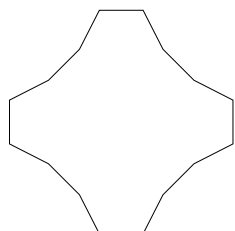


Figure 2.9: The doubly discrete Hashimoto flow on a equal sided triangle with subdivided edges.





Chapter 3

On the equivalence of the discrete nonlinear Schrödinger equation and the discrete isotropic Heisenberg magnet.

3.1 Introduction

The equivalence of the discrete isotropic Heisenberg magnet (IHM) model and the discrete nonlinear Schrödinger equation (NLSE) given by Ablowitz and Ladik is shown. This is used to derive the equivalence of two important discretizations of the NLSE found in literature. Moreover a doubly discrete IHM is presented that is equivalent to Ablowitz' and Ladik's doubly discrete NLSE.

The gauge equivalence of the continuous isotropic Heisenberg magnet model and the nonlinear Schrödinger equation is well known [FT86]. On the other hand there are several discretizations of the nonlinear Schrödinger equation in literature (e. g. . [AL76, IK81, DJM82b, QNCvdL84]). In particular there are two famous versions with continuous time. One introduced by Ablowitz and Ladik [AL76] (from now on called dNLSE_{AL}) and one given by Izgerin and Korepin [IK81] (from now on referred to as dNLSE_{IK}) (see also [FT86]). The second can be obtained from the discrete (or lattice) isotropic Heisenberg magnet model (dIHM) with slight modification via a gauge transformation [FT86].



In this chapter the gauge equivalence of the dIHM model and the dNLSE_{AL} is shown. In fact this is in complete analogy to the continuous case¹. The equivalence of the two discretizations of the nonlinear Schrödinger equation is derived from this.

In addition in Section 3.3 a doubly discrete (with discrete time) version of the IHM model is given that links in the same way with the doubly discrete NLSE introduced by Ablowitz and Ladik in [AL77]. It first appeared in a somewhat implicit form in [DJM82a, QNCvdL84].

In Chapter 2 we explained the geometric background of the interplay between IHM model and NLSE (see also [BS99, DS99]). From the geometric point of view the dNLSE_{AL} seems to be the more natural choice.

As before we will identify \mathbb{R}^3 with $\mathfrak{su}(2)$ that is the span of \mathbf{i} , \mathbf{j} , and \mathbf{k} where

$$\mathbf{i} = i\sigma_3 = \begin{pmatrix} i & 0 \\ 0 & -i \end{pmatrix} \quad \mathbf{j} = i\sigma_1 = \begin{pmatrix} 0 & i \\ i & 0 \end{pmatrix}$$

$$\mathbf{k} = -i\sigma_2 = \begin{pmatrix} 0 & -1 \\ 1 & 0 \end{pmatrix}.$$

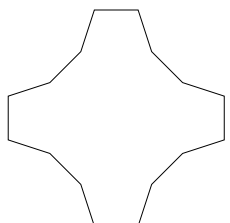
3.2 Equivalence of the discrete Heisenberg magnetic model and the nonlinear Schrödinger equation

The dIHM model and the dNLSE_{AL} are well known [AL76, FT86, BS99, Sur97]. In this section it is shown that—as in the smooth case—both models are gauge equivalent. We start by giving the discretizations.

The dNLSE_{AL} has the form:

$$-i\dot{\Psi}_k = \Psi_{k+1} - 2\Psi_k + \Psi_{k-1} + |\Psi_k|^2(\Psi_{k+1} + \Psi_{k-1}). \quad (3.1)$$

¹It seem to have first appeared in [Ish82] with no explicit reference to the IHM.





It has the following zero curvature representation (see [AL76, Sur97])

$$\hat{L}_k = \widehat{M}_{k+1} \widehat{L}_k - \widehat{L}_k \widehat{M}_k \quad (3.2)$$

with \widehat{L}_k and \widehat{M}_k of the form

$$\begin{aligned} \widehat{L}_k(\mu) &= \begin{pmatrix} \mu & \Psi_k \\ -\overline{\Psi}_k & \mu^{-1} \end{pmatrix} \\ \widehat{M}_k(\mu) &= \begin{pmatrix} \mu^2 i - i + i\Psi_k \overline{\Psi}_{k-1} & \mu i \Psi_k - \mu^{-1} i \Psi_{k-1} \\ -\mu i \overline{\Psi}_{k-1} + \mu^{-1} i \overline{\Psi}_k & -\mu^{-2} i + i - i \overline{\Psi}_k \Psi_{k-1} \end{pmatrix} \end{aligned} \quad (3.3)$$

where $\overline{}$ denotes complex conjugation. Aiming to the forthcoming theorem we gauge this Lax pair with $\begin{pmatrix} \sqrt{\mu} & 0 \\ 0 & \sqrt{\mu}^{-1} \end{pmatrix}$ and get

$$\begin{aligned} L_k(\mu) &= \begin{pmatrix} 1 & \Psi_k \\ -\overline{\Psi}_k & 1 \end{pmatrix} \begin{pmatrix} \mu & 0 \\ 0 & \mu^{-1} \end{pmatrix} \\ M_k(\mu) &= \begin{pmatrix} i\Psi_k \overline{\Psi}_{k-1} & i\Psi_k - i\Psi_{k-1} \\ -i\overline{\Psi}_{k-1} + i\overline{\Psi}_k & -i\overline{\Psi}_k \Psi_{k-1} \end{pmatrix} + \\ &+ \begin{pmatrix} 1 & \Psi_{k-1} \\ -\overline{\Psi}_{k-1} & 1 \end{pmatrix} \begin{pmatrix} i(\mu^2 - 1) & 0 \\ 0 & -i(\mu^{-2} - 1) \end{pmatrix}. \end{aligned} \quad (3.4)$$

We now turn our attention for a moment to the discrete isotropic Heisenberg magnet model. It is given by the following evolution equation

$$\dot{S}_k = 2 \frac{S_{k+1} \times S_k}{1 + \langle S_{k+1}, S_k \rangle} - 2 \frac{S_k \times S_{k-1}}{1 + \langle S_k, S_{k-1} \rangle} \quad (3.5)$$

with the S_k being unit vectors in \mathbb{R}^3 . Its zero curvature representation is given by

$$\dot{U}_k = V_{k+1} U_k - U_k V_k \quad (3.6)$$

with U_k and V_k of the form

$$\begin{aligned} U_k &= \mathbb{I} + \lambda S_k \\ V_k &= -\frac{1}{1+\lambda^2} \left(2\lambda^2 \frac{S_k + S_{k-1}}{1 + \langle S_k, S_{k-1} \rangle} + 2\lambda \frac{S_k \times S_{k-1}}{1 + \langle S_k, S_{k-1} \rangle} \right) \end{aligned} \quad (3.7)$$

if one identifies the \mathbb{R}^3 with $\mathfrak{su}(2)$ in the usual way. Now we are prepared to state



Theorem 30 *The discrete nonlinear Schrödinger equation dNLSE_{AL} (3.1) and the discrete isotropic Heisenberg magnet model dIHM (3.5) are gauge equivalent.*

Proof We use the notation introduced above. Let \mathcal{F} be a solution to the linear problem

$$\mathcal{F}_{k+1} = L_k(1)\mathcal{F}_k, \quad \dot{\mathcal{F}}_k = \widehat{M}_k(1)\mathcal{F}_k := (M_k(1) + \mathcal{F}_k c \mathcal{F}_k^{-1}) \mathcal{F}_k \quad (3.8)$$

with a constant vector c . Since $\widehat{M}_{k+1}(1)L_k(1) - L_k(1)\widehat{M}_k(1) = M_{k+1}(1)L_k(1) - L_k(1)M_k(1) = \dot{L}_k(1)$ the zero curvature condition stays valid and the system is solvable. The additional term $\mathcal{F}_k c \mathcal{F}_k^{-1}$ will give rise to an additional rotation around c in the dIHM model. The importance of this possibility will be clarified in the next section. Moreover define

$$S_k := \mathcal{F}_k^{-1} \dot{\mathcal{F}}_k. \quad (3.9)$$

Note that this implies that

$$\frac{|S_k \times S_{k+1}|}{1 + \langle S_k, S_{k+1} \rangle} = |\Psi_k|. \quad (3.10)$$

In other words: $|\Psi_k| = \tan(\frac{\phi_k}{2})$ with $\phi_k = \angle(S_k, S_{k+1})$. We will show, that the S_k solve the dIHM model (if $c = 0$). To do so we use \mathcal{F}^{-1} as a gauge field:

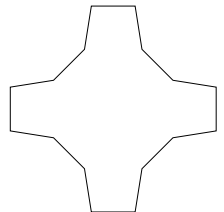
$$L_k^{\mathcal{F}^{-1}}(\mu) := \mathcal{F}_{k+1}^{-1} L_k(\mu) \mathcal{F}_k = \mathcal{F}_k^{-1} \begin{pmatrix} \mu & 0 \\ 0 & \mu^{-1} \end{pmatrix} \mathcal{F}_k$$

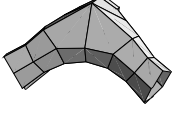
If one writes $\mu = \sqrt{\frac{1+i\lambda}{1-i\lambda}} = \frac{1+i\lambda}{\sqrt{1+\lambda^2}}$ one gets $\mu^{-1} = \frac{1-i\lambda}{\sqrt{1+\lambda^2}}$ and one can conclude that

$$L_k^{\mathcal{F}^{-1}}(\lambda) = \mathcal{F}_k^{-1} \frac{\mathbb{I} + i\lambda}{\sqrt{1 + \lambda^2}} \mathcal{F}_k = \frac{1}{\sqrt{1 + \lambda^2}} (\mathbb{I} + \lambda S_k). \quad (3.11)$$

This clearly coincides with $U_k(\lambda)$ up to the irrelevant normalization factor $\frac{1}{\sqrt{1+\lambda^2}}$. On the other hand one gets for the gauge transform of $M_k(\mu)$

$$\begin{aligned} M_k^{\mathcal{F}^{-1}}(\mu) &:= \mathcal{F}_k^{-1} M_k(\mu) \mathcal{F}_k - \mathcal{F}_k^{-1} \dot{\mathcal{F}}_k = \mathcal{F}_k^{-1} (M_k(\mu) - M_k(1) - \mathcal{F}_k c \mathcal{F}_k^{-1}) \mathcal{F}_k \\ &= \mathcal{F}_k^{-1} L_{k-1}(1) \mathcal{F}_k \mathcal{F}_k^{-1} \begin{pmatrix} i(\mu^2 - 1) & 0 \\ 0 & -i(\mu^{-2} - 1) \end{pmatrix} \mathcal{F}_k - c \end{aligned}$$





But with above substitution for μ one gets

$$\begin{pmatrix} i(\mu^2 - 1) & 0 \\ 0 & -i(\mu^{-2} - 1) \end{pmatrix} = -2 \frac{\lambda \mathbb{I} + \lambda^2 \mathbf{i}}{1 + \lambda^2} \quad (3.12)$$

and since $\mathcal{F}_k^{-1} L_{k-1}(1) \mathcal{F}_k = \mathcal{F}_{k-1}^{-1} L_{k-1}(1) \mathcal{F}_{k-1}$ we get

$$\begin{aligned} \mathcal{F}_k^{-1} L_{k-1}(1) \mathcal{F}_k &= \mathbb{I} + \mathcal{F}_{k-1}^{-1} (\text{Im}(\Psi_{k-1}) \mathbf{j} - \text{Re}(\Psi_{k-1}) \mathbf{k}) \mathcal{F}_{k-1} \\ &= \mathbb{I} + \mathcal{F}_k^{-1} (\text{Im}(\Psi_{k-1}) \mathbf{j} - \text{Re}(\Psi_{k-1}) \mathbf{k}) \mathcal{F}_k \end{aligned}$$

Remember that $S_k = \mathcal{F}_k^{-1} \mathbf{i} \mathcal{F}_k$ and $S_{k-1} = \mathcal{F}_{k-1}^{-1} \mathbf{i} \mathcal{F}_{k-1}$. Using equation (3.10) and the fact that \mathbf{i} and $\text{Im}(\Psi_{k-1}) \mathbf{j} - \text{Re}(\Psi_{k-1}) \mathbf{k}$ anti-commute we conclude²

$$\mathcal{F}_k^{-1} L_{k-1}(1) \mathcal{F}_k = \mathbb{I} + \frac{S_k \times S_{k-1}}{1 + \langle S_k, S_{k-1} \rangle}. \quad (3.13)$$

Combining this and equation (3.12) one obtains for the gauge transform of M_k

$$\begin{aligned} M_k^{\mathcal{F}^{-1}}(\lambda) &= -2 \left(\mathbb{I} + \frac{S_k \times S_{k-1}}{1 + \langle S_k, S_{k-1} \rangle} \right) \frac{\lambda \mathbb{I} + \lambda^2 S_k}{1 + \lambda^2} - c \\ &= \frac{-2}{1 + \lambda^2} \left(\lambda \mathbb{I} + \lambda \frac{S_k \times S_{k-1}}{1 + \langle S_k, S_{k-1} \rangle} + \lambda^2 \left(S_k + \frac{(S_k \times S_{k-1}) S_k}{1 + \langle S_k, S_{k-1} \rangle} \right) \right) - c \\ &= \frac{-2\lambda}{1 + \lambda^2} \mathbb{I} - \frac{2}{1 + \lambda^2} \left(\lambda \frac{S_k \times S_{k-1}}{1 + \langle S_k, S_{k-1} \rangle} + \lambda^2 \frac{S_k + S_{k-1}}{1 + \langle S_k, S_{k-1} \rangle} \right) - c \\ &= \frac{-2\lambda}{1 + \lambda^2} \mathbb{I} + V_k(\lambda) - c. \end{aligned} \quad (3.14)$$

Since the first term is a multiple of the identity and independent of k it cancels in the zero curvature condition and therefore can be dropped. This gives the desired result if $c = 0$. \square

3.2.1 Equivalence of the two discrete nonlinear Schrödinger equations

There has been another discretization of the nonlinear Schrödinger equation in the literature [IK81, FT86]. It can be derived from a

²to fix the sign of the second term one needs to look at the sign of the scalar product $\left\langle \mathcal{F}_k^{-1} (\text{Im}(\Psi_{k-1}) \mathbf{j} - \text{Re}(\Psi_{k-1}) \mathbf{k}) \mathcal{F}_k, \frac{S_k \times S_{k-1}}{1 + \langle S_k, S_{k-1} \rangle} \right\rangle$.



slightly modified diHM model by a gauge transformation. Since we showed that the dNLSE_{AL} introduced by Ablowitz and Ladik is gauge equivalent to the diHM it is a corollary of the last theorem that the two discretizations of the NLSE are in fact equivalent.

The method of getting the variables of this other discretization is basically a stereographic projection of the variables S_k from the diHM [FT86]: One defines

$$\chi_k = \chi(S_k) = \sqrt{2}(-1)^k \frac{2(S_k + \mathbf{i}) - |S_k + \mathbf{i}|^2 \mathbf{i}}{\sqrt{|S_k + \mathbf{i}|^4 + |2(S_k + \mathbf{i}) - |S_k + \mathbf{i}|^2 \mathbf{i}|^2}} \quad (3.15)$$

or

$$\begin{aligned} S_k = & (1 - |\chi_k|^2) \mathbf{i} + \text{Im} \left(\sqrt{2}(-1)^k \chi_k \sqrt{1 - \frac{|\chi_k|^2}{2}} \right) \mathbf{j} \\ & - \text{Re} \left(\sqrt{2}(-1)^k \chi_k \sqrt{1 - \frac{|\chi_k|^2}{2}} \right) \mathbf{k}. \end{aligned} \quad (3.16)$$

If one modifies the evolution (3.5) by adding a rotation around \mathbf{i}

$$\dot{S}_k = 2 \frac{S_{k+1} \times S_k}{1 + \langle S_{k+1}, S_k \rangle} - 2 \frac{S_k \times S_{k-1}}{1 + \langle S_k, S_{k-1} \rangle} - 4S_k \times \mathbf{i}. \quad (3.17)$$

Writing this in terms of the new variables χ_k gives rise to the following evolution equation (dNLSE_{IK}):

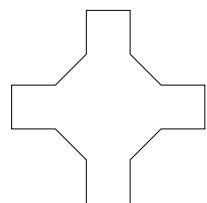
$$-i\dot{\chi}_k = 4\chi_k + \frac{P_{k,k+1}}{Q_{k,k+1}} + \frac{P_{k,k-1}}{Q_{k,k-1}} \quad (3.18)$$

where

$$\begin{aligned} P_{n,m} = & - \left(\chi_n + \chi_m \sqrt{1 - \frac{|\chi_n|^2}{2}} \sqrt{1 - \frac{|\chi_m|^2}{2}} - \chi_n |\chi_m|^2 - \right. \\ & \left. - \frac{1}{4} (|\chi_n|^2 \chi_m + \chi_n^2 \bar{\chi}_m) \frac{\sqrt{1 - \frac{|\chi_m|^2}{2}}}{\sqrt{1 - \frac{|\chi_n|^2}{2}}} \right) \end{aligned}$$

and

$$\begin{aligned} Q_{n,m} = & 1 - \frac{1}{2} \left(|\chi_n|^2 + |\chi_m|^2 + (\chi_n \bar{\chi}_m + \bar{\chi}_n \chi_m) \sqrt{1 - \frac{|\chi_n|^2}{2}} \right. \\ & \left. \cdot \sqrt{1 - \frac{|\chi_m|^2}{2}} - |\chi_n|^2 |\chi_m|^2 \right). \end{aligned}$$





This evolution clearly possesses a zero curvature condition $\dot{U}_k = \widehat{V}_{k+1}U_k - U_k\widehat{V}_k$ with

$$\widehat{V}_k(\lambda) = V_k(\lambda) - 2i \quad (3.19)$$

since one can view S_k as a function of χ_k via equation (3.16).

Theorem 31 *The dNLSE_{IK} (3.18) and the dNLSE_{AL} (3.1) are gauge equivalent.*

Proof This is already covered by the proof of theorem 30. \square

Since the S_k are given by $S_k = \mathcal{F}_k^{-1}i\mathcal{F}_k$ the χ_k are functions of the Ψ_k and vice versa, but these maps are nonlocal.

3.3 A doubly discrete IHM model and the doubly discrete NLSE

In the following we will construct a discrete time evolution for the variables S_k that—applied twice—can be viewed as a doubly discrete IHM model. In fact it will turn out that this system is equivalent to the doubly discrete NLSE introduced by Ablowitz and Ladik [AL77]. We start by defining the zero curvature representation.

$$\begin{aligned} U_k(\lambda) &= \mathbb{I} + \lambda S_k \\ V_k(\lambda) &= \mathbb{I} + \lambda(r\mathbb{I} + v_k) \end{aligned} \quad (3.20)$$

with $r \in \mathbb{R}$. The v_k (as well as the S_k) are vectors in \mathbb{R}^3 (again written as complex 2 by 2 matrix). The zero curvature condition $\widetilde{L}_k V_k = V_{k+1} L_k$ should hold for all λ giving $v_k + \widetilde{S}_k = S_k + v_{k+1}$ and $r(\widetilde{S}_k - S_k) = v_{k+1} S_k - \widetilde{S}_k v_k$. (Here and in the forthcoming we use $\widetilde{}$ to denote the time shift.) One can solve this for v_{k+1} or \widetilde{S}_k getting

$$\begin{aligned} v_{k+1} &= (S_k - v_k - r)v_k(S_k - v_k - r)^{-1} \\ \widetilde{S}_k &= (S_k - v_k - r)S_k(S_k - v_k - r)^{-1}. \end{aligned} \quad (3.21)$$

This can be interpreted in the following way: Since $S_k, v_{k+1}, -\widetilde{S}_k,$ and $-v_k$ sum up to zero they can be viewed as a quadrilateral in \mathbb{R}^3 .



But equation (3.21) says that v_{k+1} and \tilde{S}_k are rotations³ of v_k and S_k around $S_k - v_k$. So the resulting quadrilateral is a parallelogram that is folded along one diagonal. See Chapter 2 to get a more elaborate investigation of the underlying geometry.

Equation (3.21) is still a transformation⁴ and no evolution since one has to fix an initial v_0 . But in the case of periodic S_k one can find in general two fix points of the transport of v_0 once around the period and thus single out certain solutions. If on the other hand one has rapidly decreasing boundary conditions one can extract solutions by the condition that $\tilde{S}_k \rightarrow \pm S_k$ for $k \rightarrow \infty$ and $k \rightarrow -\infty$. But instead of going into this we will show, that doing this transformation twice is equivalent to Ablowitz' and Ladiks system.

Let us recall their results.

Theorem 32 (Ablowitz and Ladik 77) *Given the matrices*

$$L_k(\mu) = \begin{pmatrix} 1 & \Psi_k \\ -\bar{\Psi}_k & 1 \end{pmatrix} \begin{pmatrix} \mu & 0 \\ 0 & \mu^{-1} \end{pmatrix}$$

and $V_k(\mu)$ with the following μ -dependency:

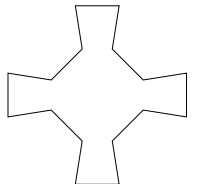
$$V_k(\mu) = \mu^{-2}V_k^{(-2)} + V_k^{(0)} + \mu^2V_k^{(2)}$$

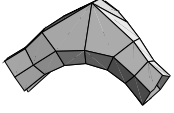
with $V_k^{(-2)}$ being upper and $V_k^{(2)}$ being lower triangular. Then the zero curvature condition $V_{k+1}(\mu)L_k(\mu) = \tilde{L}_k(\mu)V_k(\mu)$ gives the following equations:

$$\begin{aligned} (\tilde{\Psi}_k - \Psi_k)/i &= \alpha_+ \Psi_{k+1} - \alpha_0 \Psi_k + \bar{\alpha}_0 \tilde{\Psi}_k - \bar{\alpha}_+ \tilde{\Psi}_{k-1} \\ &\quad + (\alpha_+ \Psi_k \mathcal{A}_{k+1} - \bar{\alpha}_+ \tilde{\Psi}_k \bar{\mathcal{A}}_k) \\ &\quad + (-\bar{\alpha}_- \tilde{\Psi}_{k+1} + \alpha_- \Psi_{k-1})(1 + |\tilde{\Psi}_k|^2) \Lambda_k \\ \mathcal{A}_{k+1} - \mathcal{A}_k &= \tilde{\Psi}_k \bar{\tilde{\Psi}}_{k-1} - \Psi_{k+1} \bar{\Psi}_k \\ \Lambda_{k+1}(1 + |\Psi_k|^2) &= \Lambda_k(1 + |\tilde{\Psi}_k|^2) \end{aligned} \tag{3.22}$$

³Any rotation of a vector v in $\mathbb{R}^3 = \mathfrak{su}(2)$ can be written as conjugation with a matrix σ of the form $\sigma = \cos(\frac{\phi}{2})\mathbb{I} + \sin(\frac{\phi}{2})a$ where ϕ is the rotation angle and a the rotation axis with $|a| = 1$.

⁴In fact it is the Bäcklund transformation for the dIHM model!





with constants α_+ , α_0 and α_- .

In the case of periodic or rapidly decreasing boundary conditions the natural conditions $\mathcal{A}_k \rightarrow 0$, and $\Lambda_k \rightarrow 1$ for $k \rightarrow \pm\infty$ give formulas for \mathcal{A}_k and Λ_k :

$$\mathcal{A}_k = \Psi_k \overline{\Psi}_{k-1} + \sum_{j=j_0}^{k-1} (\Psi_j \overline{\Psi}_{j-1} - \tilde{\Psi}_j \overline{\tilde{\Psi}}_{j-1})$$

$$\Lambda_k = \prod_{j=j_0}^{k-1} \frac{1 + |\tilde{\Psi}_j|^2}{1 + |\Psi_j|^2}$$

with $j_0 = 0$ in the periodic case and $j_0 = -\infty$ in case of rapidly decreasing boundary conditions.

Note that this is not the most general version of their result. One can make Ψ and $\overline{\Psi}$ independent variables which results in slightly more complicated equations but the given reduction to the NLSE case is sufficient for our purpose.

Theorem 33 *The system obtained by applying the above transformation twice is equivalent to the doubly discrete Ablowitz Ladik system in Theorem 32.*

Proof The method is more or less the same as in the singly discrete case although this time we start from the other side:

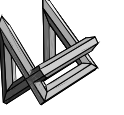
Start with a solution S_k of the ddiHM model. Choose \mathcal{F}_k such that

$$\mathcal{F}_k^{-1} \mathbf{i} \mathcal{F}_k = S_k \tag{3.23}$$

$$[(\mathcal{F}_{k+1}^{-1} \mathbf{j} \mathcal{F}_{k+1}), (\mathcal{F}_k^{-1} \mathbf{j} \mathcal{F}_k)] \parallel [S_{k+1}, S_k].$$

This is always possible since the first equation leaves a gauge freedom of rotating around \mathbf{i} . Moreover define $L_k(1) = \mathcal{F}_{k+1} \mathcal{F}_k^{-1}$ and normalize \mathcal{F}_k in such a way that $L_k(1)$ takes the form

$$L_k(1) = \mathbb{I} + A_k$$



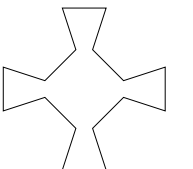
equations (3.23) ensure that $A_k \in \text{span}(\mathbf{j}, \mathbf{k})$ and thus can be written $A_k = \text{Re}(\Psi_k)\mathbf{k} - \text{Im}(\Psi_k)\mathbf{j}$ for some complex Ψ_k . Equipped with this we can gauge a normalized version of $M_k(\lambda)$ with \mathcal{F}_k and get

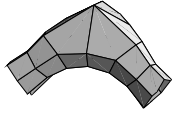
$$\begin{aligned} M_k^{\mathcal{F}} &= \frac{1}{\sqrt{1+\lambda^2}} \mathcal{F}_{k+1} M_k(\lambda) \mathcal{F}_k^{-1} = L_k(1) \frac{\mathbb{I} + \lambda \mathbf{i}}{\sqrt{1+\lambda^2}} \\ &= \begin{pmatrix} 1 & \Psi_k \\ -\overline{\Psi}_k & 1 \end{pmatrix} \begin{pmatrix} \mu & 0 \\ 0 & \mu^{-1} \end{pmatrix} \end{aligned} \quad (3.24)$$

if we write $\mu = \frac{1+i\lambda}{\sqrt{1+\lambda^2}}$ as before. On the other hand we get for an—again renormalized— $N_k(\lambda)$

$$\begin{aligned} N_k^{\mathcal{F}} &= \frac{1+\mu^2}{\mu} \tilde{\mathcal{F}}_k N_k(\lambda) \mathcal{F}_k^{-1} = \left(\frac{1}{\mu} + \mu\right) \tilde{\mathcal{F}}_k \mathcal{F}_k^{-1} + \left(\frac{1}{\mu} - \mu\right) \tilde{\mathcal{F}}_k (r + v_k) \mathcal{F}_k^{-1} \\ &= \mu^{-1} V_k^- + \mu V_k^+. \end{aligned} \quad (3.25)$$

But the zero curvature condition $\tilde{L}_k(\mu) N_k^{\mathcal{F}}(\mu) = N_{k+1}^{\mathcal{F}_k}(\mu) L_k(\mu)$ yields that V_k^+ must be lower and V_k^- upper triangular. Thus $(\tilde{N}_k^{\mathcal{F}} N_k^{\mathcal{F}})(\mu)$ has the μ -dependency as required in Theorem 32. \square





Chapter 4

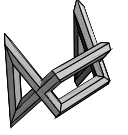
Discrete cmc surfaces from discrete curves

4.1 Introduction

As we have mentioned in Chapter 1, maps from \mathbb{Z}^2 to \mathbb{R}^3 with all elementary quadrilaterals having cross-ratio -1 can serve as discretizations of isothermic surfaces. In particular they possess the defining property of their smooth counterparts: They have a dual surface.

The condition that this dual surface can—when properly scaled—be placed in constant distance, can be used to define discrete surfaces of constant mean curvature (cmc surfaces) [BP99, HJHP99].

We also mentioned in Chapter 1 that in general one can not evolve a unique discrete isothermic surface out of a closed discrete curve, since the fix point set of the holonomy matrix may have more than two elements. In the case of discrete cmc surfaces however, we can adopt the method to produce a unique surface from a curve that allows this (not every discrete curve can serve as a curvature line of a discrete cmc surface; more precisely one needs a stripe formed by the curve and its dual). To derive this construction is the aim of this chapter.



4.2 Discrete isothermic and cmc surfaces

We start as usual with recalling some definitions. They can be found e.g. in [BP99]:

Definition 9 *A discrete isothermic surface in \mathbb{R}^3 is a map $\mathcal{F} : \mathbb{Z}^2 \rightarrow \mathbb{R}^3$ for which all elementary quadrilaterals*

$$[\mathcal{F}_{n,m}, \mathcal{F}_{n+1,m}, \mathcal{F}_{n+1,m+1}, \mathcal{F}_{n,m+1}]$$

have cross-ratio $-\frac{\alpha_n^2}{\beta_m^2}$. A dual surface \mathcal{F}^* of \mathcal{F} is given by the equations

$$\begin{aligned} \mathcal{F}_{n+1,m}^* - \mathcal{F}_{n,m}^* &= \frac{\lambda}{\alpha_n^2} \frac{\mathcal{F}_{n+1,m} - \mathcal{F}_{n,m}}{|\mathcal{F}_{n+1,m} - \mathcal{F}_{n,m}|^2} \\ \mathcal{F}_{n,m}^* - \mathcal{F}_{n,m+1}^* &= \frac{\lambda}{\beta_m^2} \frac{\mathcal{F}_{n,m+1} - \mathcal{F}_{n,m}}{|\mathcal{F}_{n,m+1} - \mathcal{F}_{n,m}|^2} \end{aligned} \quad (4.1)$$

with $\lambda \in \mathbb{R} \setminus \{0\}$. The dual surface is isothermic again.

In a narrow version of this definition one demands $\frac{\alpha_n^2}{\beta_m^2} = 1$. We will do this in the following for notational simplicity although everything can be done for the wide definition too.

Definition 10 *A discrete isothermic surface is a discrete cmc surface with mean curvature $H \neq 0$, if there is a properly scaled and placed dual surface in constant distance*

$$\|\mathcal{F}_{n,m} - \mathcal{F}_{n,m}^*\| = \frac{1}{H}. \quad (4.2)$$

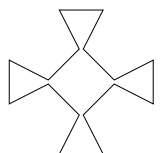
Let us compute λ . Figure 4.1 shows the two types of quadrilaterals that occur between the cmc surface and its dual.

Lemma 34 *With the notations from Figure 4.1 we have*

$$\begin{aligned} 2h^2 &= r_1^2 + r_2^2 \\ \lambda &= h^2 - r_1^2 \end{aligned} \quad (4.3)$$

Proof The proof is simple elementary geometry. \square

Note that r_1 and r_2 are constant along the surface due to the constance of h and λ and that the role of r_1 and r_2 in the figure can change depending on the sign of λ . Note also that the cross-ratios



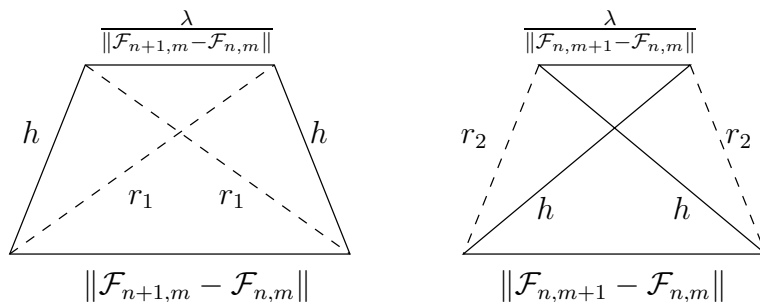
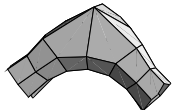


Figure 4.1: The quadrilaterals that occur between the cmc surface and its dual

of above quadrilaterals are $\pm \frac{\lambda}{h^2}$. We continue by stating a lemma that we will need in the next section (it can be found in [HJHP99]):

Lemma 35 (Hexahedron lemma) *Given a quadrilateral $[x_1, x_2, x_3, x_4]$ in the complex plane and $\lambda \in \mathbb{C}$ then for each initial point z_1 there is a unique quadrilateral $[z_1, z_2, z_3, z_4]$ such that*

$$\begin{aligned} \text{cr}(z_1, z_2, z_3, z_4) &= \text{cr}(x_1, x_2, x_3, x_4) = \mu \\ \text{cr}(z_1, z_2, x_2, x_1) &= \text{cr}(z_3, z_4, x_4, x_3) = \mu\lambda \\ \text{cr}(z_2, z_3, x_3, x_2) &= \text{cr}(z_4, z_1, x_1, x_4) = \lambda \end{aligned} \tag{4.4}$$

holds.

Remark In case of real μ and λ one can generalize this to points in \mathbb{R}^3 : Since four points with real cross-ratio always lie on a circle, the five points $[x_1, x_2, x_3, x_4]$ and z_1 define a sphere that can be interpreted as Riemann sphere¹.

4.3 CMC evolution of discrete curves

Let γ be an immersed discrete space curve. It is a strong condition, that γ possesses a “dual” curve in constant distance: Given γ_k and γ_k^* $\|\gamma_{k+1} - \gamma_k^*\| = r_1$ must hold. Thus the next point is always on a sphere of radius r_1 around the dual point of the previous (Figure 4.2). We will call such a configuration a stripe.

¹The ambiguity of orientation does not matter here

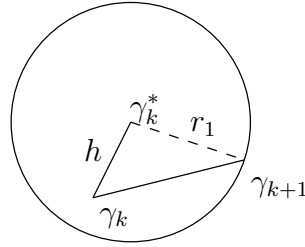
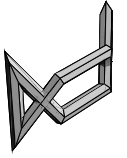


Figure 4.2: For a stripe the next point must lie in constant distance to the dual one of the previous.

Example

1. If γ is planar and arclength parametrized—say in the $\mathbf{j}\text{-}\mathbf{k}$ -plane, choosing the dual curve as $\gamma^* = \gamma + h\mathbf{i}$ gives a valid stripe.
2. If γ is a regular n -gon around 0 choosing $\gamma^* = r\gamma$ with $r \in \mathbb{R} \setminus \{0\}$ will give a stripe too.

Now we want to evolve such a stripe into a cmc surface:

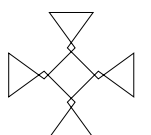
Theorem 36 *Let $\gamma_{n,0}$ and $\gamma_{n,0}^*$ form a stripe with some h and r_1 .*

1. *Choosing $\gamma_{0,1}$ on the sphere of radius $r_2 = \sqrt{2h^2 - r_1^2}$ around $\gamma_{0,0}^*$ and use it as starting point for a Bäcklundtransform $\gamma_{n,1}$ of $\gamma_{n,0}$ with $\mu = -1$ gives a new stripe $\gamma_{n,1}, \gamma_{n,1}^*$ with the same h and r_1 and $\|\gamma_{n,1} - \gamma_{n,0}^*\| = r_2$ holds for all n .*
2. *Iterating this gives raise to a discrete cmc surface.*
3. *The map sending $\gamma_{n,k+1} - \gamma_{n,k}^*$ to $\gamma_{n+1,k+1} - \gamma_{n+1,k}^*$ is a Möbius transformation of the sphere of radius r_2 . It can be represented by the complex 2×2 -matrix*

$$M = \begin{pmatrix} -\frac{1}{\mu} + (\overline{HS^{-1}})_{1,i} + r_2 \operatorname{Re}(iS^{-1}) & -2r_2((HS^{-1}\mathbf{k})_{1,i}) - r_2(iS^{-1}\mathbf{k})_{1,i} \\ \frac{1}{2r_2}(\overline{HS^{-1}\mathbf{k}})_{1,i} + r_2(\overline{iS^{-1}\mathbf{k}}) & -\frac{1}{\mu} + (HS^{-1})_{1,i} - r_2 \operatorname{Re}(iS^{-1}) \end{pmatrix} \quad (4.5)$$

with $H = \gamma^* - \gamma$.

Proof 1. follows directly from the Hexahedron lemma, since given $\gamma_{n,1}$ there are unique points $\gamma_{n,1}^*, \gamma_{n+1,1}$, and $\gamma_{n+1,1}^*$ with the necessary cross-ratios.





2. is trivial. The proof of 3. is similar to the proof of Theorem 23. To avoid repetitions we will leave it to the reader to do the details here. \square

Now we can state

Theorem 37 *Let $\gamma_{n,0}$ and $\gamma_{n,0}^*$ form a closed stripe. Then the holonomy matrix $H = \prod M_{n,0}$ has in general two fix points that give rise to an unique evolution of the curve into a cmc surface.*

4.4 Examples

4.4.1 Delaunay surfaces

As a first example we can look at the evolution of the above regular n -gon. It gives Delaunay surfaces i.e. rotational symmetric cmc surfaces. This is one of the three methods to construct them presented in this work so we refer to Chapter 5 and 6 for figures of them.

4.4.2 Wente tori

As second example let us take a discrete elastic figure eight. Since this is a planar arclength parametrized curve we can make it a stripe by taking the dual as in the first example of the last section. The surface we get is clearly a discretization of a Wente type cmc surface. One needs to adjust the cross-ratio μ however to get it a torus. Figure 4.3 shows a closed one with fourfold symmetry.² Compare these figures with Figure 7.2 and 2.4.

4.4.3 Trinoidal surfaces

The third example comes form the following observation: if for a closed stripe $\gamma_0, \gamma_0^*, g_k$, and γ_k^* lie on a straight line, one can fold the stripe along this line. This holds e.g. for a regular $2n$ -gon (see Figure 4.4.3). Moreover it holds for the whole one-parameter family

²the closedness is a numeric result but the existence of discrete cmc tori has been shown e.g. in [Haa96].

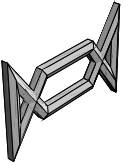


Figure 4.3: A discrete Wente torus

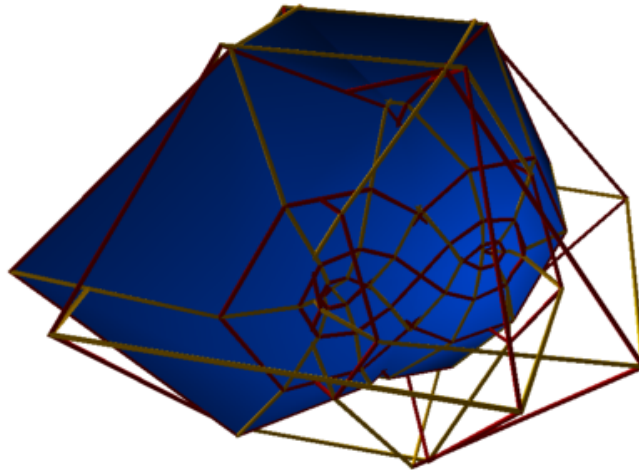
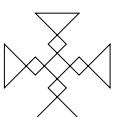


Figure 4.4: A folded regular 6-gon

of non-regular 6-gons, that preserve a two-fold symmetry. So let us fold this family by an angle $\phi = \pi - \frac{2\pi}{N}$. Evolving this gives a cmc cylinder but due to the fact that the two arcs of our initial stripe are planar we can paste N copies of the surface rotated by $k\frac{2\pi}{N}$ $k = 0, \dots, N - 1$ together. This gives a surface with the topology of a sphere with N punctures.

Of course if $N > 2$ this surface is no longer a map from Z^2 to \mathbb{R}^3 but from a graph build from quadrilaterals and two points with $2N$ outgoing edges. Since the edges are equivalents of curvature lines one should think of these points as points where more than 2 curvature lines are intersecting. This makes it natural to define these points as discrete umbilics (see also Section 6.6 where discrete versions of Smyth surfaces are introduced).





It is a natural question whether one can archive embedded ends for these surfaces, i.e. ends of Delaunay type.

Definition 11 *The polynom*

$$P(\mu) = 1/4 \operatorname{tr}(H(\mu))^2 - \det(H(\mu)) \quad (4.6)$$

is called spectral curve of the discrete curve γ

Lemma 38 *The spectral curve is invariant under the evolution.*

Proof Clear, since the holonomy matrix H evolves by conjugation. \square

Therefore a candidate for Delaunay type ends must have the same spectral curve than the circle. Figure 4.5 shows a surface with $N = 3$ and the spectral curve of the circle. Variables:

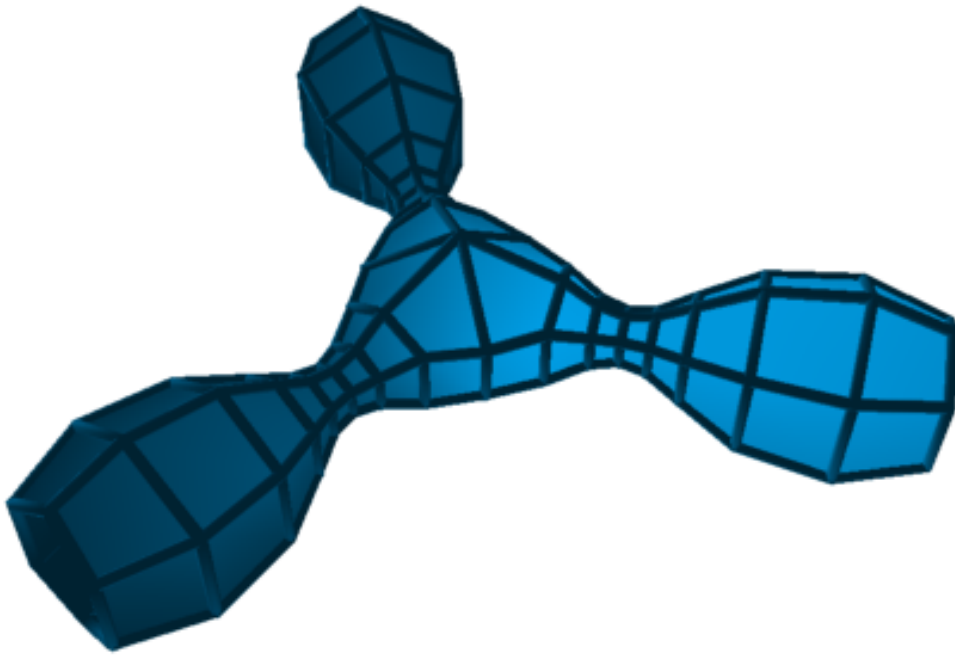
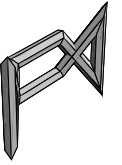
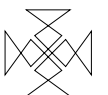


Figure 4.5: A Trinoid



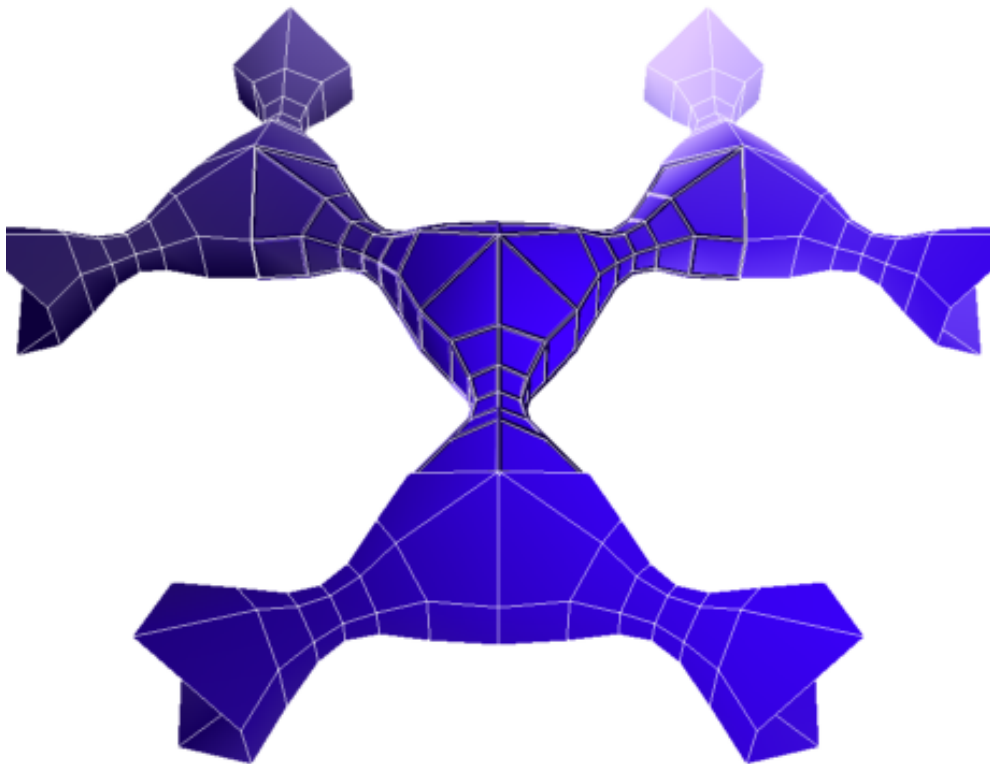
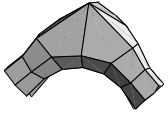


Figure 4.6: A discrete cmc surface with the topology of a tubed hexagonal grid.



Chapter 5

Discrete Rotational CMC Surfaces and the Elliptic Billiard.

5.1 Introduction

It is a well known fact, that the meridian curve of rotational constant mean curvature (cmc) surfaces (which determines the surface completely) can be obtained as the trace of one focal point of an ellipse or hyperbola when rolling it on a straight line. In this chapter it will be shown, that discrete rotational cmc surfaces can be obtained in a similar way. In fact the meridian polygons are closely related to the elliptic (or Hyperbolic) standard billiard: The discrete analogue of the ellipse or hyperbola will be the trace of a billiard in a continuous one.

In the continuous case it is well known that the rotational K and cmc surfaces are closely related and it turns out that this holds for the discrete case too: In fact they both come from the same discrete difference equation. N. Kutz showed in [Kut96] that rotational K-surfaces are equivalent to the standard billiard in an ellipse. The aim of this chapter is to show, that the billiard in turn gives discrete rotational cmc surfaces.

First we will give a very short review of the discrete surfaces we have to deal with:





5.2 Discrete rotational surfaces

It's a well known fact, that every (continuous) rotational surface allows isothermic parametrisation. We introduced the discrete analog of isothermic surfaces in Chapter 4. We will recall this definition here:

Definition 12 *A discrete isothermic surface in \mathbb{R}^3 is a map $F : \mathbb{Z}^2 \rightarrow \mathbb{R}^3$ for which the elementary quadrilaterals*

$$[F_{n,m}, F_{n+1,m}, F_{n+1,m+1}, F_{n,m+1}]$$

have crossratio¹ = -1.²

A dual surface F^* of F is given by the equations:

$$\begin{aligned} (F_{m+1,n}^* - F_{m,n}^*) &= \lambda \frac{(F_{m+1,n} - F_{m,n})}{|F_{m+1,n} - F_{m,n}|^2} \\ (F_{m,n+1}^* - F_{m,n}^*) &= -\lambda \frac{(F_{m,n+1} - F_{m,n})}{|F_{m,n+1} - F_{m,n}|^2} \end{aligned} \quad (5.1)$$

with $\lambda \in \mathbb{R} \setminus \{0\}$. The dual surface is itself isothermic again.

In general one can obtain discrete rotational surfaces by rotating a polygon $P_m \in \mathbb{R}^2$ around an axis (e.g. the x-axis): Choose $\phi \in (0, \pi)$ and define $F : \mathbb{Z}^2 \rightarrow \mathbb{R}^3$ by

$$F(n, m) = F_{n,m} := ((P_m)_1, \cos(n\phi)(P_m)_2, \sin(n\phi)(P_m)_2). \quad (5.2)$$

The condition for this surface to be isothermic is³:

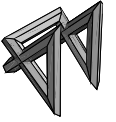
$$\|P_n - P_{n+1}\|^2 = 4|cr| \sin^2 \frac{\phi}{2} (P_n)_2 (P_{n+1})_2. \quad (5.3)$$

This is equivalent to the condition that the cross-ratio of P_n, P_{n+1} and their complex conjugates is constant. It can be interpreted as an arclength parametrisation in the hyperbolic plane.

¹As mentioned in Chapter 1 The crossratio of four complex numbers a, b, c and d is given by $cr = \frac{(a-b)(c-d)}{(b-c)(c-a)}$. It is invariant under Möbius transformations (fractional linear transformations of the complex plane). The cross-ratio is real iff the four points lie on a circle. Therefore it is possible to demand a real cross-ratio for points in space: They have to lie on a circle and this defines a plane.

²We use the narrow definition here.

³Choose $cr = -1$ for the narrow definition of discrete isothermic



5.3 Unrolling polygons and discrete rotational surfaces

Let $Q : \mathbb{Z} \rightarrow \mathbb{R}^2$ be a polygon, $p \in \mathbb{R}^2$ a fixed point. Think of this as being a set of triangles $\Delta(Q_n, Q_{n+1}, p)$. Now take these triangles and place them with the edges $[Q_n, Q_{n+1}]$ on a straight line e.g. the x -axis. The result is a sequence of points P_n . This new polygon P is the discrete trace of p when unrolling the polygon Q along the x -axis (Fig. 5.1).

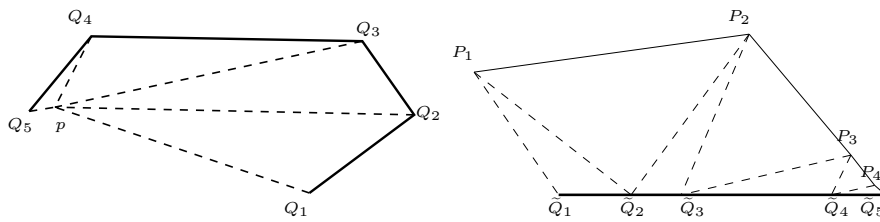


Figure 5.1: Unrolling a polygon

We can rotate this polygon P around the x -axis to obtain a discrete rotational surface: Choose $\phi \in (0, \pi)$ and define $F : \mathbb{Z}^2 \rightarrow \mathbb{R}^3$ by

$$F(n, m) = F_{n,m} := ((P_m)_1, \cos(n\phi)(P_m)_2, \sin(n\phi)(P_m)_2) \quad (5.4)$$

The condition (5.3) for F to be isothermic reads in terms of Q as follows:

$$\frac{1}{c} + 1 = \frac{1 + \cos(\alpha_n - \beta_n)}{1 + \cos(\alpha_n + \beta_n)} \quad (5.5)$$

where $\alpha_n = \angle(Q_{n-1}, Q_n, p)$, $\beta_n = \angle(p, Q_n, Q_{n+1})$ and $c = |cr| \sin^2 \frac{\phi}{2}$. Or equivalently:

$$\tan \frac{\alpha_n}{2} \tan \frac{\beta_n}{2} = \text{const.} \quad (5.6)$$

5.4 The Standard Billiard in an Ellipse or Hyperbola

Let E be a given ellipse. Choose a starting point Q_0 on E and a starting direction in Q_0 pointing to the inner of E . Shooting a ball





in that direction will give a new point Q_1 where it hits the ellipse again⁴. The new direction in Q_1 now is given by the usual reflection law: incoming angle = outgoing angle. This leads to a sequence Q_0, Q_1, Q_2, \dots (see fig. 5.3 upper left). If one thinks of these points as the vertices of a polygon, it is again a well known fact, that the edges are tangential to either a confocal hyperbola or a confocal ellipse, depending whether the first shot goes between the two foci or not [Kle26]. In an hyperbola the situation is similar with the one difference, that one has to change the branch if the shooting line doesn't hit the first branch twice (Fig. 5.2).

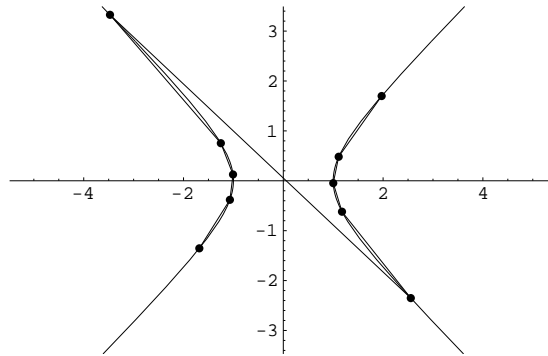


Figure 5.2: Billiard in an Hyperbola

5.5 Discrete Rotational CMC Surfaces

Now we have to recall the notion of a discrete surface of constant mean curvature first defined in [BP99]. We will give it in the following way:

Definition 13 *An isothermic surface F is a cmc surface with mean curvature $H \neq 0$ if there is a properly scaled and placed dual surface F^* of F in constant distance*

$$\|F_{n,m} - F_{n,m}^c\| = \frac{1}{H} \in \mathbb{R}.$$

⁴namely the point where the ball hits again the ellipse after moving on a straight line.

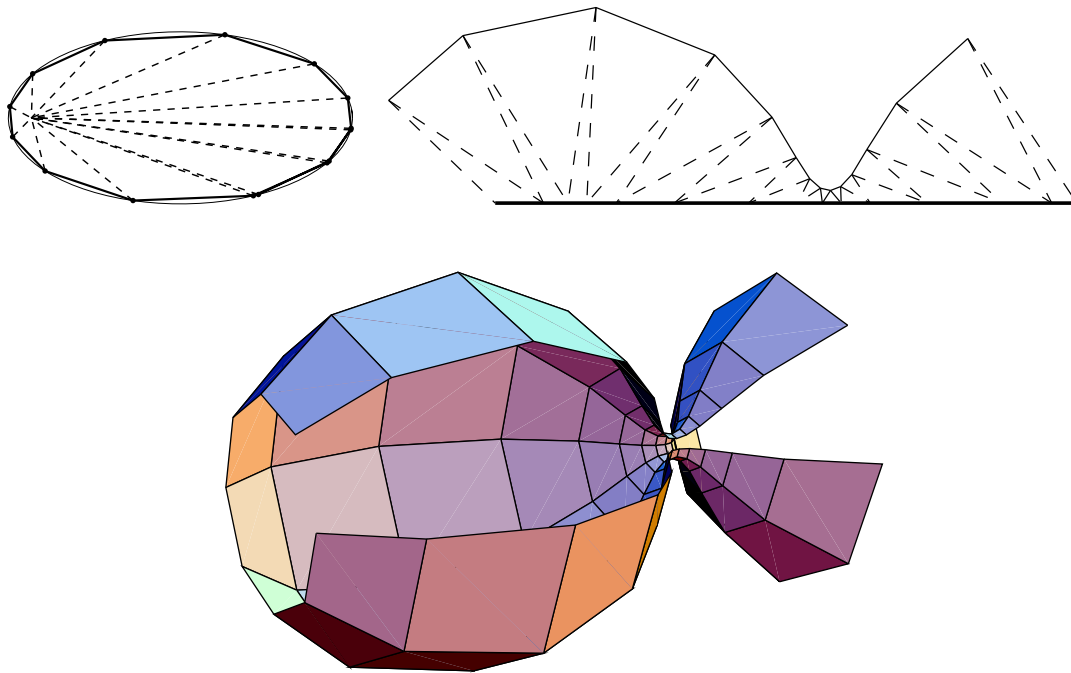
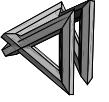


Figure 5.3: Billiard in an ellipse the meridian curve and the resulting discrete cmc surface

Examples for discrete cmc surfaces and a general construction mechanism can be found in [Hof99a].

Now we will see, that the polygon given by unrolling an elliptic or hyperbolic billiard trace is the meridian of a discrete rotational cmc surface. For shortness we will restrict ourselves to the elliptic case. First we show, that it generates an isothermic surface:

Theorem 39 *The polygon obtained by playing the standard billiard in an ellipse together with one focus satisfies condition (5.5).*

Proof Let us denote the two foci of the ellipse by \tilde{p} and p . We will use the fact, that the edges $[Q_n, Q_{n+1}]$ of the standard billiard in the ellipse are tangential to a confocal ellipse or hyperbola. We give the calculations for the case of the confocal quadric being an ellipse. The other case can be treated completely analogous.





If we look at the triangles made from \tilde{p} , Q_n and p we see that the angle at Q_n is $\alpha_n - \beta_n$. For the edges $l_n = |p - Q_n|$ and $\tilde{l}_n = |\tilde{p} - Q_n|$ one has $l_n + \tilde{l}_n = \text{const}$. Set $c = |p - \tilde{p}|$ Now we have :

$$c^2 = l_n^2 + \tilde{l}_n^2 - 2l_n\tilde{l}_n \cos(\alpha_n - \beta_n). \quad (5.7)$$

This gives:

$$1 + \cos(\alpha_{n+1} - \beta_{n+1}) = \frac{(l_{n+1} + \tilde{l}_{n+1})^2 - l_n^2 - \tilde{l}_n^2 + 2l_n\tilde{l}_n \cos(\alpha_n - \beta_n)}{2l_{n+1}\tilde{l}_{n+1}}. \quad (5.8)$$

Denote the point obtained by mirroring \tilde{p} at the straight line though Q_{n-1} and Q_n by \hat{p}_n then $|p - \hat{p}_n| = \hat{c}$ is constant too since the intersection point of $[Q_{n-1}, Q_n]$ and $[p, \hat{p}_n]$ is a point of the inner ellipse⁵. Since $|Q_n - \tilde{p}| = |Q_n - \hat{p}_n|$ and $\angle(\hat{p}_n, Q_n, p) = \alpha + \beta$ one has:

$$\hat{c}^2 = l_n^2 + \tilde{l}_n^2 - 2l_n\tilde{l}_n \cos(\alpha_n + \beta_n) \quad (5.9)$$

And therefore:

$$1 + \cos(\alpha_{n+1} + \beta_{n+1}) = \frac{(l_{n+1} + \tilde{l}_{n+1})^2 - l_n^2 - \tilde{l}_n^2 + 2l_n\tilde{l}_n \cos(\alpha_n + \beta_n)}{2l_{n+1}\tilde{l}_{n+1}} \quad (5.10)$$

Combining equations (5.8) and (5.10) one gets:

$$\begin{aligned} \frac{1 + \cos(\alpha_{n+1} - \beta_{n+1})}{1 + \cos(\alpha_{n+1} + \beta_{n+1})} &= \frac{(l_n + \tilde{l}_n)^2 - l_n^2 - \tilde{l}_n^2 + 2l_n\tilde{l}_n \cos(\alpha_n - \beta_n)}{(l_n + \tilde{l}_n)^2 - l_n^2 - \tilde{l}_n^2 + 2l_n\tilde{l}_n \cos(\alpha_n + \beta_n)} \\ &= \frac{1 + \cos(\alpha_n - \beta_n)}{1 + \cos(\alpha_n + \beta_n)} \end{aligned} \quad (5.11)$$

showing the invariance of $\frac{1 + \cos(\alpha_n - \beta_n)}{1 + \cos(\alpha_n + \beta_n)}$. \square

Discrete rotational cmc surfaces can be constructed by the general method presented in Chapter 6. Here we present an alternative method based on above continuous construction. Will show that above isothermic surfaces are even cmc—completing the analogy to the smooth construction scheme. Here is the corresponding discrete

⁵One can see this from the fact that the normal of an ellipse in a point Q cuts the inner angle $\angle(p, Q, \tilde{p})$ into half.

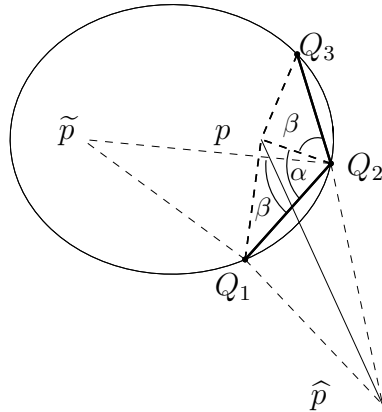


Figure 5.4:

Theorem 40 *The discrete rotational surface obtained by rotating the unrolled trace of a ball in an elliptic (or hyperbolic) billiard (see theorem 39) is a discrete rotational cmc surface.*

Proof To prove this, one has to find a dual surface in constant distance. If we trace both foci when evolving the ellipse, we get a second polygon \widehat{P} . Now mirror it along the axis (Fig. 5.5). We already saw in the proof of Theorem 39 that the distance $|P_n - \widehat{P}_n| = \tilde{c}$ is constant. From the reflection law one gets, that $|P_n - \widehat{P}_{n+1}| = |P_{n+1} - \widehat{P}_n| = c$ and therefore is constant. So $[P_n, P_{n+1}]$ and $[\widehat{P}_n, \widehat{P}_{n+1}]$ are parallel and

$$|P_n - P_{n+1}|^2 = \frac{2(c^2 - \tilde{c}^2)}{|\widehat{P}_n - \widehat{P}_{n+1}|^2}.$$

This in turn leads to

$$|P_n - P_{n+1}| = \frac{\lambda}{|\widehat{P}_n - \widehat{P}_{n+1}|}$$

with $\lambda = \frac{c^2 - \tilde{c}^2}{4}$.

□



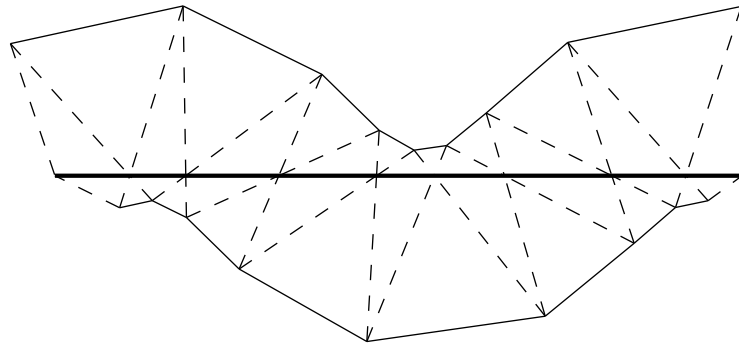


Figure 5.5: A meridian and its dual



Chapter 6

Discrete cmc Surfaces and Discrete Holomorphic Maps

6.1 Introduction

In 1994 Dorfmeister, Pedit, and Wu [DPW94] presented a method to construct all cmc surfaces in \mathbb{R}^3 by some holomorphic data. *Explicit construction*, however, is still difficult with this recipe, since one has to do some splitting in loop groups, which in general can only be done numerically and this means approximately. Therefore the results are mainly of theoretical interest. In this chapter I will present a discrete version—for discrete surfaces [BP99]—of this recipe. In spite of its continuous counterpart it is rather useful for the construction of (discrete) cmc surfaces, since it is exactly solvable in the sense that the corresponding splitting can be done explicitly. Moreover it will lead to a natural extension of the definition of discrete cmc surfaces allowing them to have umbilics. However, the construction is still difficult, since the problem is more or less reduced to the construction of discrete holomorphic maps, i.e. maps $F : \mathbb{Z}^2 \rightarrow \mathbb{C}$ with all quadrilaterals having cross-ratio -1 . This definition is due to Bobenko and Pinkall [BP96a] again. Of course the standard grid gives such a map. It will lead to the standard cylinder as the resulting cmc surface. A discrete version of the exponential map can again be found in [BP96a]. But for at least two more classical classes of cmc surfaces (rotational ones and





the Smyth surfaces also known as n -legged Mr Bubbles) we will give the generating discrete holomorphic maps.

In the rest of this chapter we will identify \mathbb{R}^3 with the imaginary quaternions in a slightly different way than before due to the conventions in above cited papers. We set $\text{Im } \mathbb{H} = \text{span}(-i\sigma_1, -i\sigma_2, -i\sigma_3) = \text{su}(2)$ where

$$\sigma_1 = \begin{pmatrix} 0 & 1 \\ 1 & 0 \end{pmatrix}, \quad \sigma_2 = \begin{pmatrix} 0 & -i \\ i & 0 \end{pmatrix}, \quad \sigma_3 = \begin{pmatrix} 1 & 0 \\ 0 & -1 \end{pmatrix}.$$

6.2 The DPW method

The method that Dorfmeister, Pedit, and Wu introduced in [DPW94] works in a more general framework, but for our purpose the following short overview shall suffice.

A main ingredient of the recipe is the interpretation of the moving frame as a map into some loop group that allows an Iwasawa-type decomposition. Therefore we introduce the following loop groups:

$$\Lambda \text{SL}(2, \mathbb{C})_\sigma = \{g : S^1 \rightarrow \text{SL}(2, \mathbb{C}) \mid g(-\lambda) = \sigma_3 g(\lambda) \sigma_3\},$$

and the splitting of $\Lambda \text{SL}(2, \mathbb{C})_\sigma$ into maps analytic inside and outside the unit circle:

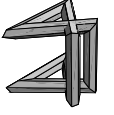
$$\Lambda^+ \text{SL}(2, \mathbb{C})_\sigma, \Lambda^- \text{SL}(2, \mathbb{C})_\sigma$$

and

$$\Lambda_*^- \text{SL}(2, \mathbb{C})_\sigma \subset \Lambda \text{SL}(2, \mathbb{C})_\sigma.$$

The subscript $*$ denotes that the members are normalized to have value \mathbb{I} at ∞ . Moreover let $\Lambda \text{sl}(2, \mathbb{C})_\sigma$ be the algebra corresponding to $\Lambda \text{SL}(2, \mathbb{C})_\sigma$. The following Lemmas are given without proof. For a detailed discussion of this subject see e.g. [AS96] and [SG85].

Lemma 41 *One has: $\Lambda_*^- \text{SL}(2, \mathbb{C})_\sigma \cdot \Lambda^+ \text{SL}(2, \mathbb{C})_\sigma$ is open and dense in $\Lambda \text{SL}(2, \mathbb{C})_\sigma$.*



Lemma 42 *The decomposition*

$$\Lambda \mathrm{SL}(2, \mathbb{C})_\sigma \cong \Lambda \mathrm{SU}(2, \mathbb{C})_\sigma \cdot \Lambda^+ \mathrm{SL}(2, \mathbb{C})_\sigma$$

is defined for all elements of $\Lambda \mathrm{SL}(2, \mathbb{C})_\sigma$.

Now we can formulate the DPW recipe [DPW94]:

1. Start with this initial condition:

$$\eta = \frac{1}{\lambda} \begin{pmatrix} 0 & f(z) \\ g(z) & 0 \end{pmatrix} dz, \lambda \in S^1 \quad (6.1)$$

where f and g are meromorphic functions with no poles at 0. Up to a constant factor fg is the Hopfdifferential Q of the immersion. This implies that one gets curvatureline parametrization iff $g = \frac{1}{\bar{f}}$ and an umbilic at p if $fg|_p = 0$.

2. Now solve the following differential equation:

$$dg_- = \eta g_-, g_-(0, \lambda) = \mathbb{I}. \quad (6.2)$$

3. Iwasawa decompose:

$$g_- = \Psi g_+^{-1}, \Psi \in \Lambda \mathrm{SU}(2, \mathbb{C})_\sigma, g_+ \in \Lambda^+ \mathrm{SL}(2, \mathbb{C})_\sigma \quad (6.3)$$

(with normalization $g_+(\lambda = 0) = \mathrm{diag}(a, a^{-1})$). The claim is that Ψ is a frame of a cmc surface f .

4. Use the Symformula to get the surface:

$$f = -\frac{1}{2H} \left(\Psi^{-1} \frac{\partial}{\partial \gamma} \Psi + \frac{i}{2} \Psi^{-1} \sigma_3 \Psi \right), \quad \lambda = e^{i\gamma}.$$

In the following sections we will develop a discrete analogue of this method that allows us to construct discrete cmc surfaces in a similar way. The discrete surfaces studied there are parametrized by conformal curvature lines, which implies that the Hopfdifferential is normalized to $Q = 1$. This reduces the initial choice to $g = \frac{1}{\bar{f}}$. This is no real restriction since every cmc surface without umbilics can be parametrized in this way, and we will see in Section 6.6.3 that we can extend the construction even to surfaces with umbilics.





6.3 Discrete cmc surfaces

Discrete cmc surfaces have been defined by A. Bobenko and U. Pinkall [BP99]. We have defined them in Chapter 4. So we will only fix the notation here:

Definition 14 • A discrete isothermic surface in \mathbb{R}^3 is a map $F : \mathbb{Z}^2 \rightarrow \mathbb{R}^3$ for which the elementary quadrilaterals

$$[F_{n,m}, F_{n+1,m}, F_{n+1,m+1}, F_{n,m+1}]$$

have cross-ratio¹ -1 .

A dual surface F^* of F is given by the equations:

$$\begin{aligned} (F_{m+1,n}^* - F_{m,n}^*) &= \lambda \frac{(F_{m+1,n} - F_{m,n})}{|F_{m+1,n} - F_{m,n}|^2} \\ (F_{m,n+1}^* - F_{m,n}^*) &= -\lambda \frac{(F_{m,n+1} - F_{m,n})}{|F_{m,n+1} - F_{m,n}|^2}, \end{aligned} \quad (6.4)$$

$\lambda \in \mathbb{R} \setminus \{0\}$. The dual surface is isothermic again.

- A discrete isothermic surface F is a discrete cmc surface with mean curvature $H \neq 0$ if there is a properly scaled and placed dual surface F^* of F at constant distance

$$\|F_{n,m} - F_{n,m}^*\| = \frac{1}{H} \in \mathbb{R}.$$

- A discrete isothermic map into the plane is called a discrete holomorphic map.

The discrete cmc surfaces can be described by a discrete moving frame: Let

$$L_{n,m} = \begin{pmatrix} a_{n,m} & \lambda b_{n,m} + \frac{1}{\lambda b_{n,m}} \\ -\frac{\bar{b}_{n,m}}{\lambda} - \frac{\lambda}{\bar{b}_{n,m}} & \bar{a}_{n,m} \end{pmatrix} \quad (6.5)$$

¹The cross-ratio of four complex numbers a, b, c , and d is given by $cr = \frac{(a-b)(c-d)}{(b-c)(c-a)}$. In a more general version of this definition the cross-ratio is of the form $\frac{\alpha_n}{\beta_m}$. It is invariant under Möbiustransformations (fractional linear transformations of the complex plane). The cross-ratio is real iff the four points lie on a circle. Therefore it is possible to demand a real cross-ratio for points in space: they have to lie on a circle and this defines a plane.



$$M_{n,m} = \begin{pmatrix} d_{n,m} & \lambda e_{n,m} + \frac{1}{\lambda e_{n,m}} \\ -\frac{\bar{e}_{n,m}}{\lambda} - \frac{\lambda}{\bar{e}_{n,m}} & \bar{d}_{n,m} \end{pmatrix} \quad (6.6)$$

satisfy the compatibility condition

$$L_{n,m} M_{n+1,m} = M_{n,m} L_{n,m+1} \quad \forall (n,m) \in \mathbb{Z}^2. \quad (6.7)$$

This gives in particular $\det L_{n,m}$ and $\det M_{n,m}$ are λ -independent and therefore:

$$\begin{aligned} \arg b &\equiv \text{const} \\ \arg e &\equiv \text{const}, \\ A = |a|^2 + |b|^2 + \frac{1}{|b|^2} &\equiv \text{const}, \\ B = |d|^2 + |e|^2 + \frac{1}{|e|^2} &\equiv \text{const}. \end{aligned}$$

$L_{n,m}$ and $M_{n,m}$ are the discrete Lax pair of the frame $\Psi_{n,m}$ of a discrete cmc surface (again see [BP99]).

$$\begin{aligned} \Psi_{n+1,m} &= L_{n,m} \Psi_{n,m} \\ \Psi_{n,m+1} &= M_{n,m} \Psi_{n,m}. \end{aligned} \quad (6.8)$$

Our goal is a discrete version of the DPW method and we will see that a normalization of $\Psi_{n,m}$ to be in $SU(2)$ is not convenient here. Note that rescaling the frame with a real function of λ will give us an additional multiple of the identity part in the Sym formula, and that $\det L$ and $\det M$ are real for $\lambda \in S^1$. Therefore we have to take the imaginary part:

$$F_{n,m} = -\text{Im} \left(\Psi_{n,m}^{-1} \frac{\partial}{\partial \gamma} \Psi_{n,m} + \frac{i}{2} \Psi_{n,m}^{-1} \sigma_3 \Psi_{n,m} \right), \quad \lambda = e^{i\gamma} \quad (6.9)$$

Im denotes the imaginary part of the quaternions.

6.4 Splitting in the discrete case

Since the Iwasawa decomposition of the solution g_- of (6.2) into the frame $\Psi \in \Lambda SU(2, \mathbb{C})_\sigma$ and $g_+^{-1} \in \Lambda^+ SL(2, \mathbb{C})_\sigma$ is a central point of





the DPW method, we will now formulate something similar for the discrete frame. The splitting can be read as a decomposition of Ψ into parts g^+ and g^- regular at 0 and ∞ . At the first glance the situation in our case is a little more complicated: if we normalize our discrete $\Psi_{n,m}$ to be in $\Lambda \text{SU}(2, \mathbb{C})_\sigma$, 0 and ∞ are not the critical points but the zeros of $\det \Psi_{n,m}$. Since

$$\begin{aligned} \det L_{n,m} &= A_m + \lambda^2 + \frac{1}{\lambda^2} \\ \det M_{n,m} &= B_n + \lambda^2 + \frac{1}{\lambda^2} \end{aligned} \quad (6.10)$$

the zeros of $\det \Psi_{n,m}$ are at $\pm\lambda_{0m}$, $\pm\frac{1}{\lambda_{0m}}$, and $\pm\lambda_{1n}$, $\pm\frac{1}{\lambda_{1n}}$ for some λ_{0m} and λ_{1n} . For notational simplicity we will omit the m and n dependence of λ_0 and λ_1 . The following results stay valid in the more general case, but the formulation would be much more complicated.

We have already seen that one can rescale a frame by an arbitrary function that does not vanish on the unit circle. In the continuous case the moving frames are typically normalized to be in $\Lambda \text{SU}(2, \mathbb{C})_\sigma$. In the discrete case, however, we will not rescale, since the fact of a missing normalization helps us to stay in the set of finite Laurent polynomials, as we will see later. One loses the group structure in this case, but looking projectively at the set brings this structure back.

Due to this and the special position of the zeros of $\det L_{n,m}$ and $\det M_{n,m}$ (and therefore the moving frame $\Psi_{n,m}$) we define the following:

Definition 15 For fixed λ_0, λ_1 define the set $G_\sigma \subset \Lambda \text{gl}(2, \mathbb{C})$ by the following conditions: The members $C(\lambda) \in G_\sigma$

1. are Laurent polynomial in λ : $C(\lambda) = \sum_{\nu=-m}^n \lambda^\nu C_\nu$
2. are twisted, that is: $C(-\lambda) = \sigma_3 C(\lambda) \sigma_3$
3. and have $\det(C(\lambda)) = (1 - \frac{\lambda_0^2}{\lambda^2})^i (1 - \frac{\lambda_1^2}{\lambda^2})^j (1 - \lambda_0^2 \lambda^2)^k (1 - \lambda_1^2 \lambda^2)^l$ for some $i, j, k, l \in \mathbb{N}$.



This set is closed under multiplication but not under inversion, so define the group PG_σ of classes of elements that are pointwise projective equivalent with elements of G_σ on S^1 .

It is obvious, that the frame $\Psi_{n,m}$ of a discrete cmc surface is in PG_σ . Now we will split elements of G_σ into a product of matrices corresponding to factors of its determinant:

Theorem 43 *Let $C \in G_\sigma$ and let $(1 - \frac{\lambda_\epsilon^2}{\lambda^{2i}})$ with $\epsilon \in \{0, 1\}, i \in \{-1, 1\}$ be a factor in above sense of $\det(C(\lambda))$. Then there exist matrices $X, \tilde{C} \in G_\sigma$ with $C = \tilde{C}X$, $X(\lambda) \xrightarrow{\lambda^i \rightarrow \infty} \mathbb{I}$ and $\det(\tilde{C}) = \det(C)/(1 - \frac{\lambda_\epsilon^2}{\lambda^{2i}})$.*

Proof Look at

$$C(\lambda_\epsilon^i) = \begin{pmatrix} a & b \\ c & d \end{pmatrix}.$$

Since $\det(C)$ vanishes at λ_ϵ^i , we have $ad - bc = 0$. Moreover, $a = b = c = d = 0$ is impossible, otherwise a, b, c , and d would have a common factor $(1 - \frac{\lambda_\epsilon^2}{\lambda^{2i}})$.

Now we make the following ansatz for a matrix \tilde{X} :

$$0 = \begin{pmatrix} a & b \\ c & d \end{pmatrix} \tilde{X}|_{\lambda_\epsilon}$$

One has to consider three cases:

1. If $b = d = 0$ we set

$$\tilde{X} = \begin{pmatrix} (1 - \frac{\lambda_\epsilon^2}{\lambda^{2i}}) & 0 \\ 0 & 1 \end{pmatrix}$$

2. If $a = c = 0$ we set

$$\tilde{X} = \begin{pmatrix} 1 & 0 \\ 0 & (1 - \frac{\lambda_\epsilon^2}{\lambda^{2i}}) \end{pmatrix}$$





3. If ab or cd is $\neq 0$ we choose f so that:

$$\tilde{X} = \begin{pmatrix} 1 & -\frac{f}{\lambda^i} \\ -\frac{\lambda_\epsilon^2}{f\lambda^i} & 1 \end{pmatrix}$$

This has a unique solution $f = \lambda_\epsilon \frac{b}{a}$ (or $f = \lambda_\epsilon \frac{d}{c}$).

Note that in all cases $\det \tilde{X} = (1 - \frac{\lambda_\epsilon^2}{\lambda^2})$. If we set

$$X^{-1} := \frac{1}{\det \tilde{X}} \tilde{X}$$

and $\tilde{C} = CX^{-1}$, we have $C = \tilde{C}X$ with $\det(\tilde{C}) = \det(C)/(1 - \epsilon \frac{\lambda_0^2}{\lambda^{2i}})$. \tilde{C} is again in G_σ since $(1 - \epsilon \frac{\lambda_0^2}{\lambda^{2i}})$ is a common factor of all of its coefficients and since $\tilde{X}(\infty) = \mathbb{I}$ one has $X(\infty) = \mathbb{I}$ too. \square

Remark We could have formulated this theorem also with splitting to the left.

Of course one can iterate this splitting until one has factorized C into a product of finitely many matrices of the above form:

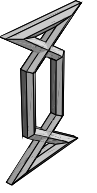
Corollary 44 *Let $C \in PG_\sigma$ with $\det(C(\lambda)) = x^2(\lambda)(1 - (\frac{\lambda_0^2}{\lambda})^2)^i(1 - (\frac{\lambda_1^2}{\lambda})^2)^j(1 - (\lambda_0^2\lambda)^2)^k(1 - (\lambda_1^2\lambda)^2)^l$ for some $i, j, k, l \in \mathbb{N}, x : \mathbb{C} \rightarrow \mathbb{C}$. Then there exist matrices $X_\nu \in G_\sigma, \nu \in \{1, i + j + k + l + 1\}$, with*

$$\begin{aligned} C(\lambda) &= x(\lambda) \prod_\nu X_\nu(\lambda) \\ \det X_1(\lambda) &= 1 \\ \det X_\nu(\lambda) &= (1 - \frac{\lambda_{\epsilon\nu}^2}{\lambda^{2\nu}}), \quad \nu \in \{2, i + j + k + l + 1\} \end{aligned}$$

and one can prescribe the order of the different types of determinants of the X_ν .

Proof Simply take the common polynomial divisor to the front and iterate Theorem 43. \square

Now we are able to split $C \in G_\sigma$ into two parts C^+ and C^- with $\det C^- = (1 - (\frac{\lambda_0^2}{\lambda})^2)^i(1 - (\frac{\lambda_1^2}{\lambda})^2)^j$, $\det C^+ = (1 - (\lambda_0^2\lambda)^2)^k(1 - (\lambda_1^2\lambda)^2)^l$ and $C^-(\infty) = \mathbb{I}$. Essentially this will be our discrete version of the



Iwasawa decomposition. Since $\Psi_{n,m} \in PG_\sigma$ (with appropriate λ_0 and λ_1) we can decompose it in this way

$$\Psi_{n,m} = G_{n,m}^+ G_{n,m}^-$$

with $G_{n,m}^-(\infty) = \mathbb{I}$. $G_{n,m}^-$ will play the role of g_- , so let us have a closer look at it: one has $\Psi_{n,m} = M_{n,m} \cdots M_{n,0} L_{n,0} \cdots L_{0,0}$. Decomposing $L_{n,m} = L_{n,m}^+ L_{n,m}^-$ gives:

$$L_{n,m}^+ = \begin{pmatrix} \frac{a_{n,m}}{\lambda_0^2 b_{n,m}^2 + 1} & \lambda b_{n,m} \\ -\frac{\lambda}{\bar{b}_{n,m}} & \frac{\bar{a}_{n,m}}{\frac{\lambda_0^2}{\bar{b}_{n,m}^2} + 1} \end{pmatrix} \quad (6.11)$$

$$L_{n,m}^- = \begin{pmatrix} 1 & \frac{f_{n,m}}{\lambda} \\ \frac{\lambda_0^2}{\lambda f_{n,m}} & 1 \end{pmatrix} \quad (6.12)$$

$$f_{n,m} = \lambda_0 \frac{\lambda_0 b_{n,m} + (\lambda_0 b_{n,m})^{-1}}{a_{n,m}} = -\lambda_0 \frac{\bar{a}_{n,m}}{\bar{b}_{n,m} \lambda_0^{-1} + \lambda_0 \bar{b}_{n,m}^{-1}} \quad (6.13)$$

and of course the same for $M_{n,m} = M_{n,m}^+ M_{n,m}^-$:

$$M_{n,m}^+ = \begin{pmatrix} \frac{d_{n,m}}{\lambda_0^2 e_{n,m}^2 + 1} & \lambda e_{n,m} \\ -\frac{\lambda}{\bar{e}_{n,m}} & \frac{\bar{d}_{n,m}}{\frac{\lambda_0^2}{\bar{e}_{n,m}^2} + 1} \end{pmatrix} \quad (6.14)$$

$$M_{n,m}^- = \begin{pmatrix} 1 & \frac{g_{n,m}}{\lambda} \\ \frac{\lambda_1^2}{\lambda g_{n,m}} & 1 \end{pmatrix} \quad (6.15)$$

$$g_{n,m} = \lambda_0 \frac{\lambda_0 e_{n,m} + (\lambda_0 e_{n,m})^{-1}}{d_{n,m}} = -\lambda_0 \frac{\bar{d}_{n,m}}{\bar{e}_{n,m} \lambda_0^{-1} + \lambda_0 \bar{e}_{n,m}^{-1}} \quad (6.16)$$

From this we see that $\Psi_{n,m}^-$ is the product of matrices of the form (6.12) and (6.15). Note that in general²

$$\Psi_{n,m}^- \neq M_{n,m}^- \cdots M_{n,0}^- L_{n,0}^- \cdots L_{0,0}^-$$

, since one has to commute minus and plus parts.

$L_{n,m}$ and $M_{n,m}$ have a very special form, so one can reconstruct them from their minus parts:

²See Section 6.6.2.





Lemma 45 *Let $L_{n,m}^-$ be of the form (6.12). Then there exists a matrix*

$$L_{n,m} = \begin{pmatrix} a_{n,m} & \lambda b_{n,m} + \frac{1}{\lambda b_{n,m}} \\ -\frac{\bar{b}_{n,m}}{\lambda} - \frac{\lambda}{\bar{b}_{n,m}} & \bar{a}_{n,m} \end{pmatrix}$$

with $\det L_{n,m} = c(1 - (\lambda_0^2 \lambda)^2)(1 - (\frac{\lambda_0^2}{\lambda})^2)$ and $L_{n,m}$ is unique up to sign.

Proof We make the same ansatz as in the proof of Theorem 43: Look at

$$\begin{aligned} \begin{pmatrix} 0 & 0 \\ 0 & 0 \end{pmatrix} &= L_{n,m}(\lambda)(L_{n,m}^-)^{-1}|_{\lambda=\lambda_0} \\ &= \begin{pmatrix} a_{n,m} & \lambda b_{n,m} + \frac{1}{\lambda b_{n,m}} \\ -\frac{\bar{b}_{n,m}}{\lambda} - \frac{\lambda}{\bar{b}_{n,m}} & \bar{a}_{n,m} \end{pmatrix} \begin{pmatrix} 1 & -\frac{f_{n,m}}{\lambda} \\ -\frac{\lambda_0^2}{\lambda f_{n,m}} & 1 \end{pmatrix}. \end{aligned}$$

This gives two equations:

$$a_{n,m} = \frac{b_{n,m} \lambda_0^2}{f_{n,m}} + \frac{1}{b_{n,m} f_{n,m}} \quad (6.17)$$

$$a_{n,m} = -\frac{\bar{f}_{n,m} b_{n,m}}{\lambda_0^2} - \frac{\bar{f}_{n,m}}{b_{n,m}}. \quad (6.18)$$

From this one gets

$$b_{n,m} = \pm \sqrt{-\frac{1 + |f_{n,m}|^2}{\lambda_0^2 + \frac{|f_{n,m}|^2}{\lambda_0^2}}}. \quad (6.19)$$

So $b_{n,m}$ and with it $a_{n,m}$ are defined up to sign. \square

Now we will focus again on the minus part $G_{n,m}^-$. It is the solution of the following difference equation:

$$\begin{aligned} G_{n+1,m}^- &= L_{n,m}^- G_{n,m}^- \\ G_{n,m+1}^- &= M_{n,m}^- G_{n,m}^- \end{aligned} \quad (6.20)$$

with $L_{n,m}^-$ and $M_{n,m}^-$ of the form (6.12). This is a discrete analogue of (6.2). The integrability condition

$$L_{n,m}^- M_{n+1,m}^- = M_{n,m}^- L_{n,m+1}^- \quad (6.21)$$

for (6.20) leads to the equations

$$f_{n,m} + g_{n+1,m} = g_{n,m} + f_{n,m+1} \quad (6.22)$$

$$\lambda_0^2 \frac{g_{n+1,m}}{f_{n,m}} = \lambda_1^2 \frac{f_{n,m+1}}{g_{n,m}} \quad (6.23)$$

One can interpret this in the following way: Equation (6.22) says that $f_{n,m}$ and $g_{n,m}$ are edges of a map $z : \mathbb{Z}^2 \rightarrow \mathbb{C}$ and (6.23) means that the elementary quadrilaterals of this map have a cross-ratio of λ_0^2/λ_1^2 . In the interesting case that $\lambda_0 \in \mathbb{R}$ and $\lambda_1 = i\lambda_0$ the map z is a discrete holomorphic map³.

Having L^-, M^- satisfying (6.21), one can solve (6.20) for a given initial value $G_{0,0}^-$ and one can split the solution $G_{n,m}^-$ in the following way: since $G_{n,m}^- = M_{n,m}^- \cdots M_{n,0}^- L_{n,0}^- \cdots L_{0,0}^-$ we can write

$$G_{n,m}^- = M_{n,m}^- \cdots M_{n,0}^- L_{n,0}^- \cdots L_{1,0}^- (L_{0,0}^+)^{-1} L_{0,0} = \tilde{G}_{n,m}^- L_{0,0}.$$

But $\tilde{G}_{n,m}^-$ is again in PG_σ and therefore we can factor out an $\tilde{L}_{1,0}^-$:

$$G_{n,m}^- = \tilde{G}_{n,m}^- (\tilde{L}_{1,0}^+)^{-1} \tilde{L}_{1,0}^- L_{0,0} = \tilde{\tilde{G}}_{n,m}^- \tilde{L}_{1,0}^- L_{0,0}.$$

We can continue with this procedure until we have

$$G_{n,m}^- = \Psi_{n,m}^+ \widetilde{M}_{n,m}^- \cdots \widetilde{M}_{n,0}^- \widetilde{L}_{n,0}^- \cdots \widetilde{L}_{1,0}^- L_{0,0}.$$

Notice that besides $L_{0,0}^-$, all the $L_{n,m}^-$ and $M_{n,m}^-$ are not the minus parts of the $\widetilde{L}_{n,m}$ and $\widetilde{M}_{n,m}$. Of course we could have changed the order to get the $\widetilde{L}_{i,j}$ and $\widetilde{M}_{i,j}$ for arbitrary $i \leq n, j \leq m$, but from the construction it is clear that

$$L_{i,j} M_{i+1,j} = M_{i,j} L_{i,j+1}.$$

Now we can formulate the discrete DPW method.

³One gets the more general definition of discrete holomorphic if λ_0^2/λ_1^2 is real negative, λ_0 is m -dependent and λ_1 is n -dependent.

6.5 The discrete DPW method

Theorem 46 *Any discrete cmc immersion $F : \mathbb{Z}^2 \rightarrow \mathbb{R}^3$ can be obtained by the following method, which is called the discrete DPW method:*

1. Choose $\lambda_0, \lambda_1 \in \mathbb{C}$ with $|\lambda_0| \neq 1$ and $\frac{\lambda_0^2}{\lambda_1^2} = -1$. Let $z : \mathbb{Z}^2 \rightarrow \mathbb{C}$ be a discrete holomorphic map and set

$$L_{n,m}^-(\lambda) = \begin{pmatrix} 1 & \frac{f_{n,m}}{\lambda} \\ \frac{\lambda_0^2}{\lambda f_{n,m}} & 1 \end{pmatrix}$$

with $f_{n,m} = z_{n+1,m} - z_{n,m}$ and

$$M_{n,m}^- = \begin{pmatrix} 1 & \frac{g_{n,m}}{\lambda} \\ \frac{\lambda_1^2}{\lambda g_{n,m}} & 1 \end{pmatrix}$$

with $g_{n,m} = z_{n,m+1} - z_{n,m}$

2. Solve

$$\begin{aligned} G_{n+1,m}^- &= L_{n,m}^- G_{n,m}^- \\ G_{n,m+1}^- &= M_{n,m}^- G_{n,m}^- \end{aligned} \tag{6.24}$$

with $G_{0,0}^- = \begin{pmatrix} 1 & 0 \\ 0 & 1 \end{pmatrix}$.

3. Split $G_{n,m}^- = \Psi_{n,m}^+ \Psi_{n,m}$.
4. Use the Sym formula (6.9) to get a discrete cmc surface $F_{n,m}$ out of $\Psi_{n,m}$.

Proof

From the previous calculations it is clear that this method gives a discrete cmc surface. On the other hand, given a discrete cmc immersion one can calculate its moving frame Ψ and its minus part in the sense of corollary 44 by

$$\Psi_{n,m} = \Psi_{n,m}^+ M_{n,m}^- \cdots M_{n,0}^- L_{n,0}^- \cdots L_{0,0}^-.$$

Again, by altering the order of the L^- and M^- one gets all of the $L_{i,j}^-$ and $M_{i,j}^-$, and from construction it is clear that they satisfy (6.21) and therefore have the edges of a discrete holomorphic map as coefficients. \square

6.6 Examples

Now let us give some special cases as examples. We will derive the holomorphic maps that lead to Delaunaytubes as well as the ones that give Smyth surfaces.

In the following we will take $\lambda_1 = i\lambda_0$ for simplicity.

6.6.1 Cylinder and two-legged Mr Bubbles

The simplest discrete holomorphic map one can think of is the identity map⁴

$$z : \mathbb{Z}^2 \rightarrow \mathbb{C}, \quad z_{n,m} = \Delta\lambda_0(n + im)$$

This gives:

$$L_{n,m}^- = \begin{pmatrix} 1 & \frac{\Delta\lambda_0}{\lambda} \\ \frac{\lambda_0}{\Delta\lambda} & 1 \end{pmatrix} \quad (6.25)$$

$$M_{n,m}^- = \begin{pmatrix} 1 & i\frac{\Delta\lambda_0}{\lambda} \\ -i\frac{\lambda_0}{\Delta\lambda} & 1 \end{pmatrix} \quad (6.26)$$

in the special case $\Delta = 1$, (6.17) and (6.19) are very easy and give $b = i$ and $a = i(\lambda_0 - \frac{1}{\lambda_0})$ (for $L_{n,m}$) and $e = 1$ and $d = i(\lambda_0 - \frac{1}{\lambda_0})$ (for $M_{n,m}$). One easily calculates

$$L_{n,m}^+ = \begin{pmatrix} -\frac{i}{\lambda_0} & i\lambda \\ i\lambda & \frac{i}{\lambda_0} \end{pmatrix}$$

$$M_{n,m}^+ = \begin{pmatrix} -\frac{i}{\lambda_0} & \lambda \\ \lambda & \frac{i}{\lambda_0} \end{pmatrix}.$$

Since the plus and the minus parts commute, it is obvious that $L_{n,m}$ and $M_{n,m}$ are constant. As one would expect, the resulting discrete surface is a cylinder.

⁴if $|\lambda_0| \neq |\lambda_1|$ set $z_{n,m} = \Delta(\lambda_0 n + i\lambda_1 m)$

If $\Delta \neq 1$, however, the situation is not that simple and the resulting surface is a two-legged Mr Bubble. These surfaces are discrete versions of Smyth surfaces (i.e. surfaces with rotational symmetric metric). Figure 6.1 shows a discrete cylinder and three Mr Bubbles for different values of Δ .

Note that in the continuous case $f = \text{const}$ produces these surfaces instead of $f(z) = z$. Nevertheless we use the edges of the discrete holomorphic map in $L_{n,m}^-$ and $M_{n,m}^-$ and one should think of them as being derivatives.

6.6.2 Delaunay tubes

A famous class of cmc surfaces is the rotational symmetric ones. We constructed them already in Chapter 4 and 5 as cmc evolution of a circle and by generating the meridian curve from a Billiard in an ellipse or hyperbola. The edges of our discrete cmc surfaces are discrete equivalents of curvature lines (again see [BP99]). Since the meridians of surfaces of revolution are curvature lines too, the rotational symmetry implies that the frame $\Psi_{n,m}$ is constant in n (or m) direction. in terms of $L_{n,m}$ this means:

$$\begin{aligned}
G_{n,0}^+ G_{n,0}^- &= L_{n-1,0} \cdots L_{0,0} \\
&= L_{n-1,0} \cdots L_{0,0}^+ L_{0,0}^- \\
&= L_{n-1,0} \cdots L_{0,0}^+ L_{0,0}^- L_{0,0}^+ L_{0,0}^- \\
&= L_{n-1,0} \cdots L_{0,0}^+ L_{1,0}^+ L_{1,0}^- L_{0,0}^- \\
&= L_{n-1,0} \cdots L_{0,0}^+ L_{1,0}^+ L_{1,0}^- L_{1,0}^+ L_{1,0}^- L_{0,0}^- \\
&= L_{n-1,0} \cdots L_{0,0}^+ L_{1,0}^+ L_{2,0}^+ L_{2,0}^- L_{1,0}^- L_{0,0}^- \\
&\vdots
\end{aligned}$$

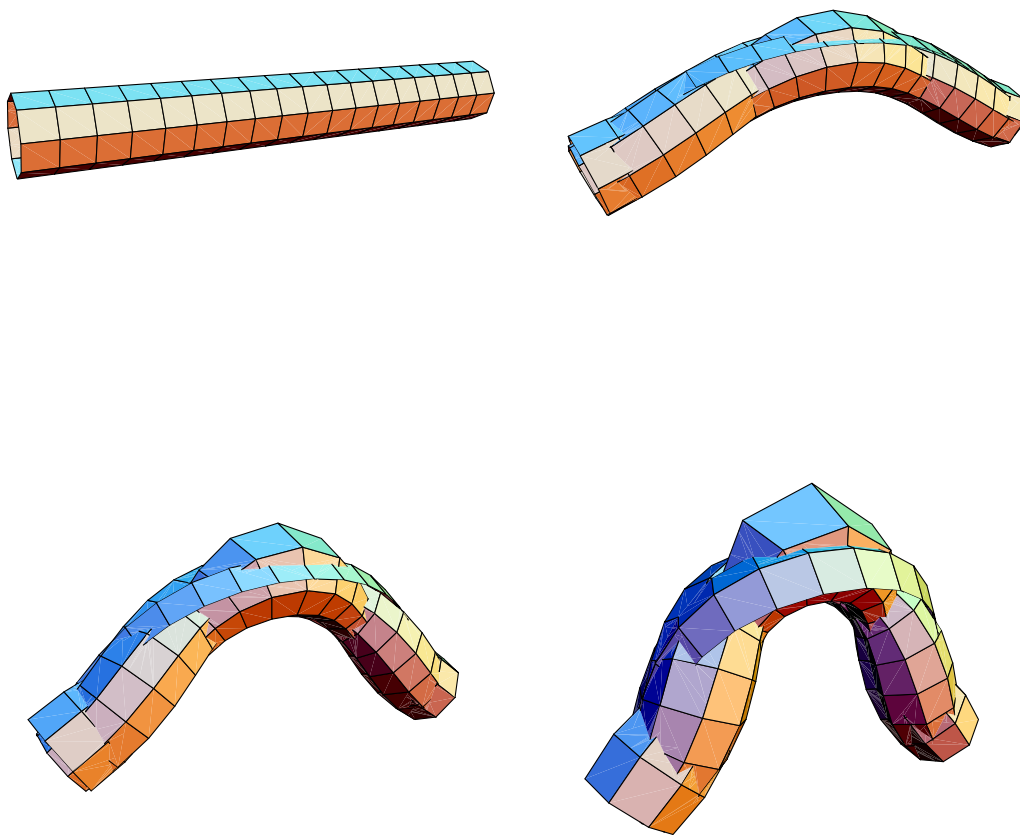


Figure 6.1: A cylinder and two-legged Mr Bubbles with $\Delta = 1.5, 2,$ and $3.$

Or in other terms: start with $L_{0,0}^-$ and solve $L_{n+1,0}^+ L_{n+1,m}^- = L_{n,0}^- L_{n,0}^+$. For the entries $f_{n,0}$ of $L_{n,0}^-$ this gives the following recursion:

$$\begin{aligned} f_{n+1,0} &= \frac{\frac{f_{n,0}}{\lambda_0^2 S_n} - p \lambda_0^2}{S_n - \frac{f_{n,0}}{p}} \\ S_{n+1} &= \frac{f_{n,0}}{\lambda_0^2 f_{n+1,0} S_n} \end{aligned} \quad (6.27)$$

with $S_0 = -\frac{1}{f_{0,0} p}$ and

$$p = \sqrt{-\frac{1 - f_{0,0}^2}{\lambda_0^2 - \frac{f_{0,0}^2}{\lambda_0^2}}}.$$

Choosing an initial $f_{0,0}$ one can compute for any $g_{0,0}$ the $g_{n,0}$ and $f_{n,1}$ by evolving the cross-ratio condition (6.23). Now we can solve the condition

$$M_{0,0} = M_{1,0}$$

in order to get $g_{0,0}$. There are two possible solutions⁵ (depending on the orientation of the first quadrilateral):

$$g_{0,0} = \pm \frac{\sqrt{f_{0,0}^2 - 2\lambda_0^4 + f_{0,0}^2 \lambda_0^4}}{-1 + 2f_{0,0}^2 - \lambda_0^4}.$$

Having this initial $g_{0,0}$ $g_{0,m}$ evolves the same way as $f_{n,0}$:

$$\begin{aligned} g_{0,m+1} &= \frac{\frac{g_{0,m}}{\lambda_1^2 T_m} - p \lambda_1^2}{T_m - \frac{g_{0,m}}{p}} \\ T_{m+1} &= \frac{g_{0,m}}{\lambda_1^2 g_{0,m+1} T_m} \end{aligned} \quad (6.28)$$

with $T_0 = -1/g_{0,0} p$. Now we have initial conditions for the discrete holomorphic map. Figure 6.2 shows a typical solution. Note the

⁵ This solution looks more complicated if $\lambda_0 \neq i\lambda_1$

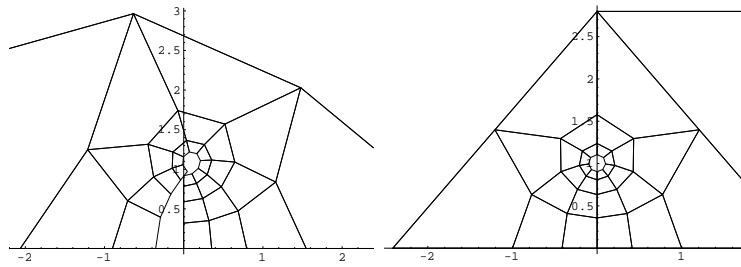


Figure 6.2: The first quadrants of a discrete holomorphic map that generates a rotational cmc surface and of a discrete tanh.

similarity to the discrete $\tanh(z)$ function⁶ given by

$$\tanh_{n,m} = \tanh\left(\frac{\rho n + i\alpha m}{2}\right) \quad (6.29)$$

with $\alpha = \frac{2\pi}{N}$ and $\rho = 2 \operatorname{arcsinh}(\sin(\frac{\alpha}{2}))$. In fact the above definition can be extended to a two-parameter family of discrete holomorphic maps containing both of them.

Figure 6.3 finally shows some of the discrete rotational surfaces we can get in this way: one Nodoid, one Undoloid, and one surface of the associated family of the Undoloid (this is no longer rotational of course).

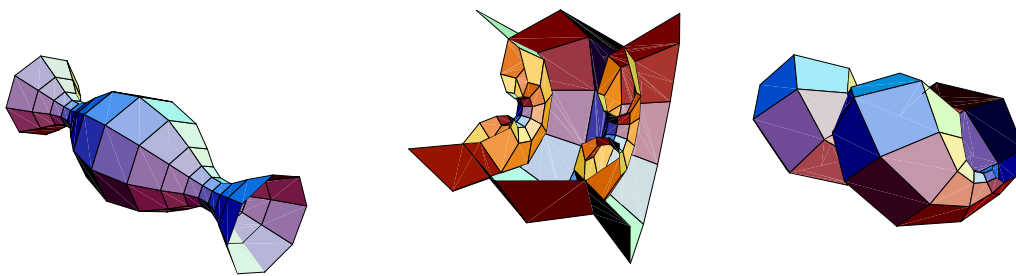


Figure 6.3: A discrete Nodoid, an Undoloid, and a member of the associated family of the Undoloid

⁶This is simply a Möbius transform of the discrete $\exp(z)$.

6.6.3 n -legged Mr Bubbles and a discrete z^α

Now we want to discretize Mr Bubbles with more than two legs. These surfaces have an umbilic. In order to get discrete cmc surfaces with umbilics we have to look at the continuous case again. In an isolated umbilic more than two curvature lines intersect. Since the edges of our discretization correspond to curvature lines, we have to change the connectivity of our lattice. Up to now we have formulated all results for maps from \mathbb{Z}^2 , but the generalization to quad-graphs with even numbers of edges per vertex (Chapter 1) is obvious.

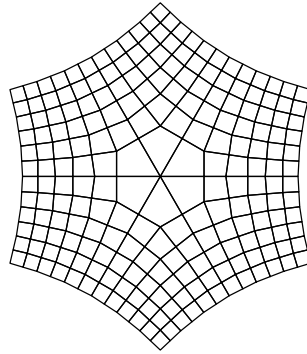


Figure 6.4: The discrete $z^{\frac{2}{3}}$

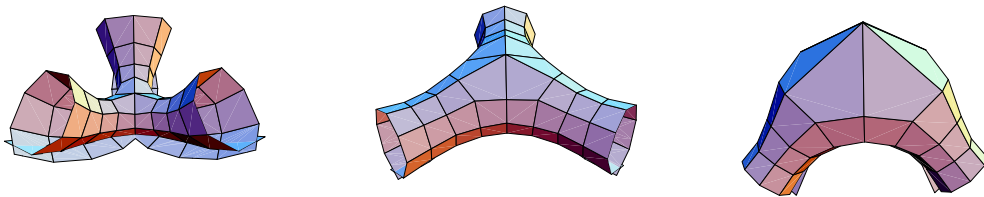


Figure 6.5: Some three-legged Mr Bubbles

Usually the meromorphic potential for the Smyth surfaces is

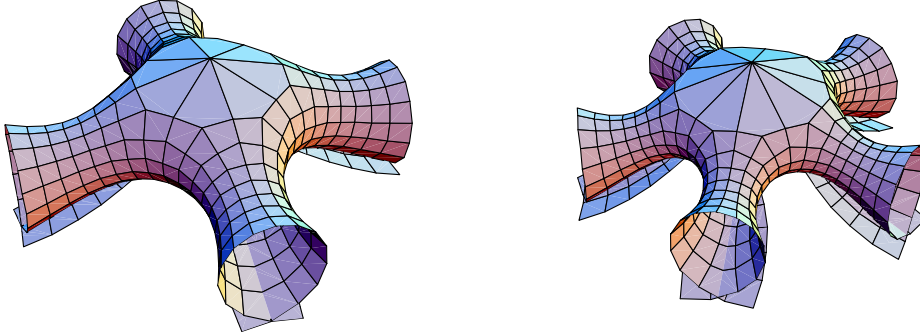


Figure 6.6: Four- and five-legged Mr Bubbles

given in the following way:

$$\eta = \frac{1}{\lambda} \begin{pmatrix} 0 & 1 \\ z^\alpha & 0 \end{pmatrix} dz \quad (6.30)$$

In this gauge the Hopf differential is not normalized to 1. Therefore we change the coordinates. Let $w = q(z)$. Then we have $dw = q'(z)dz$ and with it:

$$\tilde{\eta} = \frac{1}{\lambda} \begin{pmatrix} 0 & \frac{1}{q' \circ q^{-1}} \\ \frac{(q^{-1})^\alpha}{q' \circ q^{-1}} & 0 \end{pmatrix} dw. \quad (6.31)$$

The requirement for the Hopf differential to be 1 reads for q as $q'(z) = z^{\frac{\alpha}{2}}$ which gives $q(z) = \frac{2}{\alpha+2} z^{\frac{\alpha+2}{2}}$ and for our meromorphic potential

$$\tilde{\eta} = \frac{1}{\lambda} \begin{pmatrix} 0 & \frac{1}{(\frac{\alpha+2}{2}w)^{\frac{\alpha}{\alpha+2}}} \\ (\frac{\alpha+2}{2}w)^{\frac{\alpha}{\alpha+2}} & 0 \end{pmatrix} dw. \quad (6.32)$$

If we choose e.g. $\alpha = 1$ we get $f(w) = (\frac{3}{2}w)^{\frac{1}{3}}$ for our holomorphic function. As mentioned before the continuous map is an analogue of the derivative of the discrete one. Therefore we would have to look for a discrete $z^{\frac{2}{3}}$. It can be described in the following way: the

constraint below is compatible with the “cross-ratio equal to -1 ” evolution.

$$\alpha z_{n,m} = n D_x^h z|_{n,m} + m D_y^h z|_{n,m} \quad (6.33)$$

where D^h is the discrete harmonic derivative from Chapter 1:

$$D_x^h z|_{n,m} = 2 \frac{(z_{n+1,m} - z_{n,m})(z_{n,m} - z_{n-1,m})}{z_{n+1,m} - z_{n-1,m}}$$

With the obvious initial conditions

$$z_{0,0} = 0, \quad z_{1,0} = 1, \quad z_{0,1} = i^\alpha$$

one gets a discrete version of z^α in the first quadrant⁷. See [Bob96, AB99] for a detailed investigation of this map. Since the solution for $m = 0$ (or $n = 0$) depends on n (m) only, the solutions for different sectors are compatible. Figure 6.4 shows the complete solution for $\alpha = \frac{2}{3}$

Scaling this discrete holomorphic map leads to a one-parameter family of discrete cmc surfaces with an umbilic at the image of 0. Figures 6.5 and 6.6 show some of them and the thumb anil movie on the upper left shows a part of the one-parameter family of three-legged Mr. Bubbles.

⁷In fact these discrete maps give discrete holomorphic maps in the sense of O. Schramm [Sch97] too: one simply has to take the sublattice not including zero.

Chapter 7

Discrete K-surfaces from discrete curves

7.1 Introduction

Discrete surfaces of constant negative Gaussian curvature (discrete K-surfaces) were first investigated by Wunderlich and Sauer [Wun51]. Bobenko and Pinkall [BP96b, BP99] extended their work and made the connection to discrete integrable systems (the Hirota equation). In this chapter we want to complete our picture of the connection between discrete curves and surfaces by generating these discrete surfaces from discrete curves.

7.2 Discrete K-surfaces from curvature lines

As usual we start by recalling the definitions:

Definition 16 *A map $\mathcal{F} : \mathbb{Z}^2 \rightarrow \mathbb{R}^3$ is called a discrete K-surface if the following conditions hold:*

1. *All edges connecting to one vertex lie in a plane*
2. *All edges have the same length.*¹

¹this can be weakend to The length of edges $[\mathcal{F}_{n+1,m} - \mathcal{F}_{n,m}]$ depends on m only and the length of edges $[\mathcal{F}_{n,m+1} - \mathcal{F}_{n,m}]$ depends on n only.

The first condition clearly is a discrete version of asymptotic line parametrization the second one says that the parameter net is a (discrete) Chebychev net [BP99].

Since the edges of the discrete map play the role of asymptotic lines, the diagonals of the quadrilaterals should model the curvature lines of the surface. We will see now, that with some extra data one can recover the K-surface from such a curvature line.

Lemma 47 *Let γ be a discrete curve with edges $S_n = \gamma_{n+1} - \gamma_n$ and a vertex normal field N such that $|S_n| \leq 2$, $\angle(N_n, S_n) = \angle(N_{n+1}, S_n)$, and $N_{n+1} \times N_n \perp S_n$. Then given an angle δ , each edge can be extended to a triangle $(\gamma_n, \gamma_{n+1}, \tilde{\gamma}_n)$ such that $|\tilde{\gamma}_n - \gamma| = |\tilde{\gamma}_n \gamma_{n+1}| = 1$ and $\angle(N_n, \tilde{N}_n) = -\angle(N_{n+1}, \tilde{N}_n) = \delta$ with $\tilde{N}_n := (\gamma_{n+1} - \tilde{\gamma}_n) \times (\gamma_n - \tilde{\gamma}_n)$*

Proof Elementary geometry. □

Theorem 48 *Let γ be a discrete curve with edges $S_n = \gamma_{n+1} - \gamma_n$ and a vertex normal field N such that $|S_n| \leq 2$, $\angle(N_n, S_n) = \angle(N_{n+1}, S_n)$, and $N_{n+1} \times N_n \perp S_n$.*

Then γ can be viewed as a curvature line of a discrete k-surface and the stripe (γ, N) serves as Cauchy data.

Proof After choosing an angle δ apply above lemma. The sequence $\dots, \gamma_n, \tilde{\gamma}_n, \dots$ serves as Cauchy path (zig-zag) for a discrete K-surface. The edges S_n of γ are diagonals in elementary quadrilaterals of the K-surface. Since the edges of these quadrilaterals should be viewed as asymptotic directions γ can be viewed as a curvature line. □

Example In particular plane elastic curves (with edge length 2) can serve as curvature lines for discrete K-surfaces if one assigns normals perpendicular to the plane as stripe normals.

Figure 7.2 shows a K-surface generated from an discrete elastic figure eight.

7.3 Discrete K-surfaces from asymptotic lines

The maybe more natural approach is however to evolve discrete K-surfaces out of their asymptotic lines. for this one must start with a arclength parametrized discrete curve with constant torsion (we have defined in Chapter 2 what that means).

Lemma 49 *Let γ be an arclength parametrized discrete curve with constant torsion. Choose a point $\tilde{\gamma}_0$ in the osculating plane of γ_0 (the plane spanned by γ_{-1} , γ_0 , and γ_1). Then the Bäcklund transformation in the sense of Definition 8 with angle δ_1 equal to the torsion of γ will yield a curve $\tilde{\gamma}$ with $\tilde{\gamma}_k$ in the osculating plane of γ_k for all k .*

Iterating this procedure gives rise to a discrete K-surface.

Proof Since the osculating planes of two neighbouring points have constant angle δ_1 , it is quite clear that when starting in the osculating plane the Bäcklund transformation will preserve this. Moreover is the distance of γ and $\tilde{\gamma}$ 1 so both conditions for discrete K-surfaces from Definition 16 are fulfilled when iterating the Bäcklund transformation. \square

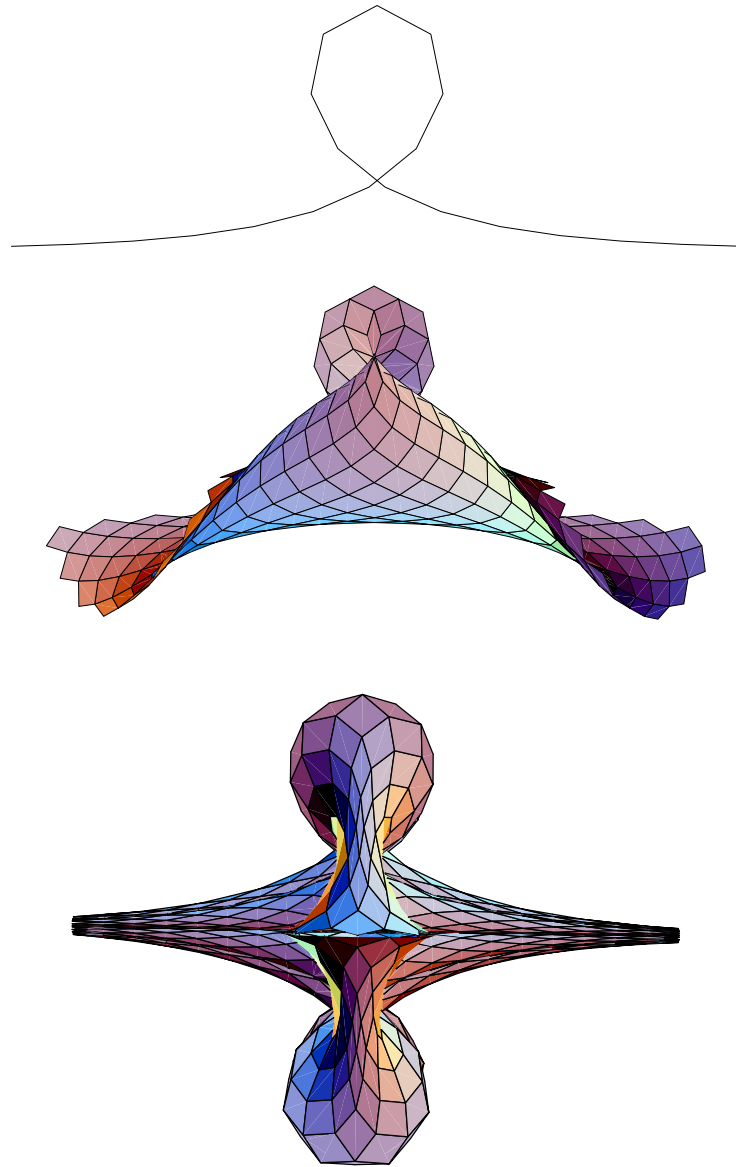


Figure 7.1: An elastic Euler loop and two Kühn surfaces generated from it.

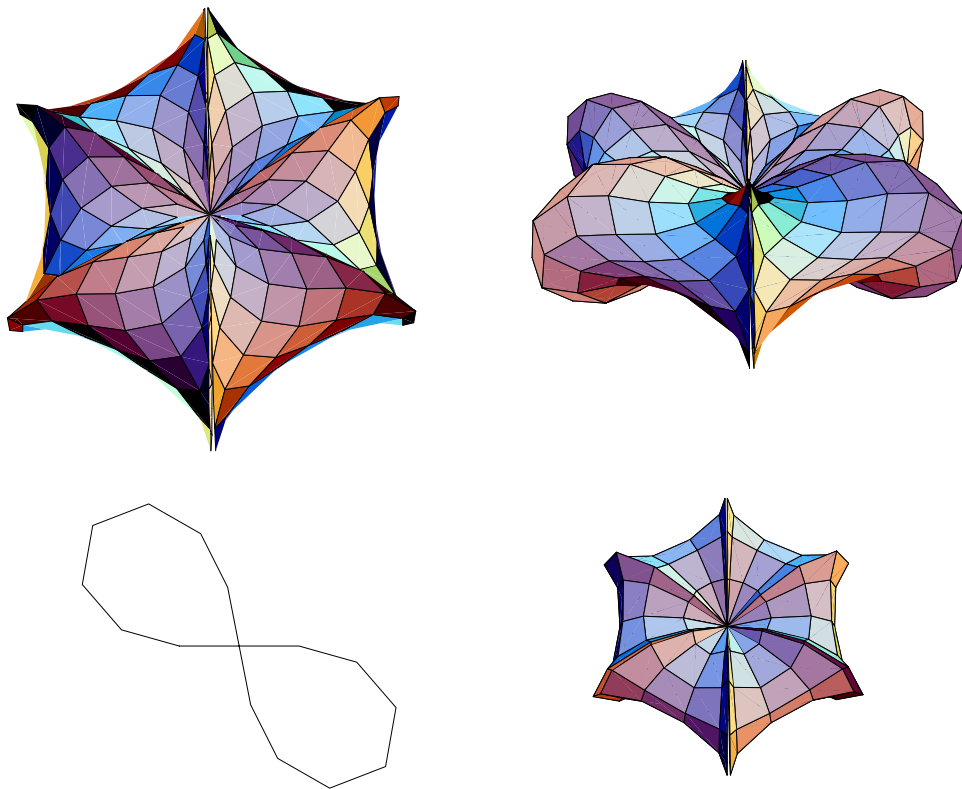


Figure 7.2: A compact K-surface and the elastic figure eight it is generated from.

Acknowledgments

I would like to thank Ulrich Pinkall and Sasha Bobenko for their constant support and many helpful and enlightening discussions. I learned a lot from them. I also would like to thank Y. Suris for helpful hints on the NLSE and the Volterra model, N. Kutz and E.-H. Tjaden for teaching me about the billiards in quadrics, and G. Haak and I. Sterling who first brought up the idea of finding the discrete analogue of the smooth construction of rotational cmc surfaces.

I owe special thanks to Nadja and Zora Kutz whose support made this work possible.

The figures in this work are made with xfig, MATHEMATICA, AVS, and Softimage.

Bibliography

- [AB99] S. I. Agafonov and A. I. Bobenko. Discrete z^γ and Painlevé equations. Sfb 288 Preprint No. 404, accepted for Int. Math. Res. Notices, 1999.
- [AL76] M. J. Ablowitz and J. F. Ladik. Nonlinear differential-difference equations and Fourier analysis. *Stud. Appl. Math.*, 17:1011–1018, 1976.
- [AL77] M. J. Ablowitz and J. F. Ladik. A nonlinear difference scheme and inverse scattering. *Stud. Appl. Math.*, 55:213–229, 1977.
- [AS96] Pressley A. and G. Segal. *Loop Groups*. Oxford University Press, 1996.
- [Bob96] A. Bobenko. Discrete conformal maps and surfaces. GANG Preprint, University of Massachusetts, to be published in the proceedings SIDE II Conference, Canterbury, July 1–5 1996, Cambridge University Press, eds.: P. Clarkson and F. Nijhoff., 1996.
- [BP96a] A. Bobenko and U. Pinkall. Discrete isothermic surfaces. *J. reine angew. Math.*, 475:178–208, 1996.
- [BP96b] A. Bobenko and U. Pinkall. Discrete surfaces with constant negative caussian curvature and the hirota equation. *J. Diff. Geom.*, 43:527–611, 1996. to appear in *Jorn Diff. Geom.*

- [BP99] A. Bobenko and U. Pinkall. Discretization of surfaces and integrable systems. In Bobenko A. and Seiler R., editors, *to appear in Discrete Integrable Geometry and Physics*. Oxford University Press, 1999.
- [BS99] A. Bobenko and Y. Suris. Discrete time Lagrangian mechanics on Lie groups, with an application to the Lagrange top. *to appear in Comm. Math. Phys.*, 1999.
- [DJM82a] E. Date, M. Jimbo, and T. Miwa. Method for generating discrete soliton equations. I. *J. Phys. Soc. Japan*, 51(12):4116//4127, 1982.
- [DJM82b] E. Date, M. Jimbo, and T. Miwa. Method for generating discrete soliton equations. IV. *J. Phys. Soc. Japan*, 52(3):761–765, 1982.
- [DPW94] J. Dorfmeister, F. Pediti, and H. Wu. Weierstrass type representation of harmonic maps into symmetric spaces. *G.A.N.G. Preprint III.25 Amherst*, 1994.
- [DS99] A. Doliva and Santini. Geometry of discrete curves and lattices and integrable difference equations. In A. Bobenko and R. Seiler, editors, *Discrete integrable geometry and physics*, chapter Part I 6. Oxford University Press, 1999.
- [FT86] L. D. Faddeev and L. A. Takhtajan. *Hamiltonian methods in the theory of solitons*. Springer, 1986.
- [Haa96] G. Haak. Discrete surfaces of constant mean curvature via dressing. sfb288 preprint No. 293, 1996.
- [Has77] H. Hashimoto. A soliton on a vortex filament. *J. Fluid Mech.*, 51:477–485, 1977.
- [HJHP99] U. Hertrich-Jeromin, T. Hoffmann, and U. Pinkall. A discrete version of the Darboux transformation for

- isothermic surfaces. In Bobenko A. and Seiler R., editors, *Discrete Integrable Geometry and Physics*. Oxford University Press, 1999.
- [HJMP98] U. Hertrich-Jeromin, J. MacIntosh, and F. Pedit. Discrete conformal maps. unpublished, 1998.
- [Hof99a] T. Hoffmann. Discrete cmc surfaces and discrete holomorphic maps. In Bobenko A. and Seiler R., editors, *Discrete Integrable Geometry and Physics*. Oxford University Press, 1999.
- [Hof99b] T. Hoffmann. On the equivalence of the discrete nonlinear Schrödinger equation and the discrete isotropic Heisenberg magnet. sfb288 preprint No. 381, submitted to Phys. Lett. A., 1999.
- [IK81] A. G. Izergin and V. E. Korepin. A lattice model associated with the nonlinear Schrödinger equation. *Dokl. Akad. Nauk SSSR*, 259:76–79, 1981. Russian.
- [Ish82] Y. Ishimori. An integrable classical spin chain. *J. Phys. Soc. Jpn.*, 51(11):3417–3418, November 1982.
- [Kle26] F. Klein. *Vorlesungen über höhere Geometrie*. Springer, 1926.
- [Kut96] N. Kutz. *The Doubly Discrete Sine-Gordon Equation in Geometry and Physics*. PhD thesis, TU Berlin, 1996.
- [QNCvdL84] G. R. W. Quispel, F. W. Nijhoff, H. W. Capel, and J. van der Linden. Linear integral equations and nonlinear difference-difference equations. *Physica*, 125A:344–380, 1984.
- [Sch97] O. Schramm. Circle patterns with the combinatorics of the square grid. *Duke Math. J.*, 86(2):347–389, 1997.

- [SG85] G. Segal and Wilson G. Loop groups and equations of kdv type. *Publ. Math. I.H.E.S.*, 61:5–65, 1985.
- [Sur94] Y. Suris. A discrete-time Garnier system. *Phys. Lett. A*, 189:281–289, 1994.
- [Sur97] Y. Suris. A note on an integrable discretization of the nonlinear Schrödinger equation. *Inverse Problems*, 13:1121–1136, 1997.
- [Sur99] Y. Suris. unpublished, 1999.
- [Wun51] W. Wunderlich. Zur differenzengeometrie der flächen konstanter negativer krümmung. *Sitzungsber. Ak. Wiss.*, 160:39–77, 1951.